Calibration and Study of the Contoured Nozzle of the T5 Free-Piston Hypervelocity Shock Tunnel

Thesis by

Bernard ROUSSET

In Partial Fulfillment of the Requirements
for the Degree of
Aeronautical Engineer

California Institute of Technology
Pasadena, California

1995

(Submitted December 6, 1994)

To my Mum & Dad,

To my Beloved Sabine,

And to our Kids-to-be ...

Acknowledgments

First of all, I would like to thank the entire T5 team for their help during this series of shots, for their advice on setting up this calibration, and for all the time we shared building up this project.

This includes Jacques BELANGER, for sharing his expertise of T5, Eric CUMMINGS, for his help with the optics, Jean-Paul DAVIS, for his general help, Patrick GERMAIN, for the electric connections, Patrick LEMIEUX, for the X-Window version of DAS, Matthias NOEKLER, for working with me on some SURF computations, Simon SANDERSON, for his explanations on the DAS and for the pitot-tip design, Prof. Bradford STURTEVANT, for his advice on the instrumentation of the rake, Kenji TOGAMI, for his early and friendly recommendations concerning models, Barham VALIFERDOWSI, for making all these shots possible, Chihyung WEN, for his general advice, and Karen CHEETHAM, our dear and kind secretary.

I would like also to include Larry FRAZIER, Joe HAGGERTY, and Phil WOOD, from the machine shop, for building my "Rack R13" (first name of the pitot-rake!).

Special thanks go to my advisor Prof. Hans HORNUNG, who, in addition, supervised this whole project all along. I enjoyed his company, his teaching, our discussions and reflexions, and simply sharing friendly ideas with him. He has always been present when I needed him, and that's also what made him a great advisor.

I am extremely grateful to Philippe ADAM for going through all the corrections of my thesis. This was already very painful for him, when we wrote the report on the Electre experiment. I consider him to be the "English translator" of this thesis!

I would like to express sincere thanks to DASSAULT Aviation (especially to Cécile GIRAUD), and to the "Ministère des Affaires Etrangères" for their trust and financial support, without which I could simply not have been here.

And I would also like to thank all those who supported me during these years and beyond, in one way or an other, here or abroad, all my Friends (French-speaking or not!), especially Laure, Christèle, Muriel & Flavio, my Parents and my Family.

A very special "Merci" goes to my beloved Sabine, who has always encouraged me. She has made many efforts to share only the "better" with all her love, especially these last months, besides my grouchy temper!

Abstract

A pitot pressure survey of the contoured nozzle of the T5 shock tunnel was performed over a wide range of reservoir conditions and in the region of the exit plane of the nozzle. A rake of thirteen pitot probes was used for this purpose. The survey includes an investigation of the repeatability of the facility and an analysis of the accuracy of the measurements. The features of the pitot pressure distribution across the exit plane are a pronounced minimum near but not exactly on the centerline, and a pronounced drop near the nozzle wall. The concave profile may be quantified in terms of the curvature of the pitot pressure distribution, which increases markedly as the enthalpy is decreased and as the area ratio is increased. The normalized value of the minimum pitot pressure is found to be independent of the reservoir enthalpy, in contrast to the behavior obtained by numerical computation of inviscid flows. The results of this survey show clearly, that the use of a contoured nozzle should be restricted to conditions very close to the design condition. Since flexibility in the reservoir enthalpy and pressure, as well as area ratio, is an important feature of a shock tunnel, the results of this survey strongly suggest the use of a conical nozzle.

Contents

List of Figures

List of Tables

List of Symbols

Symbols related to Parameters

p_4	Burst Pressure
p_0	Nozzle Reservoir Pressure
v_S	Shock Speed
h_0	Reservoir Enthalpy, derived by $(v_S)^2$
p_t	Pitot Pressure
p_{min}	Minimum of the Pitot Pressure Distribution
a, "a"	Curvature of the Pitot Pressure Distribution

Symbols related to the Parabola

a, b, c	Coefficients of the Parabola
x	Coordinates for the Parabola
x_S	Coordinate of the Symmetry Axis

Indexes

avg	Average of North and South traces
N, S	North and South respectively

Abbreviations

ave	Average on different shots
dev	Deviation around the average 'ave'
#	Equivalent in %, for a deviation 'dev'
Cond	Condition
BL, EL	Boundary layer, External layer
FL	Core (Flow layer)

Initials related to T5

2R	Second Reservoir (High Pressure Air)
CT	Compression Tube
ST	Shock Tube
DT	Dump Tank

Calibration and Study of the Contoured Nozzle of the T5 Free - Piston Hypervelocity Shock Tunnel

Introduction

The free-piston shock tunnel is one of the facility types used for ground simulation of hypervelocity flows. One such shock tunnel, known as T5, was recently built at GALCIT. T5 is the last improvement in the series of Australian free-piston shock tunnels, known as Stalker's tubes, starting with the very small facility T1. T5 was brought into operation in December 1990. The transition from shake-down to routine operation took place in September 1991.

The state of the gas in the reservoir region of the nozzle in such a facility is typically at a pressure of 60 MPa and a specific enthalpy of 20 MJ/kg. In this state, the molecular species in air are partially dissociated, and they recombine partially during the cooling that accompanies the expansion in the nozzle. In other words, T5 allows to experimentally study flows up to orbital speed, involving real gas effects.

The nozzle currently in use on the T5 shock tunnel has the same shape as the nozzle designed for T4, with air as test gas, at a specific reservoir enthalpy of 25 MJ/kg. The design is based on the scheme that the upstream part, in which significant recombination occurs, is conical. Some distance downstream of the place where the recombination freezes, the mixture may be treated as a perfect gas to good accuracy, and the method of characteristics may be used without the complication of chemical reactions in order to design the contour for optimum exit-plane uniformity of the flow.

The nozzle was designed for a nominal area ratio around 100, with a throat diameter around 30 mm and an exit diameter of 314 mm. For a number of reasons, it is occasionally desirable to operate this nozzle off-design. This may be done by running the facility either at a different reservoir enthalpy, with a different test gas, or with a different nozzle throat diameter. The latter becomes necessary when the desired density is so low that it can not easily be achieved by lowering the reservoir pressure. This was the case, for example, in the recent experiments on the Electre model of ESTEC, most of which were run with a 20 mm diameter throat [Adam and Rousset, 1993].

A first calibration was performed by Rocketdyne at the beginning of the tunnel's routine operation. However, a more detailed calibration of the nozzle exit and a study of the shock tube proved to be necessary. Furthermore, the design of a second contoured nozzle was being considered. For these reasons, a careful pitot pressure calibration of the existing nozzle was conducted, to be compared with the calculations of the program SURF (SUpersonic Reacting Flow) written by Rein [1989], the program which was going to be used for the new design.

In fact, the present work was more than a pitot pressure calibration. It was a general study of the dependence of the pitot pressure distribution in the nozzle exit plane, on various shock tube parameters, for different test gases, and with two nozzle area ratios. Special emphasis was placed on the calibration in the off-design conditions of the T5 contoured nozzle with the 20 mm diameter throat with air and nitrogen as test gas. However, the flow with other test gases (carbon dioxide and hydrogen), and with the design throat diameter (30 mm) were also examined. The measured pitot pressure distribution was

compared with that obtained by numerical computation based on the measured initial shock tube conditions, shock speed, and reservoir pressure.

The layout of the thesis follows the sequence of the tests performed, because the findings of each test series influenced decisions about the next steps.

After getting familiar with the facility and the type of conditions occurring in the test section, a pitot rake was specially designed and instrumented for this project (Section 1). Then, an extensive study was made of different methods of data reduction of the general test parameters from the raw traces (Section 2). Before the calibration study, the repeatability was checked at a particular tunnel condition (Section 3). The calibration of the T5 nozzle was investigated, first with the 20mm throat (Section 4), then with the 30mm throat, with air as the test gas (Section 5). Flows with other test gases, N_2, CO_2 and H_2, were also investigated, both with the 20mm and the 30mm throats (Section 6). Finally, some of the experimental results were compared with computations using the reacting nozzle flow program SURF (Section 7).

SECTION 1 :

Experimental Facility

and Apparatus

1.1. The T5 Hypervelocity Shock Tunnel Facility

The T5 Hypervelocity Shock Tunnel

The term "hypervelocity" is more restrictive than the general "hypersonic" notion. The latter means only that the velocity of the flow relative to a body is several times higher than the speed of sound - conventionally a Mach number M higher than 5. However, hypervelocity implies not only that this ratio M is large, but also that the velocity itself and therefore the stagnation enthalpy is high enough to generate deviations from perfect-gas behavior, such as vibrational excitation and dissociation of gas molecules.

Free-piston shock tunnels, such as T5, are capable of generating these very high enthalpy flows at high densities (Figure 1.1). These facilities are therefore well suited to simulating the chemical nonequilibrium effects that occur during the reentry of vehicles through planetary atmospheres, such as the Space Shuttle (USA), and conceptual vehicles like NASP (USA), HERMES (Europe) or HOPE (Japan).

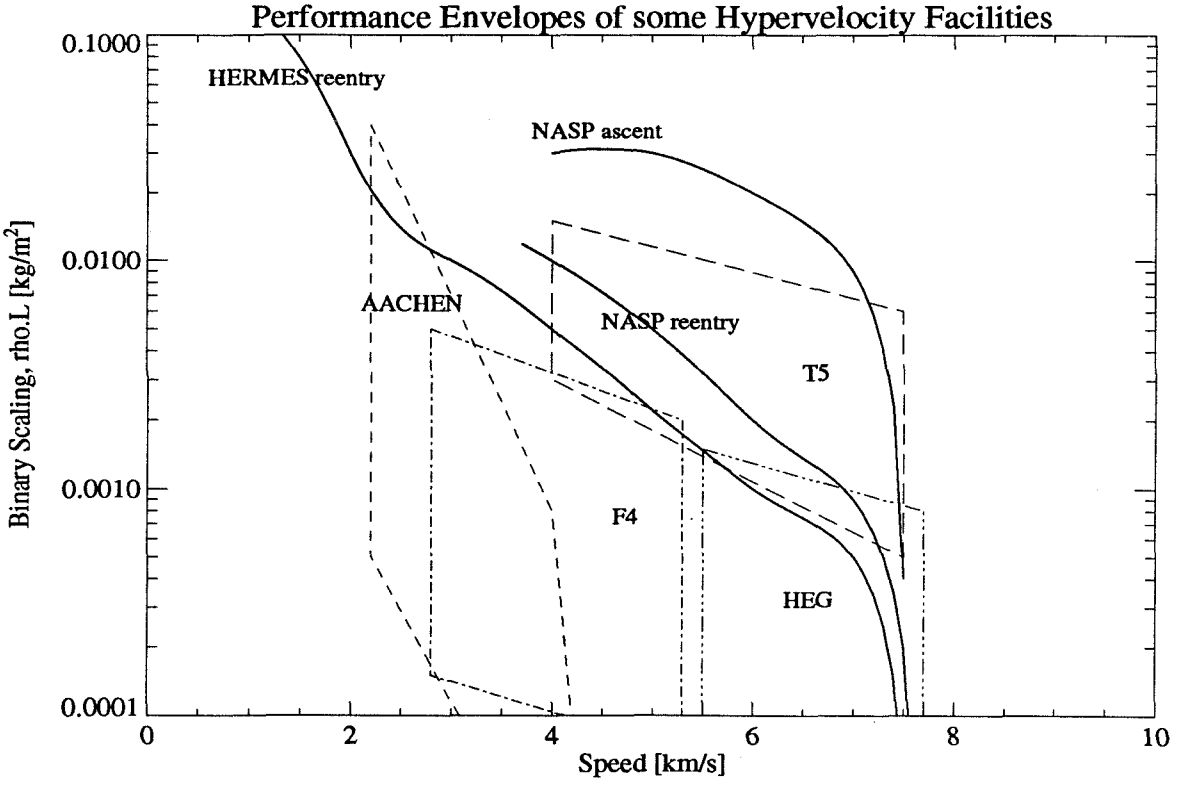

Figure 1.1. Performance Envelopes of some Hypervelocity Facilities, and some Vehicles Trajectories.

A Typical T5 Run

A typical T5 shot reflects the general free-piston technique (Hornung, 1992).

High pressure compressed air (typically 8 MPa) is released from a secondary reservoir (2R), thus pushing a reusable 120 kg piston down the compression tube (CT). The monatomic driver gas - usually a He/Ar mixture - in front of the accelerating piston, is compressed to about 1/50 of its original volume, reaching a temperature of about 4000 K, a speed of sound of 3700 m/s (for pure Helium), and a desired pressure p_4 determined by the diaphragm burst pressure (typically 90 MPa). When the diaphragm bursts, a shock wave is created in the test gas contained in the shock tube (ST), and travels at about $v_s = 4$ km/s. Once the shock reaches the end of the ST, it is reflected and stops the flow. In that region, the test gas reaches the "stagnation" conditions, namely a temperature of about 8000 K and a pressure p_0 (60 MPa) (called "nozzle reservoir pressure") somewhat lower than the burst pressure. The gas is then expanded through a contoured nozzle with an usual area ratio of 100 into the test section.

As the piston accelerates along the CT, there is a shift in center of mass which is compensated by a recoil of the CT, shock tube (ST), and the attached nozzle. The secondary air reservoir (2R) recoils in the opposite direction under the action of the thrust of the outflowing air which drives the piston down the CT. The test section and dump tank (DT) remain stationary.

A sketch of T5 detailing these major parts is shown in Figure 1.2 .

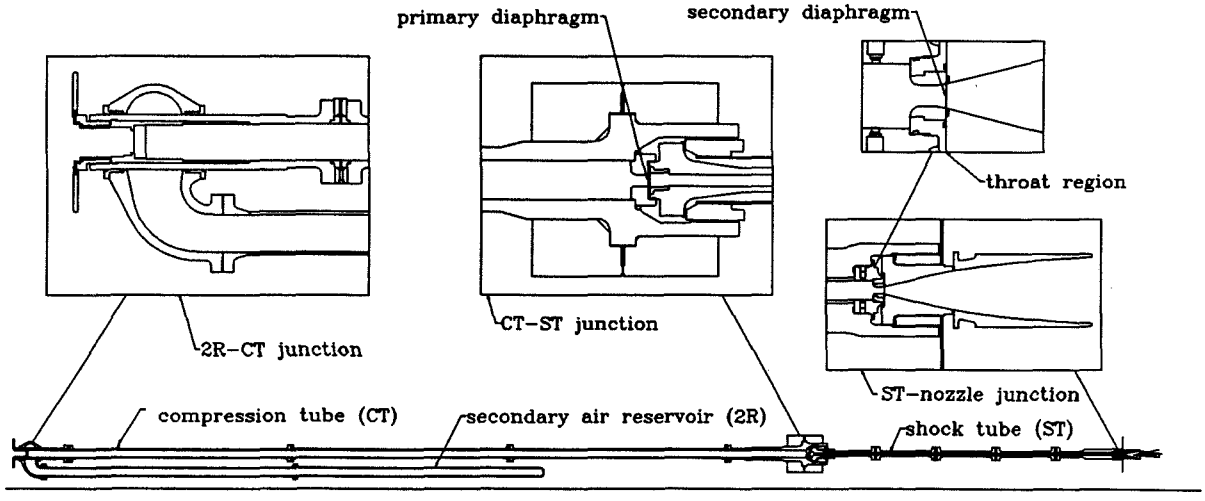

Figure 1.2. Sketch of the T5 Hypervelocity Shock Tunnel

T5 Performance Envelope

In typical T5 shots, the burst pressure (p_4) ranges from 30 MPa to 120 MPa depending on the diaphragm and its indentation. The nozzle reservoir pressure (p_0) can be made to vary from 13 MPa to 80 MPa, and the enthalpy (h_0) from 3 MJ/kg to 25 MJ/kg, depending on the conditions. The CT-ST-Nozzle recoil is about 8 cm.

Throats of different diameters (14 mm, 20 mm, 30 mm) are available for operation with different area ratios (450, 225, 100), in order to match other parameters such as the density. They are made of molybdenum, in order to sustain a heat flux of about 1 GW/m^2 without melting. The standard throat, for which the contoured nozzle is designed, is 30 mm in diameter. The exact nozzle exit diameter is 314 mm.

While the typical recording time (for the test section) is of the order of 20 ms, the useful "steady" window is about 1 ms, depending strongly on the specific enthalpy.

One can use many different test gases, such as Air, N_2, CO_2, and even H_2 or Ar.

Further information on T5 can be found in Hornung [1990, 1992], Bélanger [1993], Germain [1994]

1.2. The R13 Pitot Pressure Rake

The R13 Pitot Rake [General Requirements]

A pitot pressure rake has been designed specifically for the present calibration tests (Figure 1.3.). Among the requirements were many conflicts, such as adjustability and strength, maximum coverage of the exit and cost, sensitivity of the transducers and robustness to sustain the severe test section conditions. It happened that the best configuration (over cost) required 13 pitot pressure transducers, hence the name "R13". Three view drawings of R13 are shown in appendix 1.

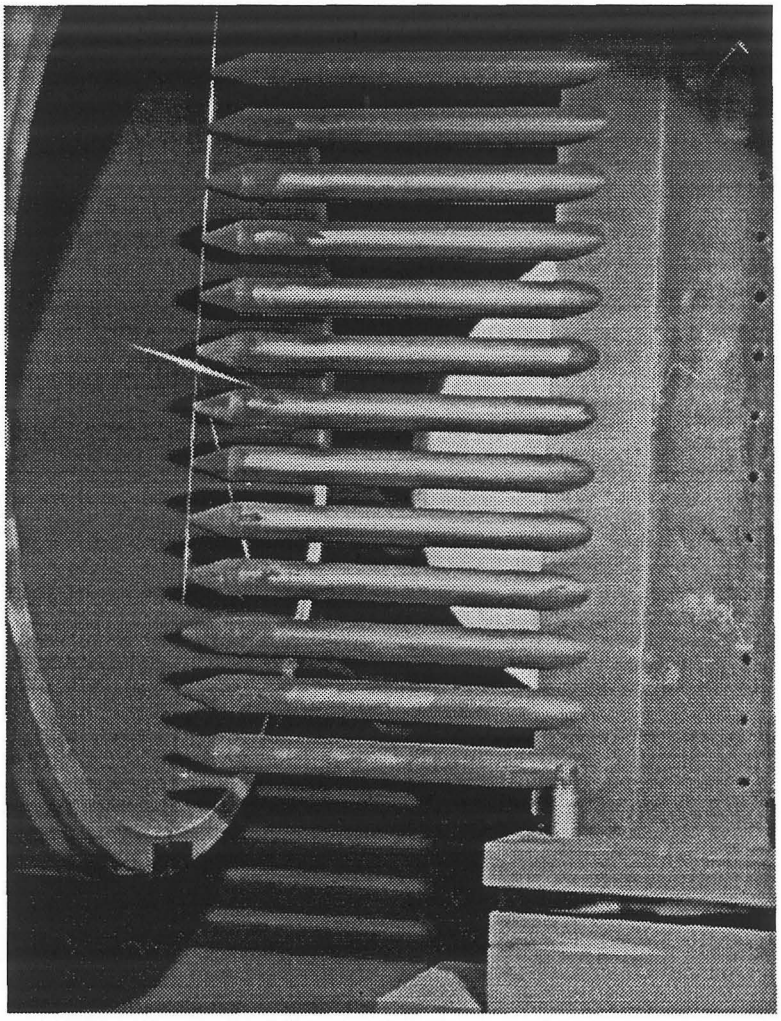

Figure 1.3.
Photo of the
R13 Pitot Rake.

The rake can translate along the 3 principal axes: along the nozzle axis, laterally in the exit plane (horizontally), and along the vertical diameter. While the lateral axis is adjusted only once (per series) to position the rake in the vertical diameter plane, the two other degrees of motion were used, one to calibrate the nozzle upstream and downstream of the exact exit plane (adjustment along the nozzle axis), and the other one to obtain more densely spaced measurements with intermediate points with the help of spacers.

Positioning in the Test Section

The reference and axes orientation are shown on figure 1.4.

The 13 pitot pressure transducers are equally spaced by 3/4 in (1.905 cm), and the actual vertical resolution (using different shots and spacers) is 3/8 in(0.9525cm).

A careful measurement of the geometric center of the nozzle (at the exit plane) with respect to the rake, has been conducted several times, before and after the series of shots. A correction (vertical) distance was therefore introduced in the plotting programs. This distance, which is the difference between the theoretical center (expected to locate on one specific tip) and the measured one, appears to be 0.25 in(0.635 cm).

The longitudinal positioning is adjusted by fixing the rake onto the two rails at the bottom of the test section, and blocking the final position of the DT with respect to the ST, and thus the nozzle. In general, the rake was placed at the level of the optical windows, similarly to the other models. The final DT position was then set every 2 cm.

The horizontal positioning is made possible by a transverse support plate. The alignment associated with the center was adjusted only using rulers.

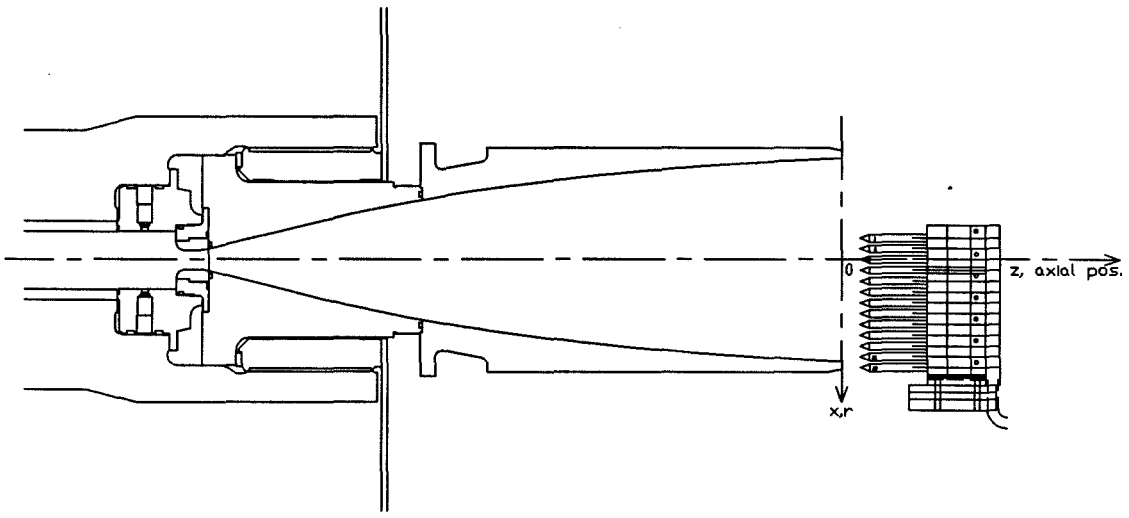

Figure 1.4. Axes Convention associated with the R13 Rake

Instrumentation

All 13 transducers are from PCB Piezotronics. They are low impedance piezoelectric quartz dynamic pressure transducers. Model 113A26 was chosen in the 113A20 series with built-in amplifier, because of its specifications such as range, maximum pressure, resolution, rise time, and maximum temperature (see appendix 1).

The calibration values used in the data reduction programs, are the ones given directly by the manufacturer. The consistency of these calibrations was tested by interchanging transducers in repeat shots. This does not provide an absolute calibration, of course, but it is easy to note when a calibration is not valid any more for a given transducer.

1.3 The DAS : Data Acquisition System

The data acquisition system consists of several CAMAC Analog/Digital converter channels (by DSP Technology), digitizers, PCB power supplies for pressure transducers, and amplifiers for thermocouples, all controlled by software run on a Sun SPARCstation computer. Data are first stored during the test in transient recorders before being down-loaded to the computer's hard drive. Trigger generators, threshold detectors and counters are also used to determine the beginning of the sampling time, the speed of the shock down the ST and to synchronize the flow visualization equipment.

All the channels are triggered at the exact same time. While different sampling rates and pre-trigger lengths are applied to record the different traces, it is important to note that the nozzle reservoir pressure and the pitot pressure traces are recorded on the same box set, each channel having a 4k bytes length, 1/8 pre-trigger, and sampling rate of 200 kHz.

Photographs can be taken with a 4in x 5in camera on black and white film. The test section is illuminated by a pulsed laser and the image focused by a series of filters, lenses and mirrors on the photographic plate. Finite and infinite fringe differential interferometry is usually the technique of choice to visualize the flow.

SECTION 2 :

Test Parameter Traces

and Data Reduction,

"from Traces to Data"

2. Test Parameter Traces and Data Reduction

The principal parameters measured in T5 are the burst pressure p_4, the nozzle reservoir pressure p_0, the shock speed v_s, and the CT-ST-nozzle recoil. A good first approximation of the reservoir enthalpy h_0 is given by the square of the shock speed v_s.

2.1. The Burst Pressure p_4

The burst pressure p_4 is derived from the two p_4 traces, North and South, taken by two PCB transducers, sampling every 32 μs (Figure 2.1.1).

It is estimated that the diaphragm takes around 0.2 ms to open completely [Brouillette, 1991]. Thus, in order to get a reasonable value, and to remove the high frequency noise, the traces are smoothed out over 15 points, i.e. every point is averaged with the 7 previous ones and the 7 next ones. This is equivalent to a time window of 0.480 ms.

The maxima of these two smoothed traces are then taken and averaged together to get $p_{4,avg}$ (Figure 2.1.2).

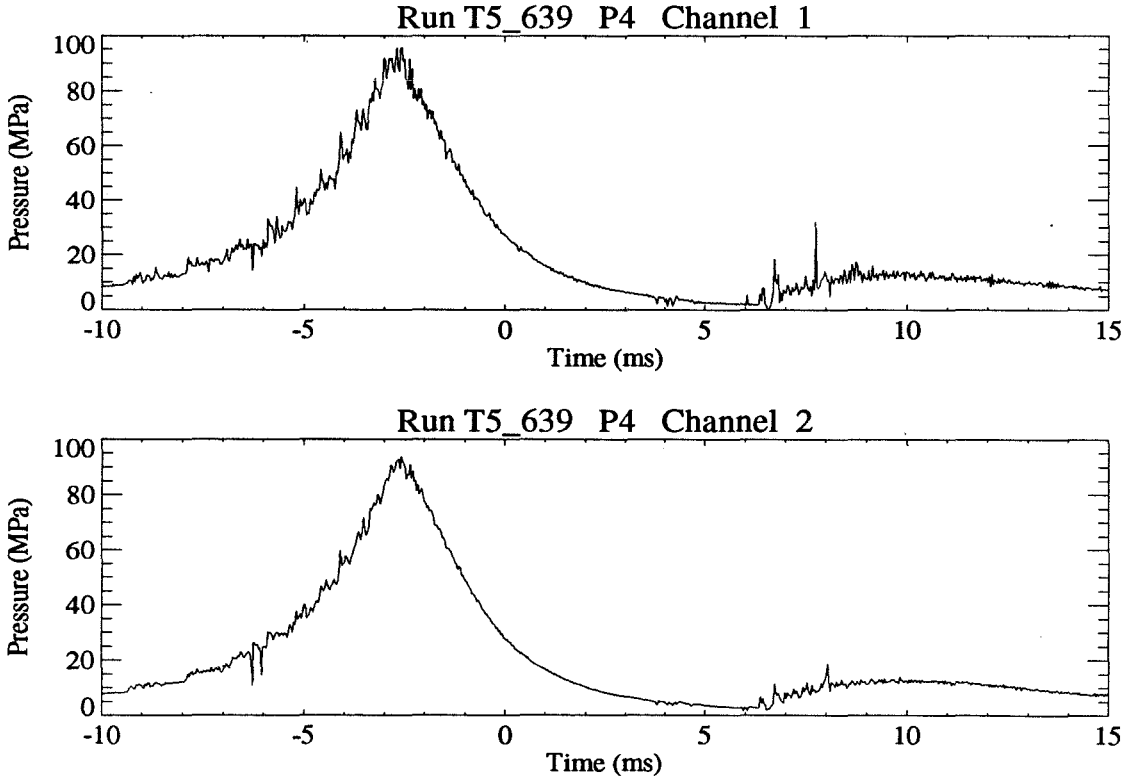

Figure 2.1.1. Example of p_4 Traces (Long Time Range).

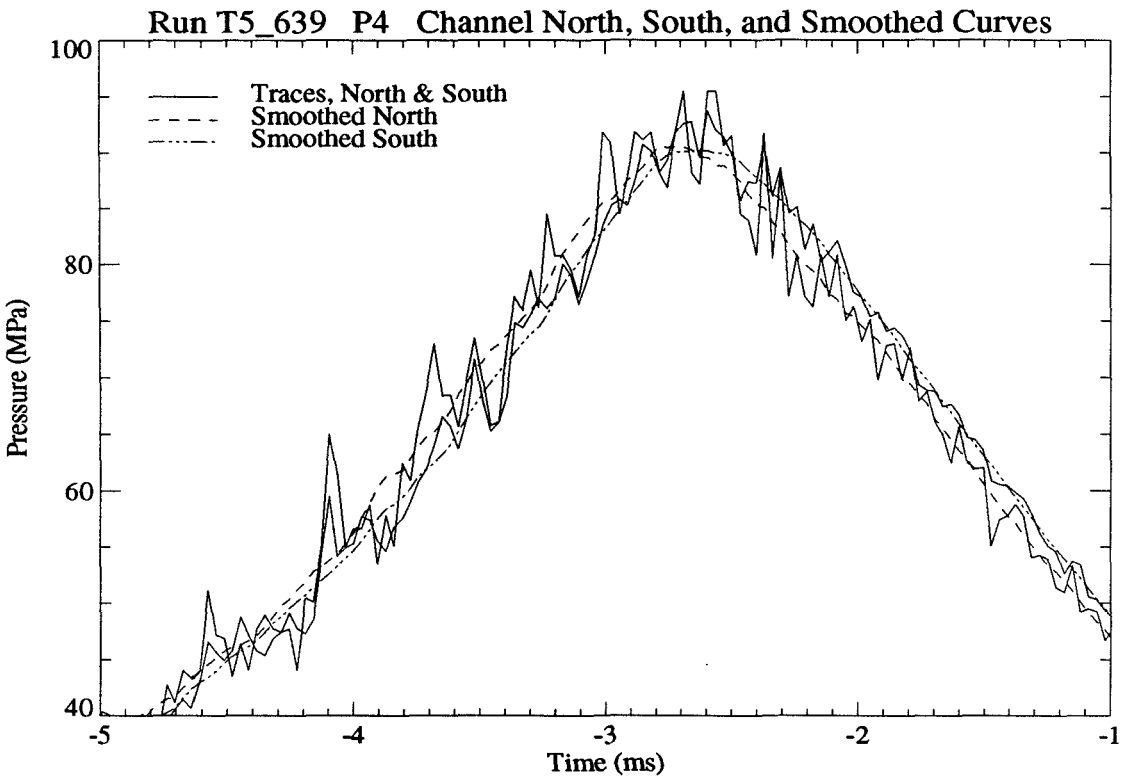

Figure 2.1.2. Example of Determination of p_4 (Short Time Range around the Burst).

2.2. The Nozzle Reservoir Pressure p_0

The nozzle reservoir pressure p_0 is also evaluated from two traces, North and South, taken by PCB transducers, but this time sampled at 200 kHz (same sampling rate as the test section data) (Figure 2.2.1).

The traces are smoothed out over 19 points to remove the high frequency noise - the time window is 0.090 ms. Then, time windows for the overshoot, the steady period, and the decreasing period, are visually established for a given condition and remain the same for all runs of a given enthalpy.

Averages are then taken over the entire steady period (Figure 2.2.2). Usually, this period lasts around 1 ms for low enthalpy runs, to 0.5 ms for high enthalpy ones. Once again, the two averages (North and South) are averaged together to get $p_{0,avg}$.

Note that the "0" trigger time is at shock reflection.

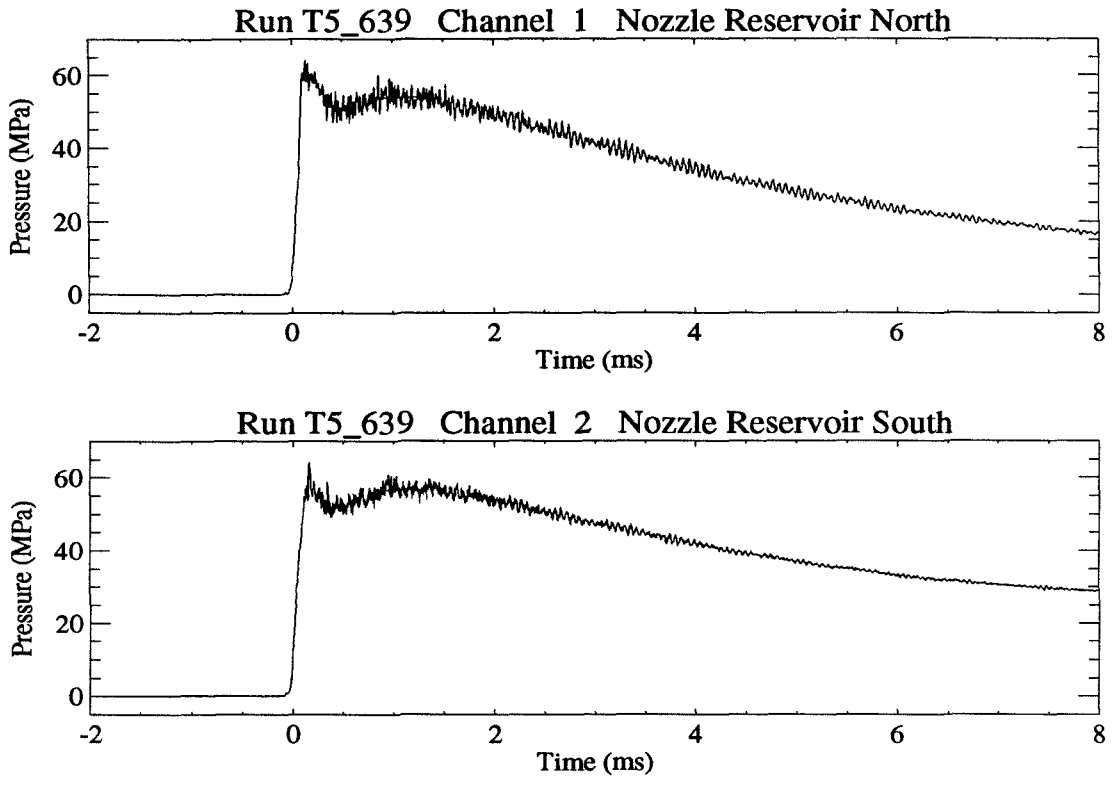

Figure 2.2.1. Example of p_0 Traces.

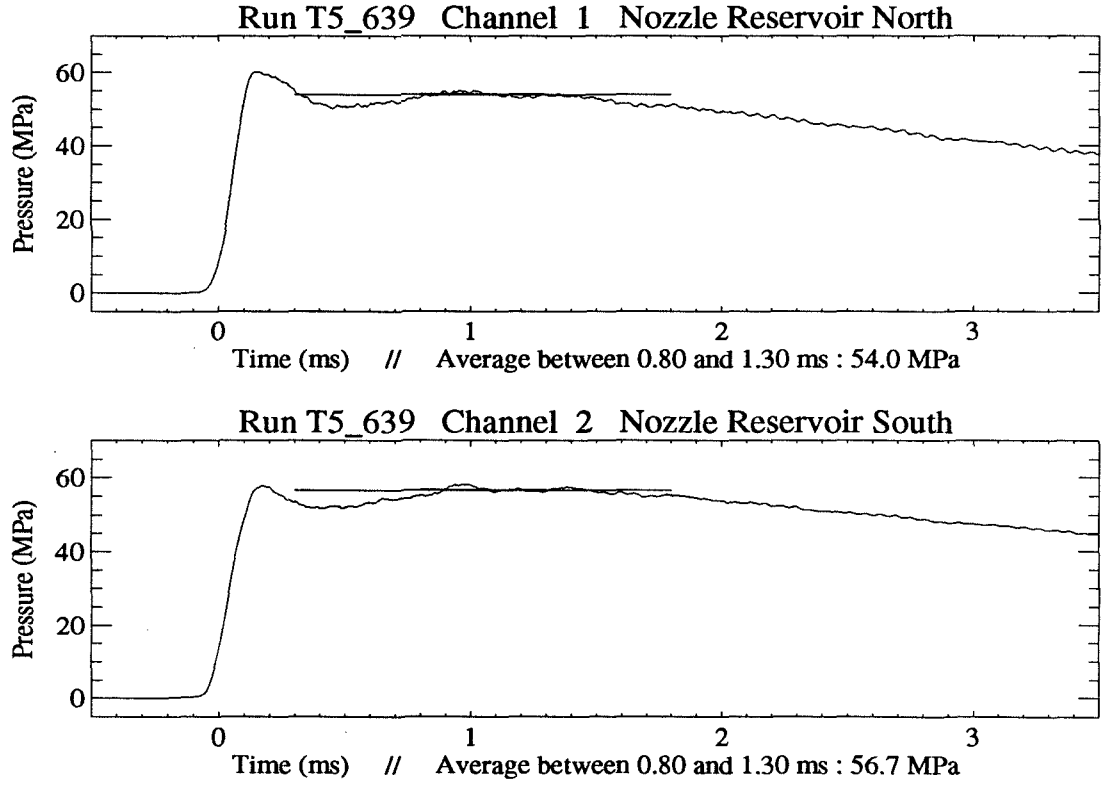

Figure 2.2.2. Example of Determination of p_0.

2.3. The Shock Speed v_s

The shock speed v_s is derived from four traces, given by three PCBs placed along the ST, and one nozzle reservoir pressure trace.

The shock is caught by the sudden rise in the pressure and the time is recorded. Note that the trigger is exactly the same for all the traces because it is given by the same box. Knowing the exact distance between the transducers, three speeds are derived.

Only the middle one is used as a parameter, corresponding to the averaged shock speed along the ST. The slowing down of the shock is mainly due to friction [see Bélanger, 1994].

The specific reservoir enthalpy h_0 is then approximated by the square of that shock speed (for Air and N_2 shots). That approximation matches the ESTC (Equilibrium Shock Tube Calculation) results within a few percents.

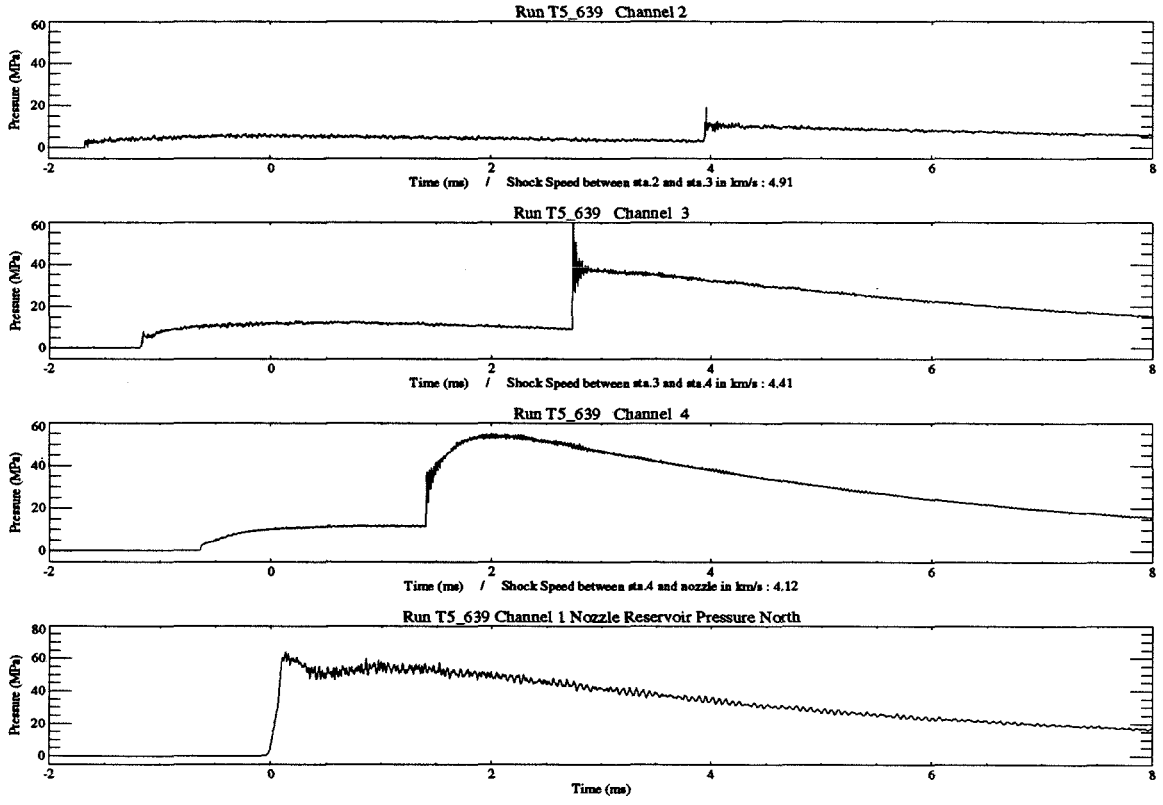

Figure 2.3. Example of Traces used for the Shock Speed.

2.4. The CT - ST - Nozzle Recoil

The CT recoil (which is also the ST and Nozzle recoil) is given by an LVDT. The value is read directly on the trace, just after 0 ms. Knowing the recoil is important as it gives the position of the nozzle exit with respect to the stationary test section during the actual shot.

Also the 2R recoil is obtained from the CT and differential recoil. The latter is recorded in order to evaluate the stress held by the launch manifold, where the compressed air is transferred from the 2R to the back of the CT in order to accelerate the piston.

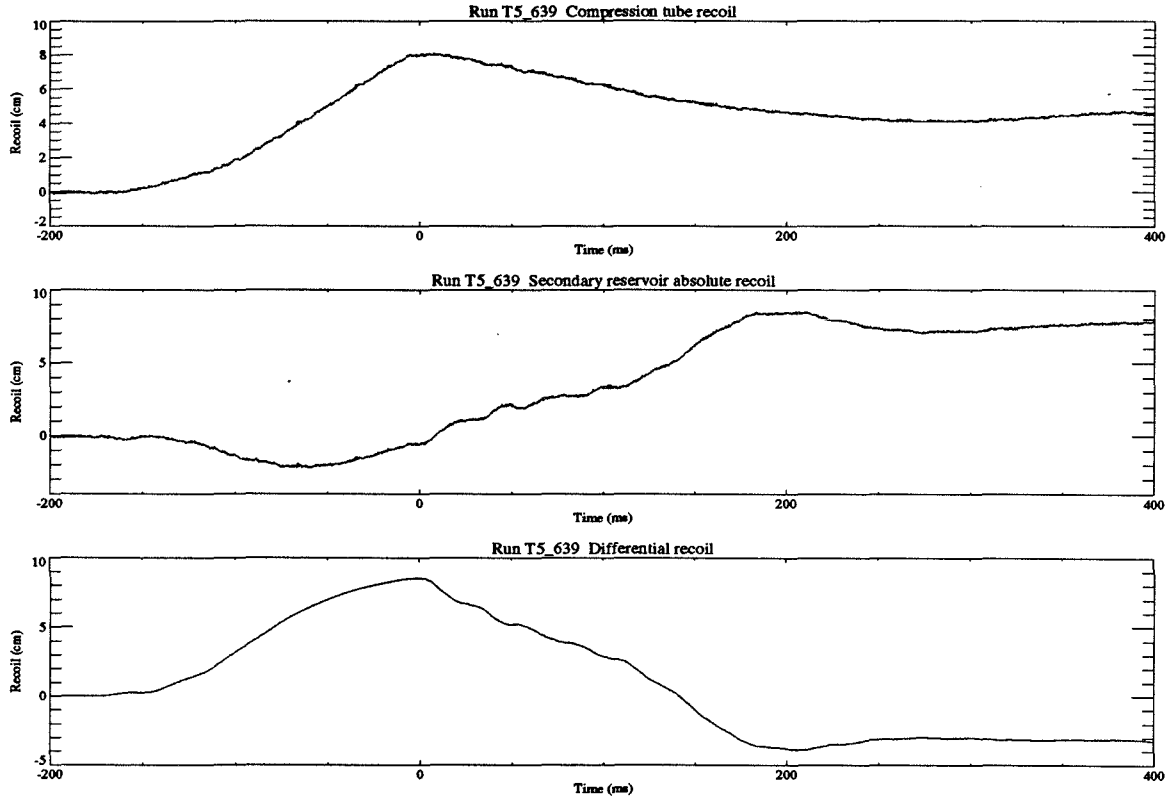

Figure 2.4. Example of Recoil Traces.

2.5. The Pitot Pressure Distribution

In order to calibrate the present T5 contoured nozzle, the pitot pressure distribution along the vertical diameter was measured with the R13 rake in the test section, at the exit plane to compare with SURF calculations, and also further downstream where the models are usually tested. The techniques to extract averages from the original traces, and then calibration parameters from these averages are described in the present chapter.

2.5.1. Visualizing the Traces

Several ways have been investigated in order to visualize and extract data - and then meaningful parameters - from the 13 simultaneous traces recorded on the R13 rake. These different attempts respond to the quest for a pitot pressure "plateau", i.e. a region of constant pressure. In this region, the flow is approximately steady along the radius and during a certain time. 3D plots, contour plots, and movies, not only give spectacular visualizations, but also help in localizing this steady plateau, the arriving shock, the pressure decrease period, and the variation along the radius down to the boundary layer. Some examples of these visualizations are shown in appendix 2.

The most useful method remains the "traditional" one, i.e. getting an average on that steady period for every trace (figure 2.5.1).

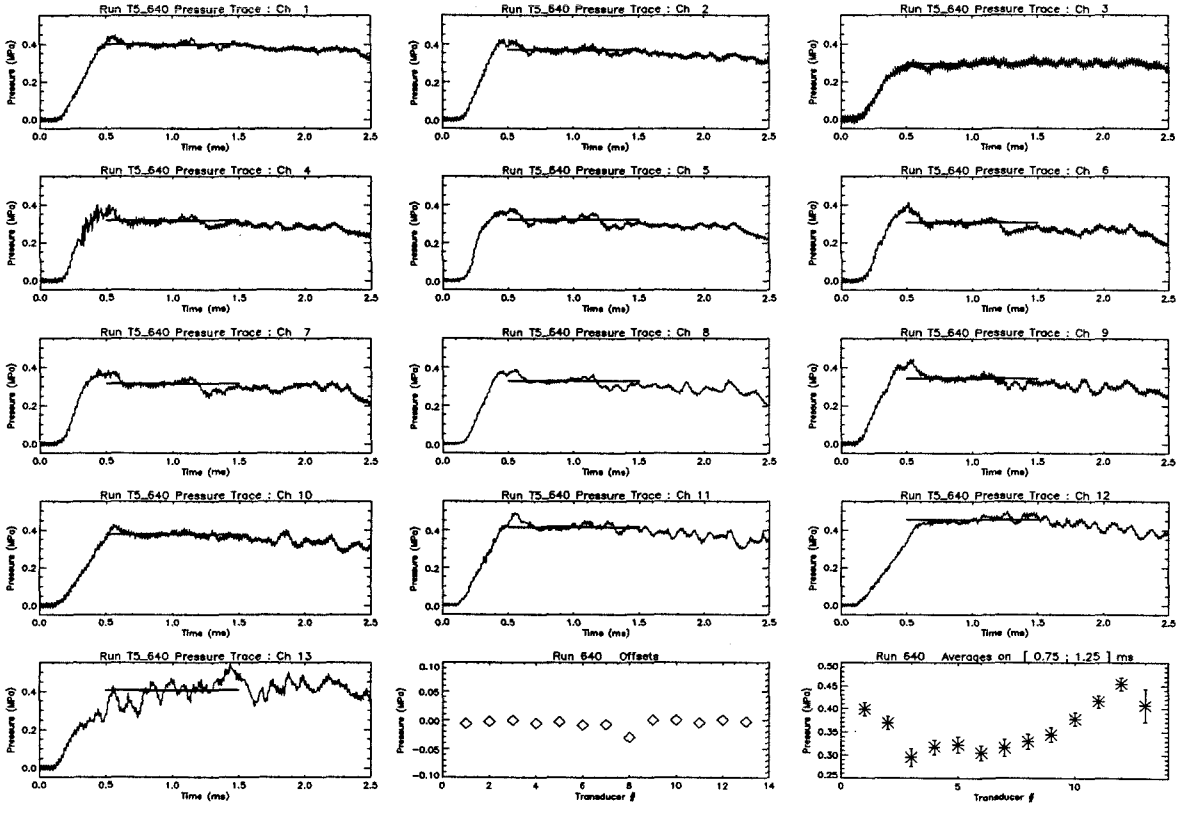

Figure 2.5.1. Example of Pitot Pressure Traces.

2.5.2. Extraction of Data from 13 Traces

The technique used to extract the averages from the traces is similar to the one for the burst pressure and the nozzle reservoir pressure. On one hand, it is simpler here since there is only one trace giving the averaged value. But on the other hand, 13 traces have to be taken into account at the same time.

In general, the time range for taking the average is determined by the steady period defined as for the nozzle reservoir pressure. In fact the traces look very similar to the nozzle reservoir pressure traces, with some more fluctuations. This range usually lasts the same time for both types of traces. Usually, the range for the pitot pressures starts 0.1 ms to 0.2 ms after the nozzle reservoir pressure ones, depending on the enthalpy. At high enthalpy, there is almost no delay. Note that the sampling frequency is the same, i.e. 200 kHz, and the trigger is still zero.

Concerning the error made on one pitot pressure value, it is due essentially to two factors : the high frequency and electric noise, and the fluctuations during the steady period. The noise is of the order of (the equivalent of) 0.02 MPa, but can be easily removed by smoothing the trace. Then there remains an error margin during the steady period, ranging on the average from 0.02 to 0.05 MPa, due to oscillations since there is no true "steady period" and due to the uncertainty on the time range too.

The high frequency and electric noise is therefore removed by smoothing the traces on 15 points (equivalent to 0.07 ms). The offsets are corrected for each trace, every shot.

2.5.3. Correction and Parabola Fit

The position of each transducer is derived carefully, taking into account the number and size of spacers, and the geometric center correction. Then these 13 averages are plotted versus their position along the vertical diameter of the exit plane -or a plane similar to that one downstream or upstream. Obviously (see figure 2.5.2) the distribution along the radius is not as uniform as expected; instead, it has the shape of a parabola in the core region.

So, when a point is thought to be "wrong" -usually really low and noisy compared to its neighbors-, it is replaced by the average of these two neighbors. When two successive points are thought to be "wrong", the substitution is made by a weighted average of the two surrounding points (linear correction). A point is considered to be "wrong", when its trace shows some electrical problems, but also, for some points near the centerline, when the flow perturbations are too important - this was the case for some 20mm runs. One must not forget that these "replaced" points have no physical meaning but are just useful in order to get a consistent parabola fit (equally spaced points everytime, same balance for a given distribution).

The experimental points and these "corrected" ones (in fact, only the points within the core) are then fitted by a parabola (second order polynomial), with the 3 coefficients free. This kind of fit was used instead of the general [average & standard deviation]

derivation, because of several considerations.

The [average & standard deviation] derivation assumes that the curve is relatively flat and centered around a constant value. Obviously here, it gives the average pressure across the exit diameter, and the deviation with respect to that average. Actually, these are not parameters of first interest because a model does not occupy the whole exit disk, but only the region near the centerline. On the other hand, the parabola fit gives the minimum pressure on the centerline, and a better understanding of the deviation of that value along the diameter, by its second derivative, called hereafter "curvature"*. This latter technique also brings out information on the symmetry of the flow.

In fact, the parabola fit appears to be the simplest technique, giving 3 essential flow parameters (value at the center, deviation from this value, and symmetry), from 3 free coefficients.

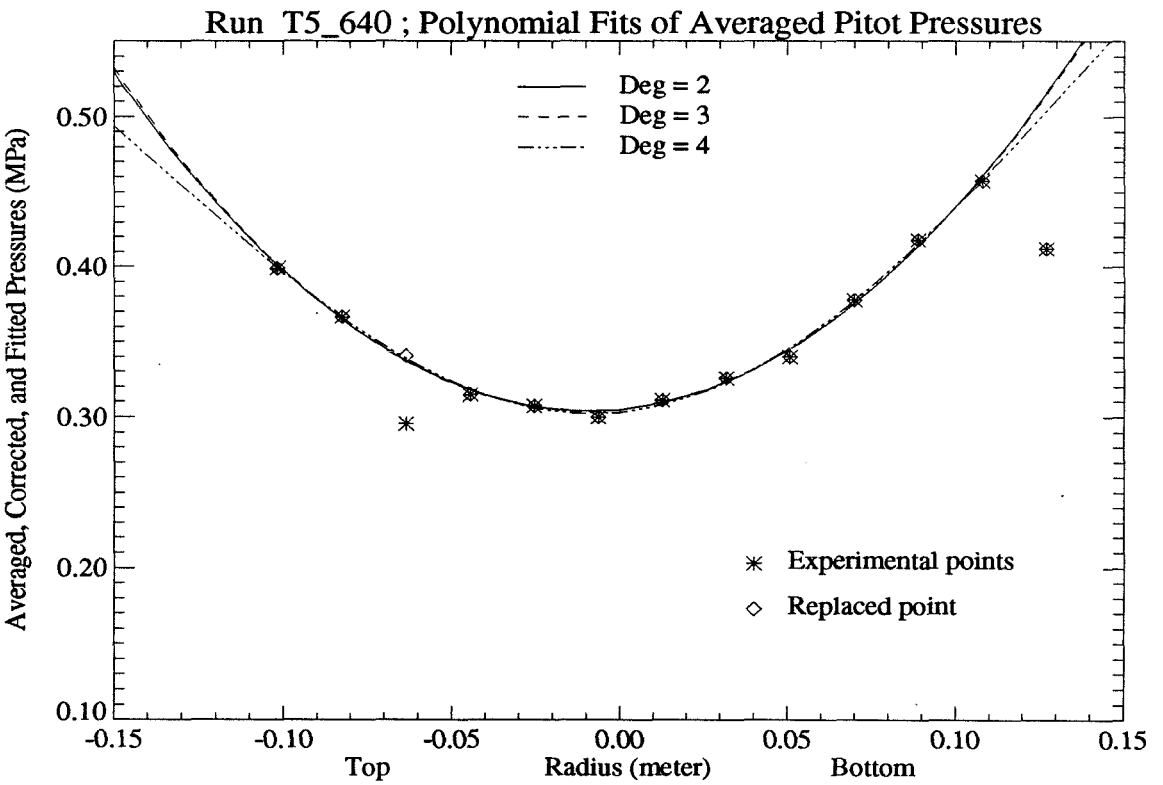

Figure 2.5.2. Example of Parabola Fit.

* This is not the mathematical definition of the curvature of a function, but it can be easily derived that the curvature of a parabola, for x near the symmetry axis, in that new translated coordinates ($X = 0$ on that axis), is in a first approximation the second derivative.

SECTION 3 :

Repeatability of Test Conditions,

Based on One Given Condition :

High_Enthalpy - Medium_Pressure,

20mm Throat - Area Ratio of 225

3.1. Description of the Repeated Shots

During the fall of 1993, a series of 19 shots was conducted in T5, focusing on one specific condition, to be then compared with SURF* calculations.

The main concerns in this calibration have been, on one hand, to check T5 repeatability, especially as far as the SURF parameters are concerned, and on the other hand, to develop a new method to get a good estimate (value and error) of the center pressure at the exit plane, and a good measure of the variation of that pressure along a radius.

The chosen condition is one of the most commonly used ones in T5, called "High Enthalpy - Medium Pressure", namely h_0 =21 MJ/kg and p_0 =55 MPa. Originally, the condition was to be tested only with air and an area ratio of 225 (nozzle with the 20mm throat). Note : this is an off-design condition for the contoured nozzle. The design area ratio is 100.

First, 4 runs (627 to 630) were made to find the optimum tailored-interface condition, but are not taken into account in this study, since they are slightly off the repeated condition. Furthermore, the ST copper sleeve (just upstream of the throat) had to be replaced after its melting during the shot 629.
Next, 13 runs (631 to 643) were fired at this specific condition, 10 times with air, and 3 times with N_2, giving enough data to check the T5 repeatability and to run both the ESTC and SURF programs. These repeated shots also gave a good range of the calibration parameters, such as the center pressure at the nozzle exit plane, the deviation of that pressure along the radius, the quality of the axisymmetry, and even the thickness of the boundary layer.
Finally, 2 runs (644 and 646) were fired with the 30mm diameter throat, for the sake of comparison. Both air and N_2 were used as test gases.

In this following section, only the 13 repeated shots (631 to 643) are presented. However, some references to the first 4 preliminary shots (627 to 630), and the 2 last ones with the 30mm throat (644 and 646) may appear for the sake of comparison. First are presented the parameters related to T5 as well as the study of the repeatability of the condition. Then follows the study of the parameters related to the calibration of the nozzle.

The detailed log of this whole series of shots is given in appendix 3.

---

* SURF : SUpersonic Reacting Flow, [Rein, 1989]

3.2. T5 Repeatability

Repeatability of an experiment is obviously always a main concern. This series of shots made it possible to check the repeatability of the T5 facility. It was even more important for this calibration, since one needs a quite good estimate (value and error range) for the basic T5 parameters, such as the nozzle reservoir pressure and the shock speed, in order to make non-dimensional ratios meaningful and to get reliable inputs for ESTC and SURF programs.

3.2.1. T5 Measurements, Data and Parameters

All the T5 parameters, for shots 631 to 643, are given in table 3.1. Explanations on the derivations and notations can be found in section 2.

	Burst Pressure (MPa)				Nozzle Res. Pres. (MPa)				(km/s)	(MJ/kg)	Test
Shot	$P_{4,N}$	$P_{4,S}$	$P_{4,avg}$	%	$P_{0,N}$	$P_{0,S}$	$P_{0,avg}$	%	V_s	h_0	Gas
631	91.6	89.3	**90.5**	1.2	51.6	48.7	**50.2**	2.9	4.44	19.8	Air
632	91.4	89.9	**90.7**	0.9	53.9	51.2	**52.5**	2.5	4.44	19.8	Air
633	94.2	91.9	**93.0**	1.2	54.2	51.9	**53.0**	2.1	4.47	20.1	Air
634	89.8	89.8	**89.8**	-0.0	54.3	51.9	**53.1**	2.3	4.35	18.9	Air
635	88.2	86.4	**87.3**	1.0	49.7	46.9	**48.3**	2.9	4.29	18.4	Air
636	84.5	82.8	**83.7**	1.0	53.4	52.0	**52.7**	1.3	4.48	20.1	Air
637	90.8	90.8	**90.8**	-0.0	54.8	54.3	**54.6**	0.5	4.44	19.8	Air
638	88.6	87.6	**88.1**	0.6	54.5	54.6	**54.6**	-0.1	4.38	19.2	Air
639	90.5	90.2	**90.4**	0.2	54.0	56.7	**55.3**	-2.4	4.41	19.5	Air
640	92.2	90.3	**91.3**	1.1	52.5	52.4	**52.5**	0.1	4.51	20.4	N_2
641	89.7	87.9	**88.8**	1.0	50.1	51.3	**50.7**	-1.2	4.48	20.1	Air
642	92.4	91.2	**91.8**	0.6	53.3	(48.6)	**52.5**	(4.6)	4.58	21.0	N_2
643	83.8	82.4	**83.1**	0.9	55.5	(29.6)	**55.5**	(30.4)	4.65	21.6	N_2

Table 3.1 - T5 Parameters (Shots 631-643)

Notation : "%" $= \frac{P_{4,N}-P_{4,S}}{P_{4,N}+P_{4,S}} * 100$, for P_4; idem for P_0.

Recall : h_0 is taken in a first appoximation as v_s^2.

A study of each of these T5 parameters was conducted for this series of repeat shots, deriving averages and standard deviations for the burst pressure, nozzle reservoir pressure, total enthalpy and shock speed.

3.2.2. The Burst Pressure

The averaged burst pressure $p_{4,avg}$ (hereafter abbreviated p_4) is plotted for every shot on Figure 3.1. These values depend a lot on the diaphragm, and the cross indentation in it. However, thanks to a careful calibration of these diaphragms, the standard deviation is quite low : less than 5% for the whole series. By omitting the last shot (643), whose diaphragm was from a new batch and not yet calibrated, the deviation is less than 3%.

The error made on the averaged burst pressure $p_{4,avg}$ on a given shot is mainly due to the high frequency noise and oscillations due to expansion-compression reflected shocks into the CT. But once corrected by smoothing the North and South traces, there remains only a small difference between the two channels on the order of 1% (example in section 2). The noise and oscillations around the burst pressure are of the order of 10%. On figure 3.1, the error bars go between the north and south values.

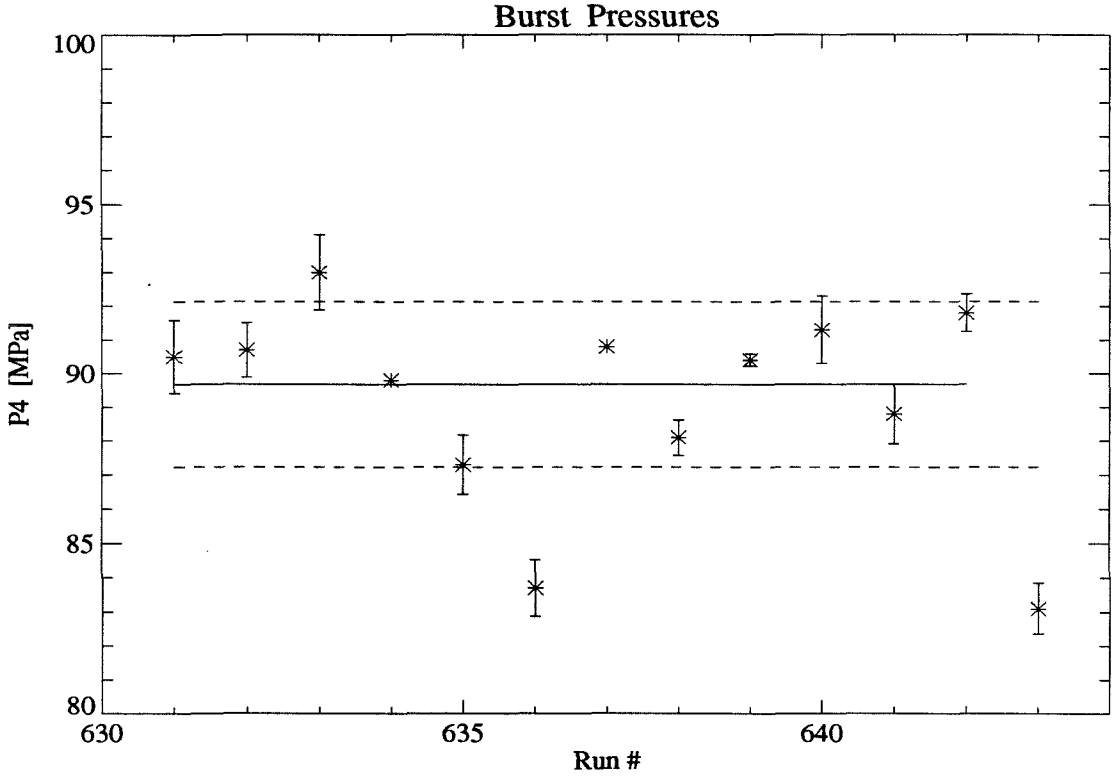

Figure 3.1. Burst Pressures p_4 vs Runs.

Following are the main results of that study :

Shots Range	P_4 Average	Standard Dev.
[631 : 642]	89.7 MPa	± 2.5 MPa # 2.7%
[631 : 643]	89.2 MPa	± 3.0 MPa # 3.3%

Note that all the shots can be used for that parameter with no distinction, since the burst pressure should depend only on the diaphragm.

3.2.3. The Nozzle Reservoir Pressure

The same procedure was followed for the nozzle reservoir pressure, even more carefully, studying also both $p_{0,North}$ and $p_{0,South}$ (See Figure 3.2). A systematic error appears between North and the South of 2% on the average, reaching sometimes 3%. Each channel has a standard deviation around 5%, implying a 5% deviation on $p_{0,ave}$. Again, noise and oscillations imply an error around 10%, but after smoothing, that error drops down to 1%, due essentially to the lack of precision on the time range of the steady period (example in section 2).

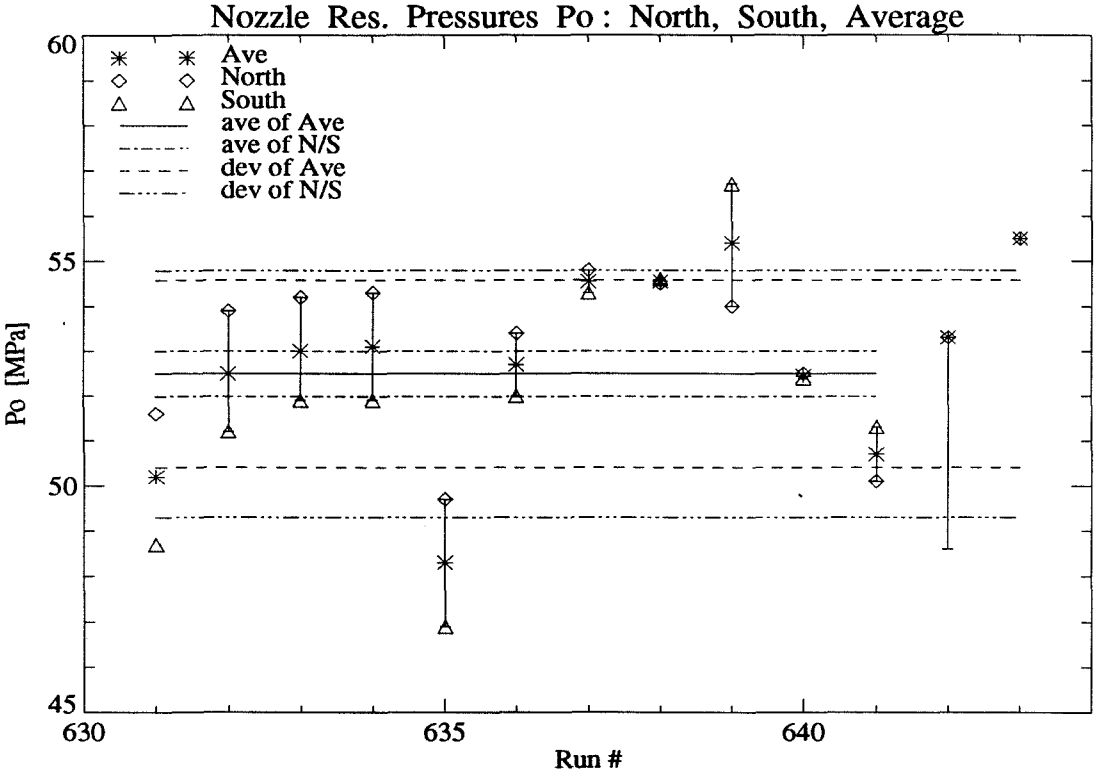

Figure 3.2. Nozzle Reservoir Pressures p_0 vs Runs.

Following are the main results ; averages and standard deviations are in MPa :

Shots Range	$P_{0,North}$ ave, dev, %	$P_{0,South}$ ave, dev, %	$P_{0,ave}$ ave, dev, %
[631 : 641]	53.0 ±1.8 # 3.5%	52.0 ±2.7 # 5.2%	52.5 ±2.1 # 4.0%

[631 : 641] are all the shots where both north and south traces are available. For the last shots (642, 643), only the north trace is used. Shot 635 remains low with no apparent explanation. Note also that there is no significant difference between air and N_2 tests, nor between 20mm and 30mm throat tests, even considering shots 644 and 646 (not shown).

Therefore, despite these non-negligible errors, but thanks to an adequate method, good repeatability is shown, and a good evaluation of $p_{0,ave}$ for this series of calibration shots appears to be 52.5 MPa ± 5%, i.e. roughly between 50 and 55 MPa.

3.2.4. Ratio of P_0/P_4

A first non-dimensional ratio, the "recovery factor" p_0/p_4, was studied, since the evaluation of the burst pressure p_4 is usually better than that of p_0. Having a good evaluation of that ratio would therefore allow a better evaluation of the nozzle reservoir pressure p_0.

Unfortunately, it appears that there is no direct correlation between these two parameters, since the standard deviation on the repeated shots increases to more than 4% (even 5.5% considering the whole series).

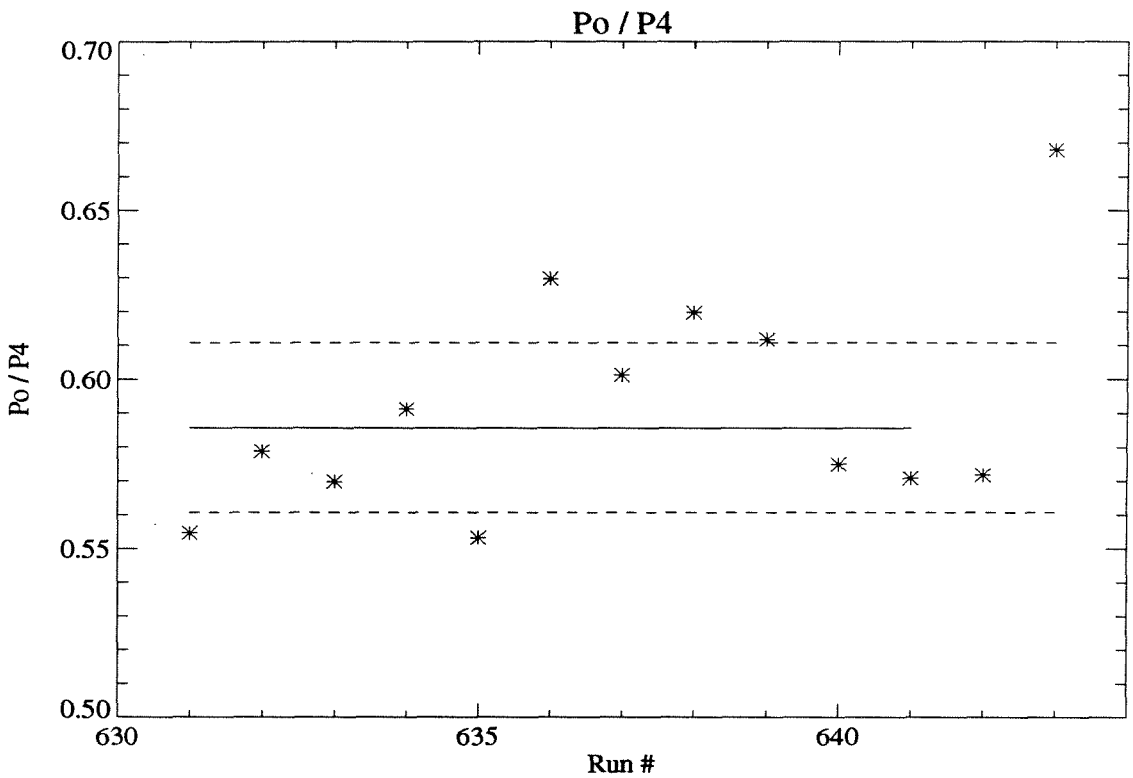

Figure 3.3. Ratios p_0/p_4 vs Runs.

The main results are presented in the following table :

Shots Range	**p_0/p_4 ave, dev, %**
[631 : 641]	0.587 ±0.026 # 4.4 %
[631 : 642]	0.586 ±0.025 # 4.3 %

Note that this ratio is nevertheless a good way to point out when the piston is leaking, as in shot 643 - p_0 has a standard value, while the ratio is quite high - or when the nozzle reservoir transducers are not working correctly - p_4 now has a standard value, while the ratio is quite low (shot 630, not shown here, is a good example).

3.2.5. The Shock Speed and Specific Total Enthalpy

The same study was then conducted for the total enthalpy h_0, which is taken in a first approximation as the square of the speed of the shock traveling in the ST denoted v_s. As said previously, the speed v_s is taken only between stations 3 and 4 (which corresponds approximately to the end of the second third of the ST). This value is measured quite accurately (error of less than 1%). However, the deviation of the shock speed along the shock tube (ST) is quite important, decreasing by around 20% between station 2 and the end of the ST.

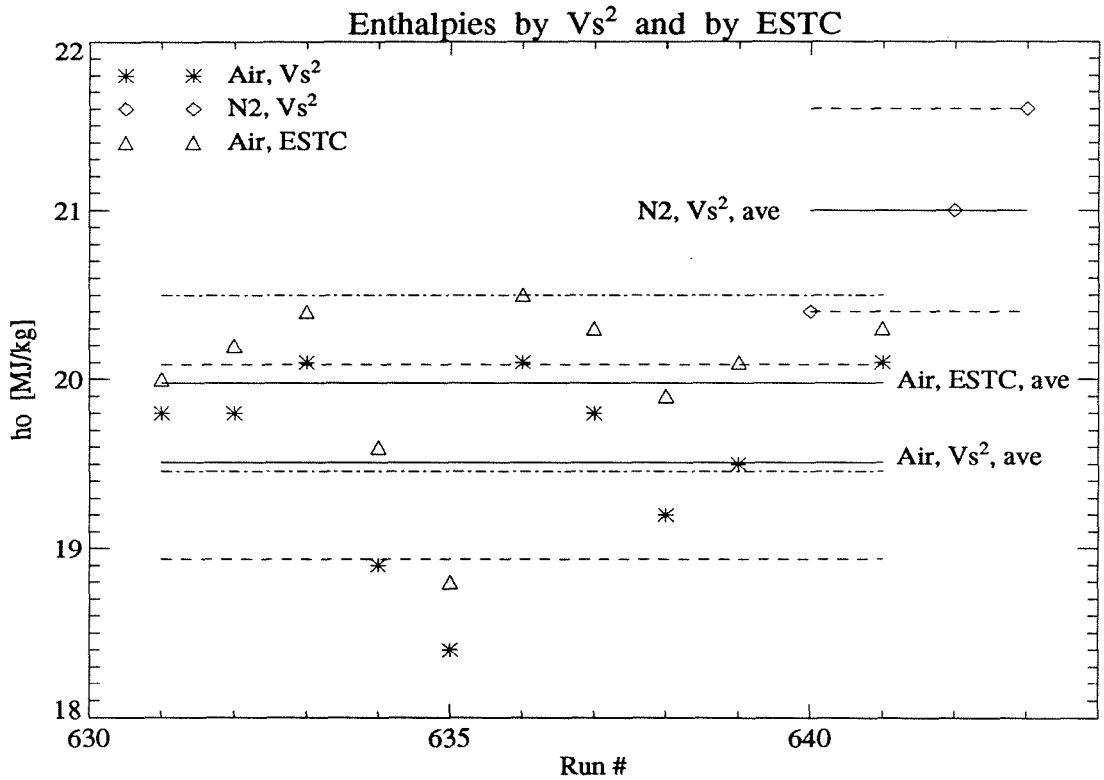

Figure 3.4. Enthalpies h_0 vs Runs.

The air shots have to be studied separately from the N_2 shots, since for the same filling ST pressure (30 kPa), the shock speed is higher for the lighter gas. Both 20mm and 30mm throat shots can be studied together, since they are both small enough to have no influence on p_0. These two statements are well confirmed by the data.

More accurate calculations have also been performed with ESTC. The results are always slightly higher by around 2% than the approximated v_s^2. Therefore, the approximation of h_0 by simply v_s^2 is considered satisfactory. The main question that stays, is when to take v_s, or how to derive a representative average (along the ST), in order to evaluate h_0 in the nozzle.

The main results (based on v_s^2 as usually used on T5) are presented in the following table ; averages and standard deviations are in [MJ/kg] :

Shots Range	**h_0 ave, dev, %**	**Comments**
[631 : 641]	19.5 ±0.6 # 2.9 %	Air only
640/642/643	21.0 ±0.6 # 2.9 %	The 3 N_2 shots

Therefore, despite an important uncertainty on where to estimate the shock speed, the repeatability was again shown less than 3%. One can evaluate roughly h_0 between 19 and 20 MJ/kg for air, and between 20.5 and 21.5 MJ/kg for N_2. This corresponds almost exactly to the expected change in shock speed according to the molecular weight.

3.2.6. Conclusion on the Repeatability of T5

Even if the accuracy for one specific shot is not so good, especially for the nozzle reservoir pressure, it can be concluded from the preceding studies that the repeatability of T5 is quite good. Deviations on the parameters for this series of 13 shots are of the order of 3 to 4 %. All basic theoretical statements can be clearly visualized when comparing shots.

3.3. Nozzle Calibration

The other main purpose of this series of shots was to calibrate the present T5 nozzle, especially at the exit plane to compare with SURF calculations, and further downstream where models are usually tested. The techniques used to visualize and extract averages from traces, and then the ones used to compute calibration parameters from these averages by means of parabola fits, are described in section 2. In the present section, the results of this calibration are presented in terms of minimum pressure around the centerline, deviation of this value along the radius, position of the centerline, and thickness of the boundary layer.

3.3.1. Calibration Coefficients and Parameters

The coefficients, given by the parabola fit, are listed in table 3.2.

It should be noted that :

$$p_t(x) = a.\,x^2 + b.\,x + c\,, \qquad a\ in\ [MPa/m^2]\ ,\ b\ in\ [MPa/m]\ ,\ c\ in\ [MPa]$$

$$p_t(x - center) = p_{min} + a.\,x^2\,, \qquad p_*\ in\ [MPa]\ ,\ x\ and\ center\ in\ [m]$$

A "C" following the shot number means that one point has been replaced ; a "C!" that 2 points have been replaced, and/or the transducer range has been restricted.

The "Data used" column shows the transducer number range used for the fit.

Ave3 is the average between the theoretical center -projection of the true geometric nozzle center on the rake- and the 2 adjacent points ; Ave5 is the same with the 4 adjacent points (2 right, 2 left) ; and Dev% is the standard deviation of the previous 5 points with respect to Ave5.

Shot #	Data used	By Parabola Fit : Coef & Parameters c MPa	b MPa/m	a MPa/m^2	Center m	P_{min} MPa	By Data Points Ave3 MPa	Ave5 MPa	Dev %	Test Gas
631C!	1-11	0.3504	0.5683	5.7820	- 0.049	0.336	0.354	0.358	6.97	Air
632	1-11	0.3613	0.3334	5.2822	- 0.032	0.356	0.368	0.369	5.90	Air
632C!	1-11	0.3557	0.3217	5.8920	- 0.027	0.351	0.359	0.362	4.58	Air
633	1-12	0.3404	0.3680	7.0505	- 0.026	0.336	0.344	0.348	6.04	Air
634	1-13	0.3483	0.0556	2.9219	- 0.010	0.348	0.354	0.353	1.86	Air
635	1-11	0.3170	0.1723	4.2486	- 0.020	0.315	0.319	0.321	2.72	Air
636	1-11	0.3480	0.1671	3.7446	- 0.022	0.346	0.350	0.352	2.95	Air
637	1-12	0.3553	0.1188	3.6974	- 0.016	0.354	0.361	0.360	2.34	Air
637C!	1-12	0.3487	0.1188	4.4810	- 0.013	0.348	0.352	0.354	1.46	Air
638	1-12	0.3504	0.1939	4.6124	- 0.021	0.348	0.354	0.356	2.65	Air
639	1-12	0.3420	0.0958	5.9084	- 0.008	0.342	0.347	0.349	1.67	Air
641	1-13	0.3072	0.1410	8.8122	- 0.008	0.307	0.313	0.316	2.81	Air
640	1-12	0.3069	0.2082	11.153	- 0.009	0.306	0.314	0.319	4.28	N_2
640C	1-12	0.3049	0.2132	11.388	- 0.009	0.304	0.311	0.317	4.53	N_2
642	1-13	0.2670	0.0929	14.074	- 0.003	0.267	0.264	0.273	6.17	N_2
643	1-12	0.2947	0.2211	15.378	- 0.007	0.294	0.296	0.303	7.97	N_2

Table 3.2 - Parabola Fit Coef. and Parameters & [ave+dev] Results (Shots 631 to 643)

3.3.2. Center Pitot Pressure

3.3.2.a. Minimum Pressure p_{min}

For every shot, the minimum value of the parabola was recorded as the "Center Pitot Pressure" or p_{min}. Actually, it is better to speak in terms of minimum, since it does not correspond exactly to the geometric center of the nozzle, as will be shown later. These values were compared with all shots on Figure 3.5. The error on p_{min} made with the parabola fit, by the software package PV-Wave, using the least-squares method, is hard to quantify.

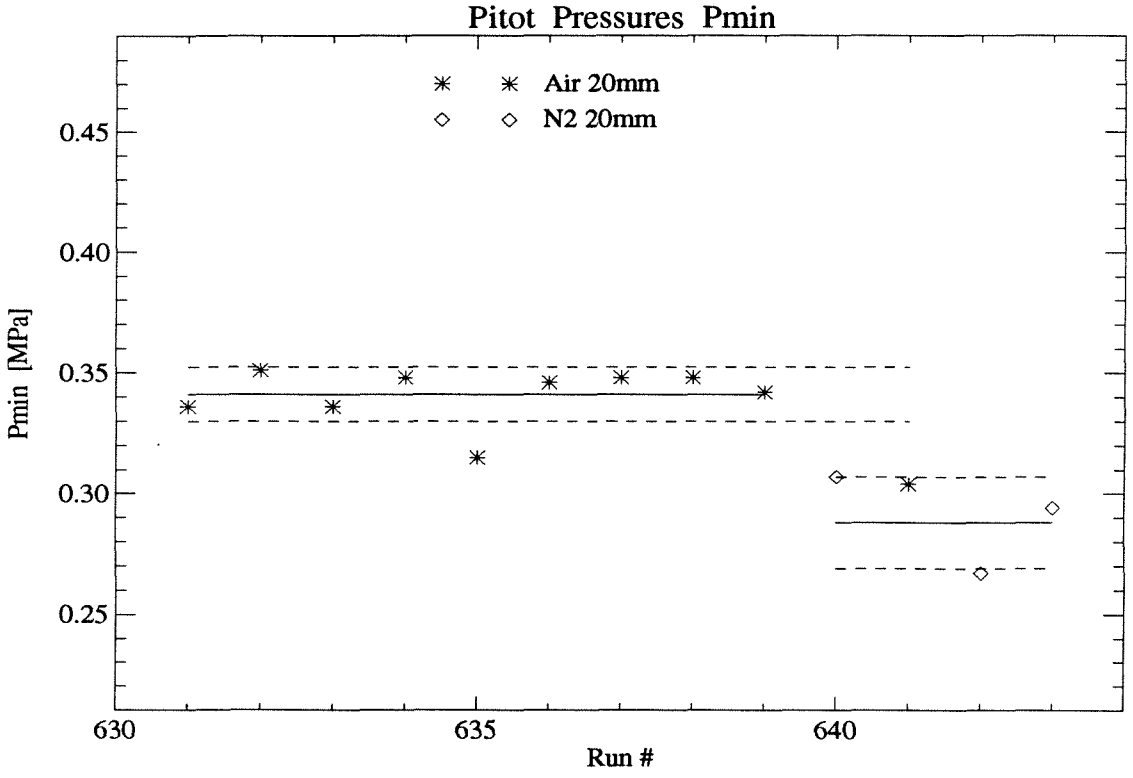

Figure 3.5. Minimum Pitot Pressures p_{min} vs Runs.

Initial remarks can be made at first glance : the 30mm throat (last 2 shots, not shown here), equivalent to an area ratio of 100, gives higher p_{min} than the 20mm throat (area ratio of 225) as expected ; and the N_2 shots give a lower p_{min} than the air shots.

The main results are presented in the following table (averages and deviations in [MPa]) :

Shots Range	P_{min} ave, dev, %	Comments
[631 : 643]	0.326 ±0.026 # 8.1 %	All 20mm, just for comparison
[631 : 639]	0.341 ±0.011 # 3.3 %	Air
640/642/643	0.288 ±0.019 # 6.6 %	The 3 N_2 shots

It is thought that shot 641 was contaminated by the previous N_2 shot, and was therefore not taken into account. The results confirm the first observations. The standard deviation around the values, when the shots are chosen carefully, are fairly good.

3.3.2.b. Non-dimensionalized p_{min} / p_0

The ratio P_{min} / P_0 (minimum pitot pressure at the exit over nozzle reservoir pressure) was studied, in order to non-dimensionalize P_{min}. All the ratios are plotted in Figure 3.6. Note that the same derivations on the first 4 shots (627 to 630), with non-tailored-interface condition, give points out of range (not shown for convenience).

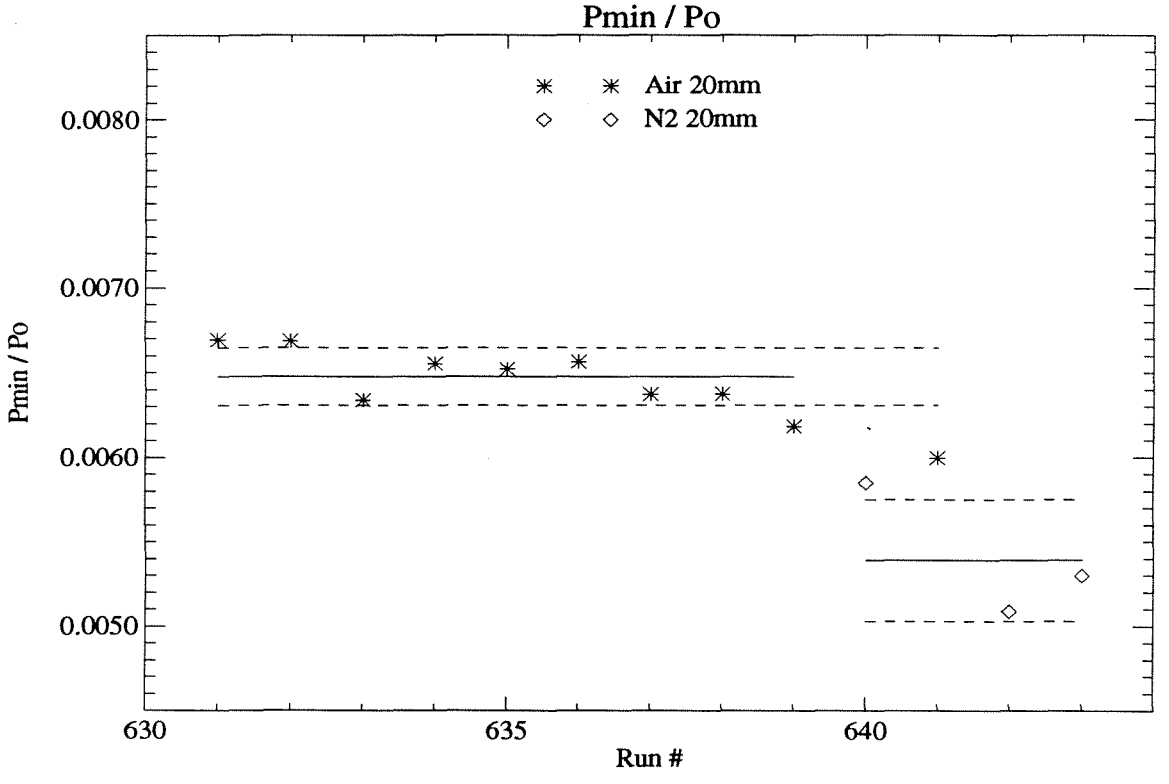

Figure 3.6. Ratios p_{min}/p_0 vs Runs.

The main results are :

Shots Range	P_{min} / P_0 ave, dev, %	Comments
[631 : 639]	6.48 E–03 $\pm 0.17E-03$ # 2.6 %	Air
640/642/643	5.39 E–03 $\pm 0.36E-03$ # 6.7 %	The 3 N_2 shots

The fact that the standard deviation becomes so low -less than 3% for air-, shows that there is a quite good correlation between the 2 parameters, as well as very good repeatability of the condition in the test section. For the N_2 shots, one has to note that the standard deviation is based on only 3 points, and furthermore, values of P_0 are based on only one transducer.

Good correlation is also clearly shown by the shot 635 : while p_0 is lower than for the other shots, and while p_{min} is also on the lower edge of the standard deviation range, the ratio is one of the closest to the averaged ratio value.

Unfortunately, the error bar on one point, in figure 3.6, is of the order of 10%. This is too large with respect to the standard deviation of the mean value, to be able to conclude anything about the variation of the pressure versus the axial position. In fact, it seems that p_{min} is almost constant at the different axial positions ranging from -3.5 cm inside the nozzle to +7.5 cm outside.

3.3.3. "Curvature"

3.3.3.a. "a", coefficient of X^2 in a Parabola

A study similar to the previous ones was conducted for the second derivative of the parabola fit, hereafter referred to as "curvature" (Figure 3.7). In fact, the study is on the coefficient of X^2, called "a", which is half the second derivative. The error made on that coefficient with the parabola fit, using PV-Wave least-squares method, is again unknown.

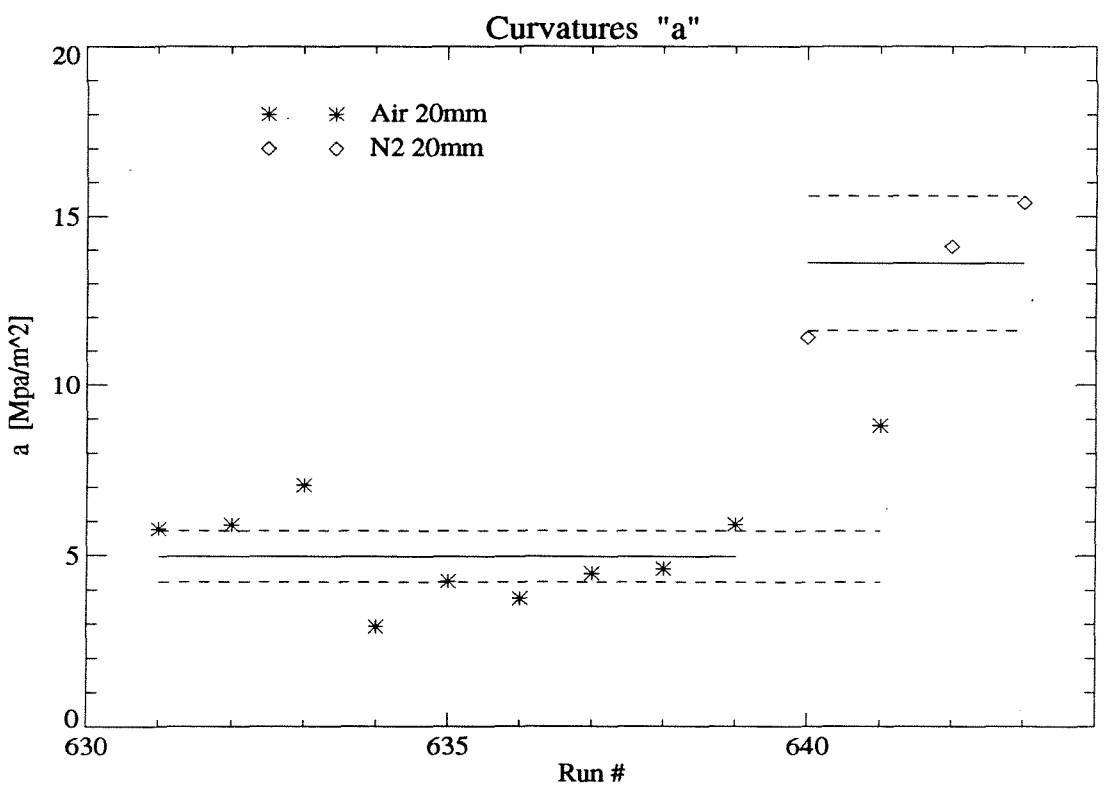

Figure 3.7. Curvatures "a" vs Runs.

As for the p_{min} plot, initial remarks of the same type can be easily made. The 30mm throat shots exhibit a higher curvature than the 20mm ones. The N_2 shots have a higher curvature than air shots. Shot 641, with air, seems again to have been contaminated by

the previous N_2 shot, as its curvature is abnormally high. Shots 633 and 634 are far from the average of all other 20mm throat air shots, for no apparent reason, and have a large standard deviation.

The main results are, with the averages and deviations of "a" in [MPa/m^2] :

Shots Range	**"a" ave, dev, %**	**Comments**
[631 : 639]	4.96 ±1.29 # 26. %	All Air, 20mm, except 641
[631 * 639]	4.97 ±0.76 # 15. %	As above, less 634 and 635
640/642/643	13.6 ±2.03 # 15. %	The 3 N_2 shots, 20mm

Again, it is impossible to make any statement regarding the variation of the curvature versus the axial position, despite the high standard deviation. However, the different conditions (air/N_2, 20/30mm throat) can be really easily identified.

3.3.3.b. Scaled Ratio "a"/p_0

When p_{min} is scaled by p_0, so is the coefficient "a". Figure 3.8 shows this ratio for various runs. Unlike p_{min}/p_0, there is no improvement here in the standard deviation when the curvature is scaled. Note nevertheless that p_0 varies by up to 5% on [631, 639], and since the deviations do not add up, this implies some correlation between the two parameters.

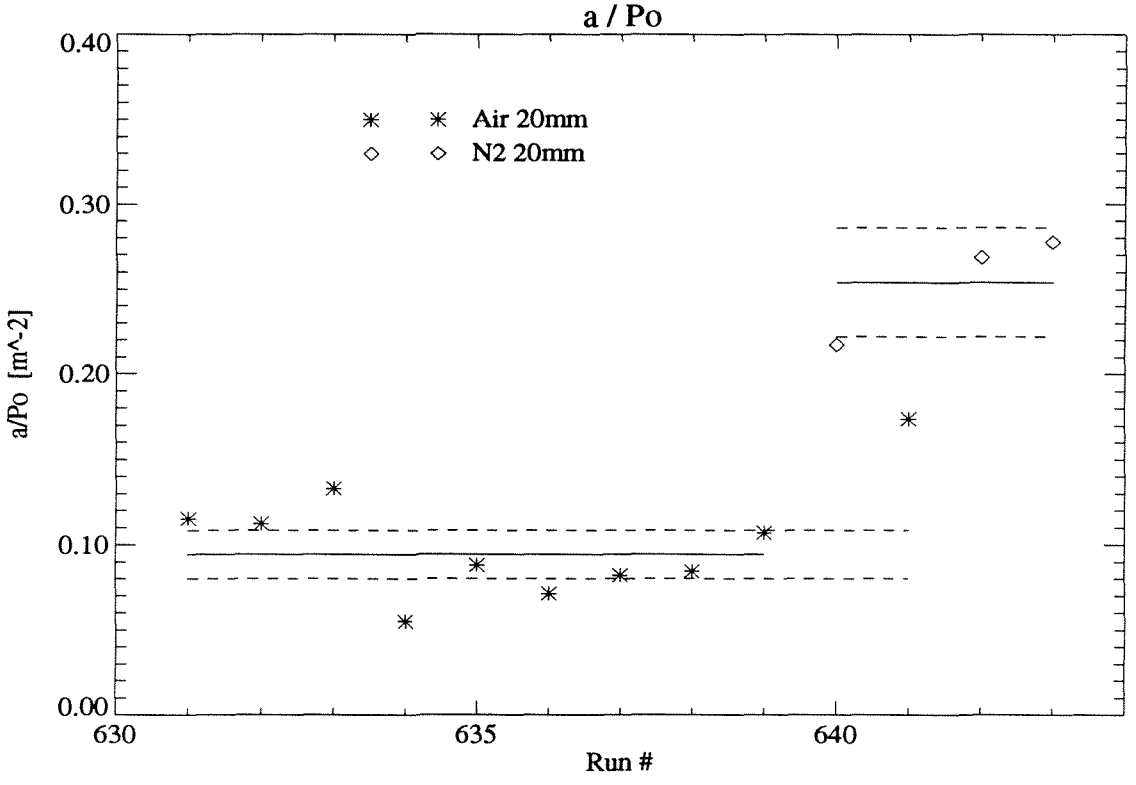

Figure 3.8. Ratios "a"/p_0 vs Runs.

The main results for the scaled curvature "a"/p_0, in $[(m^2)^{-1}]$, are :

Shots Range	"a"/P_0 ave, dev, %	Comments
[631 : 639]	0.094 ±0.024 # 26. %	All Air, 20mm, except 641
[631 * 639]	0.095 ±0.014 # 15. %	As above, less 634 and 635
640/642/643	0.254 ±0.032 # 13. %	The 3 N_2 shots, 20mm

3.3.4. Symmetry and Center Axis

With this parabola fit, one can easily find the vertical symmetry axis location, which should correspond with the geometric center, i.e. $r = 0$. However, as can be seen on Figure 3.9, results show quite a few differences. The error made on this location is thought to be at least half the distance between two transducers, i.e. around 1 cm.

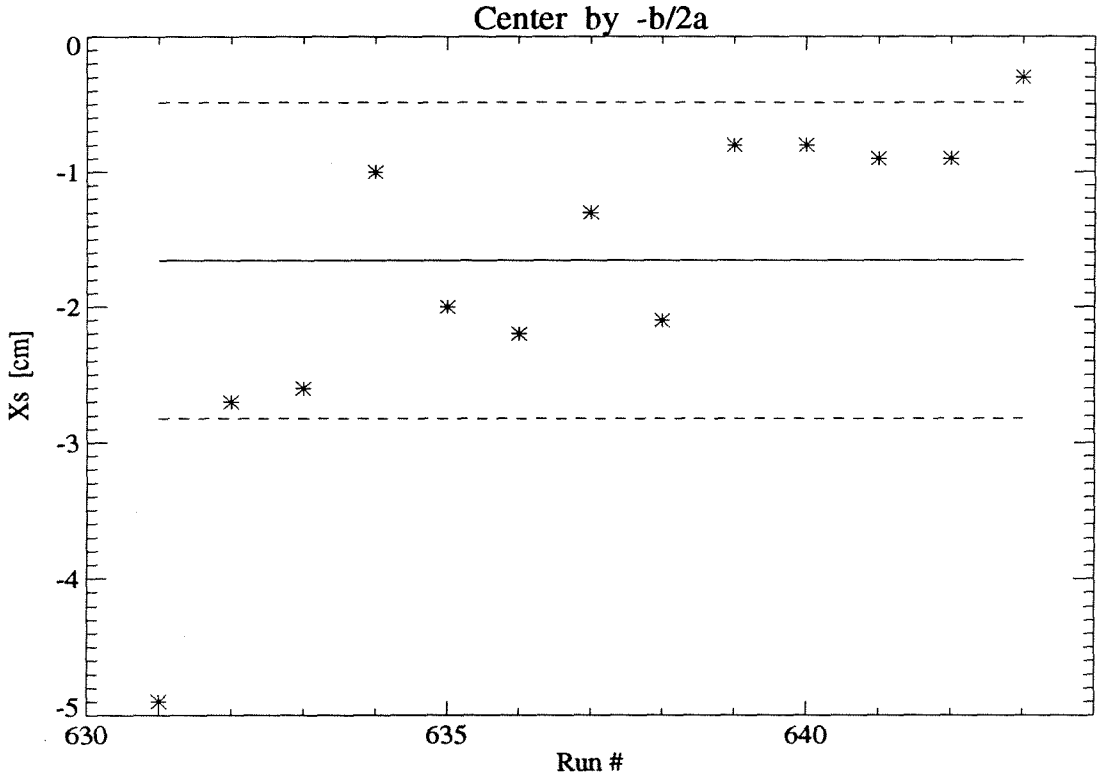

Figure 3.9. Symmetry Axis Locations X_s vs Runs.

Shots Range	$x_s = -b/2a$: ave, dev, %	Comments
All	-1.7 cm ±1.2*cm* # 71. %	All parabola fits

The exact reasons for such a shift, and such a large deviation around the averaged value, are still unknown. It does not seem to depend on the test gas nor the throat. It should be noted that the average shift is around 3/4 of an inch, which is the space between two

transducers, and also the "unit" of the spacers (3/4" thick or half of it). But until now, all the checks, as far as the elevation of the rake is concerned, as far as the geometric center position is taken into account, were in vain. Checks are also possible with the contour plots, giving approximately the same values, while looking for a symmetry axis.

3.3.5. Boundary Layer

Estimates of the boundary layer thickness were also conducted. In fact, it would be better to speak in terms of "flow layer radius", since some of the data were taken outside the nozzle. This radius was taken as the distance between the symmetry axis (as determined in the previous paragraph) and at first, the location of the maximum pitot pressure (location of one transducer in the lower part of the rake). However, the error on that distance was on the order of 2cm, and again was too large to be able to study the variation of that flow layer versus the axial position. Contour plots were therefore used to determine the maximum pressure radius (at the bottom of the nozzle) with a general error around 0.5 cm.

Figure 3.10 shows the values obtained by the two methods for all the shots. The exit nozzle radius is 15.7 cm, and a top line is drawn as a reference.

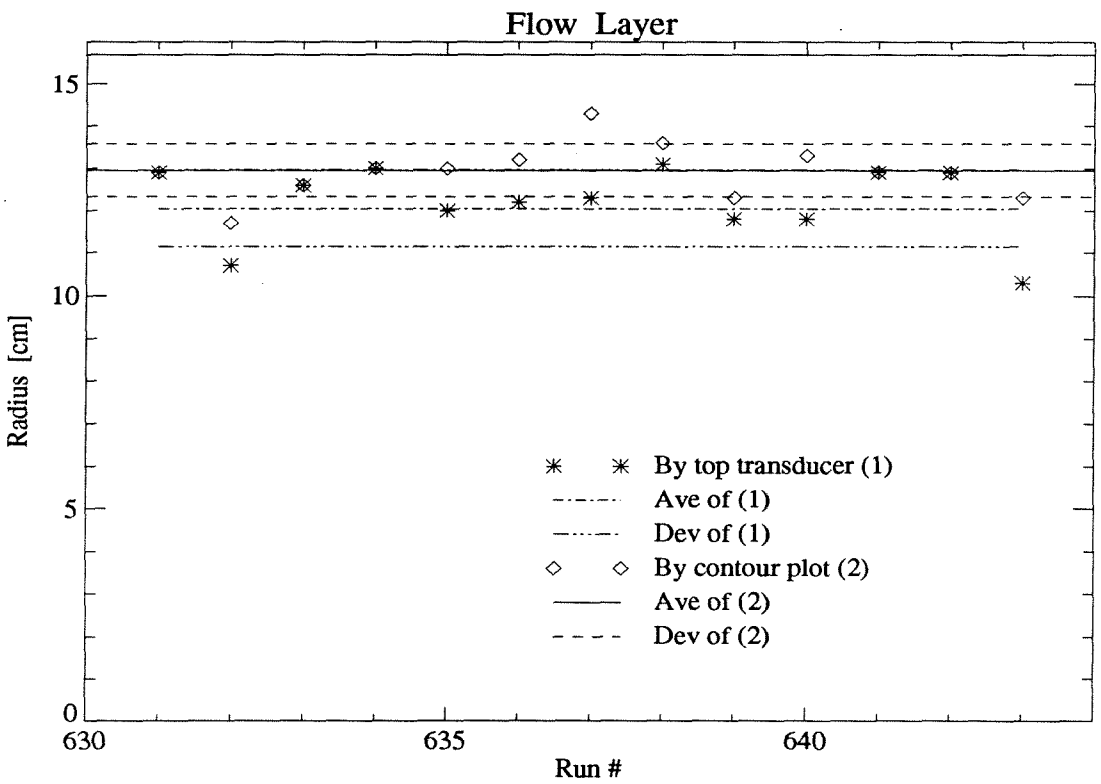

Figure 3.10. Boundary/ Flow Layers vs Runs.

The main results are summarized below :

Shots Range	Flow Layer ave, dev, %	Comments
All	12.1 cm $\pm 0.9cm$ # 7.6 %	By top transducer
All	13.0 cm $\pm 0.6cm$ # 4.8 %	By contour plot

Using contour plots, the values seem to be accurate enough to be used to study the variation of the flow layer versus the axial position. Following are the averaged flow layer radii per axial position for each condition. All these values have to be taken into account very carefully, because of the error made on each value and the small number of shots available for each case. The "Exit - 0.5 cm" one may be more useful in order to compare with computations.

Gas	Throat	Axial Pos.	By top transd.	By contour plot	Number of shots
Air	20mm	- 0.5 cm	12.8 cm	12.4 cm	4 shots
		+3.0 cm	12.3 cm	12.7 cm	4 shots
		+6.5 cm	12.4 cm	13.4 cm	4 shots
N_2	20mm	- 0.5 cm	12.4 cm	13.1 cm	Only 2 shots
		+6.5 cm	10.3 cm	12.3 cm	Only shot 643
Air	30mm	- 0.5 cm	10.7 cm	12.7 cm	Only shot 645
N_2	30mm	- 0.5 cm	11.6 cm	13.6 cm	Only shot 646

3.4. Conclusion on repeated shots

This series of 13 shots has lead to a successful calibration of the T5 facility, and in particular the contoured nozzle with the 20mm throat, for the "High_Enthalpy - Medium_Pressure" (off-design) condition with air and N_2 as test gases.

On one hand, the T5 parameters such as the nozzle reservoir pressure p_0, and the enthalpy h_0, are known for that condition, within 3 to 4%. A summary, useful as inputs for ESTC and SURF programs is given at the end of Ch.3.3 .

On the other hand, the present contoured nozzle -with an area ratio of 225- has been calibrated, by means of parabola fits, yielding the minimum pressure on the symmetry axis, p_{min}, and the curvature of the distribution along the radius, "a". Differences between air and N_2 can be easily identified. The value for p_{min} is within 3% (Air) to 7% (N_2), while the one for "a" is of the order of 15%.

Finally, a study of the symmetry and center of the airflow was conducted, but with no definitive conclusions, implying an uncertain conclusion on the flow layer.

SECTION 4 :

Calibration of the T5 Nozzle

with the 20mm Throat

(Area Ratio of 225)

for Common Conditions, with Air

4.0. Calibration with the 20mm Throat, Introduction

When lower densities are required in the test section for simulating flights at higher altitudes (like reentry in the atmosphere), one way to reach the condition is to increase the area ratio of the nozzle. Since the exit is fixed, it is done by changing the throat. Instead of the conventional 30mm diameter one (corresponding to the design condition of the contoured nozzle with an area ratio around 100-110), a 20mm (area ratio around 225-250) or even a 14mm (area ratio around 450-500) one can provide the required conditions. While the 14mm throat has never been used for testing a model, the 20mm one was used with a ESA model. This made calibrating for the common T5 conditions using this throat necessary.

The different conditions have been investigated during the second calibration series (shots 581 to 605) during the summer of 1993 (mid July to mid August), before the ESA tests [Adam & Rousset, 1993]. The entire T5 envelope was covered. Air was the only test gas considered. Different axial positions, and height (along the exit diameter) of the pitot rake R13, were investigated.

Furthermore, results from the repeat series, found in the previous section, are included in the present section, under a box (called R1). They give a good idea of the error bars related to the repeatability.

The procedure followed in the calibration study, especially as far as the parameters and the scaling are concerned, was first developed during the present study. The resulting scheme was then applied for the 30mm throat calibration, with air and other test gases (presented in the next sections).

After locating the shots on the common p_4 *vs* h_0 and p_0 *vs* h_0 plots, the (discrete) conditions are defined and the calibrated envelope visualized. The scheme goes then to test section results. The parabola fit technique provides three major pieces of information about the pitot pressure distribution : the minimum, the curvature, and the location of the flow symmetry axis. The minimum pitot pressure, located on the symmetry axis close to the nozzle centerline, is first plotted versus h_0 to confirm the condition classification. Then, the plot versus the other reservoir parameter p_0 results in a correlation plot. Since p_{min} and p_0 appear proportional, the ratio (p_{min}/p_0) is studied versus the two reservoir parameters, p_0 and h_0. Then, the curvature of the distribution, approximated by twice the quadratic coefficient "a", is studied in a similar fashion, including the scaling by p_0. Finally, the location of the flow symmetry axis with respect to the nozzle centerline is investigated. Some estimations of the extent of the core, or the thickness of the boundary layer, are presented at the end of this section.

4.1. History of the Second Series, Shots 581 to 605

The following history of the second series of tests, performed in order to calibrate the T5 nozzle with the 20mm throat (area ratio of 225) at various common conditions, is thought to be needed since information on the rake position (before the shot), or on how the condition were reached (filling pressures) may be useful. Some comments may help in identifying the condition and following the modifications.

Most of the information included is related to operations before the shot, so is the "axial position" of the rake given during the preparation. The only exceptions are the wellness of the buffers after the shot, and the changes between two shots.

Notes on the following table

In table 4.1, the "axial position" is given before the shot, in other terms before the recoil. In order to know the exact axial position during the test, one has to take into account the "compression tube recoil" (CT recoil). The CT recoil is the same as the shock tube is and therefore the nozzle is, since these three pieces are held together.

The "unit" of height for the rake position is a spacer of 3/4 of an inch. This corresponds also to the space between two transducers on the rake. The "0.0" was the first position tested, as the easiest one. It gives around 5 points in the expansion-fan, but unfortunately, not enough points in the core to be able to study it in detail (especially as far as the symmetry is concerned). On the opposite side, the "+2.5" position roughly centers the rake into the nozzle, and thus allows the experimentalist to insert the rake 11 cm into the nozzle (the "IN" position). This position gives 12 to 13 points (all of the transducers) in the core, with very little information on the boundary layer (BL).

The pressure units are the common ones used on T5. Following are the main conversions, specially useful for the 2R filling pressures :

$$1\ atm\ =\ 1.01\ E05\ Pa\ =\ 14.65\ psi$$

$$(y\ in\ psi)\ =\ (x\ in\ psig)\ +\ 1\ atm$$

$$(y\ in\ kPa)\ =\ 6.894\ *\ (x\ in\ psig)\ +\ 101\ (kPa)$$

For the CT, when it is not filled with pure Helium (100%), it is a mixture of Helium and Argon (5% to 15%), in order to match the ratio of the sound speeds (of the driver and driven gas) needed to establish a tailored interface.

This whole series used exclusively air as the test gas, since nitrogen was not thought to be significantly different as far as the results would have been concerned.

Shot #	Positions Axial cm	High *3/4"	Filling Conditions ST kPa	CT, %He kPa	2R psig	Comments
581	+5 (Out)	0.0	50, Air	116, 95%	1120	T5 & Nozzle rusted, Buffers hit hard
582	0 (Flush)	0.0	50, Air	116, 95%	1120	Overshoot & pb BL, Nozzle cleaned
583	0 (Flush)	0.0	40, Air	116, 95%	1120	Try to lower the overshoot
584	+5 (Out)	0.0	45, Air	116, 95%	1120	Try to adjust the tailored condition
	Burst & Nozzle Reservoir Transducers checked (Serial numbers and sensitivities too)					
585	+5 (Out)	0.0	85, Air	116, 85%	1110	Condition # 2
586	no change	0.0	40, Air	116, 100%	1110	Cond.# 4, Buffers smashed
587	NO DATA, Piston leaked, Diaphragm did not burst, No trigger —> Piston changed					
588	no change	+1.5	50, Air	143, 100%	1720	Cond.# 6, Buffers crashed
589	no change	+1.5	40, Air	145, 100%	630	Cond.# 1, Buffers OK
590	no change	+1.5	85, Air	116, 85%	1110	Cond.# 2, as 585, Buffers OK
	Nozzle Reservoir Transducers checked ; South black of soot (was leaking)					
	New ST sleeve (design in "2 layers"), New Nozzle Reservoir holders					
591	no change	+1.5	40, Air	116, 100%	1110	Cond.# 4, as 586, Buffers smashed
592	no change	+1.5	30, Air	116, 100%	1000	Modif. of 591, Buffers hardly touched
593	no change	+1.5	30, Air	116, 95%	1000	Modif. of 592, Buffers saved
594	no change	+1.5	30, Air	116, 95%	950	Modif. of 593, Buffers OK, Tailored
595	no change	+1.5	85, Air	116, 85%	1110	Repeat of 590, Buffers OK
596	no change	+1.0	85, Air	116, 85%	1110	Repeat of 595, Intermediate pts
597	no change	+1.0	40, Air	145, 100%	630	Repeat of 589, Intermediate pts
598	no change	+1.0	45, Air	143, 95%	1600	Modif. of 588, Buffers destroyed
	Pitot transducers #05 & #02 changed, and pitot-tips interchanged					
599	no change	+1.0	45, Air	116, 95%	1120	Repeat of 584
600	no change	+1.0	20, Air	116, 95%	950	Condition # 5, Very-high h_0
601	no change	+1.0	30, Air	116, 95%	950	Repeat of 594, Intermediate pts
	Position rake "IN", up by +2.5 spacers, upstream by 10cm, DT upstream by 6cm (total of 16cm)					
602	IN, -11cm	+2.5	40, Air	116, 100%	1110	Repeat of 586, High overshoot
603	IN, -11cm	+2.5	45, Air	116, 90%	1000	Modif. of 599, Buffers saved
604	IN, -11cm	+2.5	40, Air	145, 100%	630	Repeat of 597
605	IN, -11cm	+2.5	85, Air	116, 85%	1110	Repeat of 596, Piston leaked

Table 4.1 - Rake Positions, Filling Pressures, and Comments, for Shots 581 to 605

4.2. T5 Parameters and Conditions

4.2.1. T5 Repeatability, Errors, and Results from the Third Series

The remarks and results about the repeatability of T5, and the fluctuations around an averaged value, taken as the main (non-rectifiable) error sources, are described in section 3.

The results from these repeated shots (third series), presented also in section 3, are used in the following study, and appear as a box named "R1" on the plots. This box is centered around the averaged value of that specific condition, and its sides are the deviations from that value, or in other terms the error-bars, in both the x and y directions.

4.2.2. T5 Parameters Results

4.2.2.a. Table of Results

The following table (4.2) presents the results of the main T5 parameters for the whole series. These results are supposed to be insensitive to the downstream throat diameter, but to depend only on the filling pressures and the diaphragm burst pressures.

In fact, 6 different major conditions have been calibrated (c.f. figure 4.1 and 4.2), with some modifications for some of them, all of them with air as the test gas.

For the nozzle reservoir pressure p_0, when 'South' or 'North' is specified instead of a "%", it means that only that channel is available to get $p_{0,avg}$. For shots 589 and 590, neither of the two traces is reliable, and therefore the value is taken from an exact repeat.

Note that for "R1", the "%" value represents in fact the deviation around the average.

Shot	Burst Pres. (MPa) $P_{4,avg}$	%	Nozzle Res. (MPa) $P_{0,avg}$	%	(km/s) V_s	(MJ/kg) h_0	Test Gas	Cond. #
581	84.6	0.3	59.7	South	3.95	15.6	Air	3
582	87.3	0.8	60.3	-0.8	4.05	16.4	Air	3
583	87.6	0.2	60.6	-2.9	4.23	17.9	Air	3
584	85.2	1.9	60.2	North	4.08	16.7	Air	3
585	94.0	0.5	55.5	North	3.31	11.0	Air	2
586	87.4	0.4	62.0	North	4.32	18.6	Air	4
587	No Data		No Data	No Data	No Data	No Data		
588	107.7	0.0	74.5	North	4.35	18.9	Air	6
589	32.1	2.4	25.7	597+604	3.35	11.2	Air	1
590	84.0	0.9	58.8	as 596	3.26	10.6	Air	2
591	85.5	0.7	51.6	-0.3	4.51	20.4	Air	4
592	85.1	0.9	50.3	0.1	4.72	22.3	Air	5
593	81.4	1.5	49.0	1.1	4.44	19.8	Air	4
594	81.0	1.1	47.4	0.5	4.62	21.3	Air	4
595	83.2	0.6	58.8	-0.1	3.30	10.9	Air	2
596	83.0	1.1	58.8	-0.2	3.31	11.0	Air	2
597	32.1	2.5	24.4	1.7	3.45	11.9	Air	1
598	113.1	-0.8	74.3	-0.3	4.38	19.2	Air	6
599	87.5	0.7	59.7	0.3	4.14	17.1	Air	3
600	78.4	0.7	43.9	-0.6	4.69	22.0	Air	5
601	74.7	1.2	46.5	0.3	4.35	18.9	Air	4
602	85.5	0.5	57.6	3.0	4.29	18.4	Air	4
603	76.4	1.2	53.0	2.8	3.90	15.2	Air	3
604	32.2	2.5	26.9	5.9	3.55	12.6	Air	1
605	82.3	0.9	61.5	2.7	3.26	10.6	Air	2
R1	89.7	2.5	52.5	2.1	4.42	19.5	Air	4

Table 4.2 - T5 Parameters for Shots 581 to 605

Notation : "%" $= \frac{P_{4,N}-P_{4,S}}{P_{4,N}+P_{4,S}} * 100$, for P_4, as for P_0.

$P_{4,\,(N\text{ or }S)}$ is the maximum of the curve, smoothed over 15 pts, *i.e.* 0.5 ms.

V_S = Shock Speed between station 3 and 4;

h_0 is taken in a first appoximation as $(V_S)^2$.

4.2.2.b. Conditions in terms of p_4

Figure 4.1 shows the measured burst pressures p_4 versus the reservoir specific enthalpy h_0, approximated by ${v_s}^2$ as is usually done in T5.

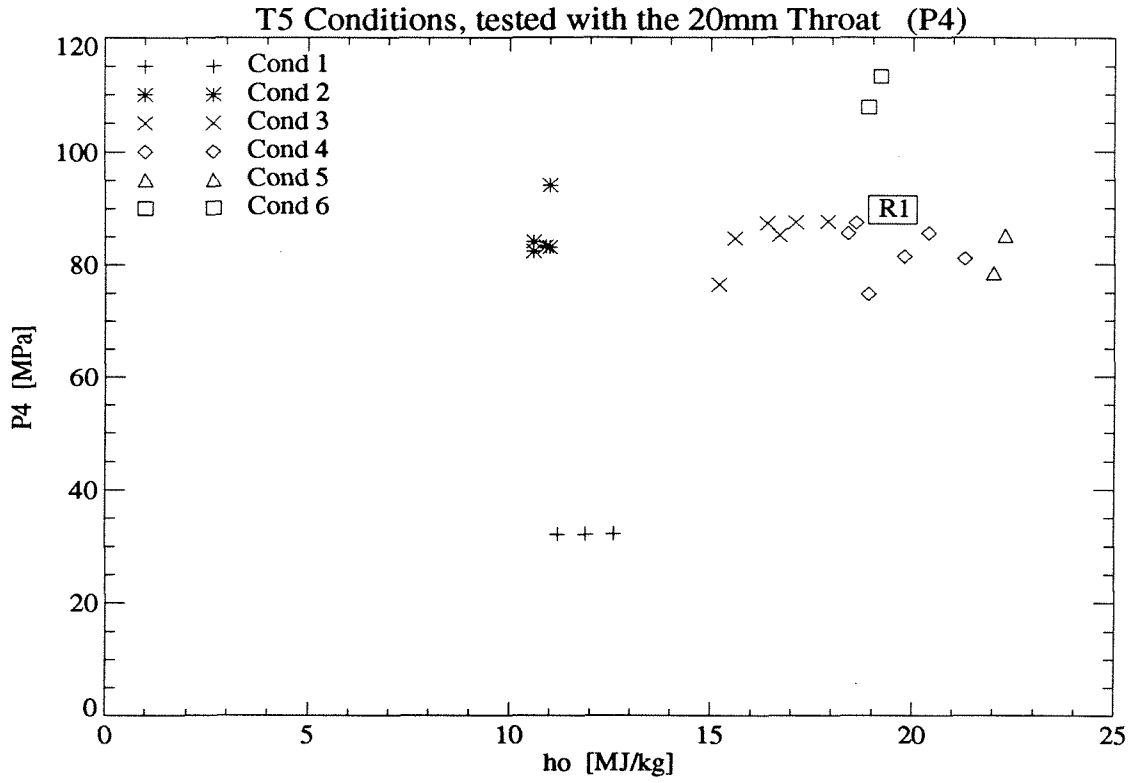

Figure 4.1. Burst Pressures p_4 vs h_0.

The 6 conditions are named, accordingly with the plot, as follows :

Condition 1 : Low_Pressure - Low_Enthalpy
Condition 2 : Medium_Pressure - Low_Enthalpy
Condition 3 : Medium_Pressure - Medium_Enthalpy
Condition 4 : Medium_Pressure - High_Enthalpy
Condition 5 : Medium_Pressure - VeryHigh_Enthalpy
Condition 6 : High_Pressure - High_Enthalpy

While the variation of p_4 for condition 1 & 6 (low and high pressure) is really low, it can reach 10% for the medium burst pressure (theoretically 90 MPa) cases. This is usually due to the fact that the diaphragms come from different batches, and therefore have a different thickness, so that the remaining thickness (the only important parameter for the burst pressure) varies.

Note that the "R1 box" lies in the middle of the shots for condition 4.

4.2.2.c. Conditions in terms of p_0

More conventionally for the T5 team, the following plot presents the conditions defined in terms of the nozzle reservoir pressure p_0 versus the reservoir specific enthalpy h_0.

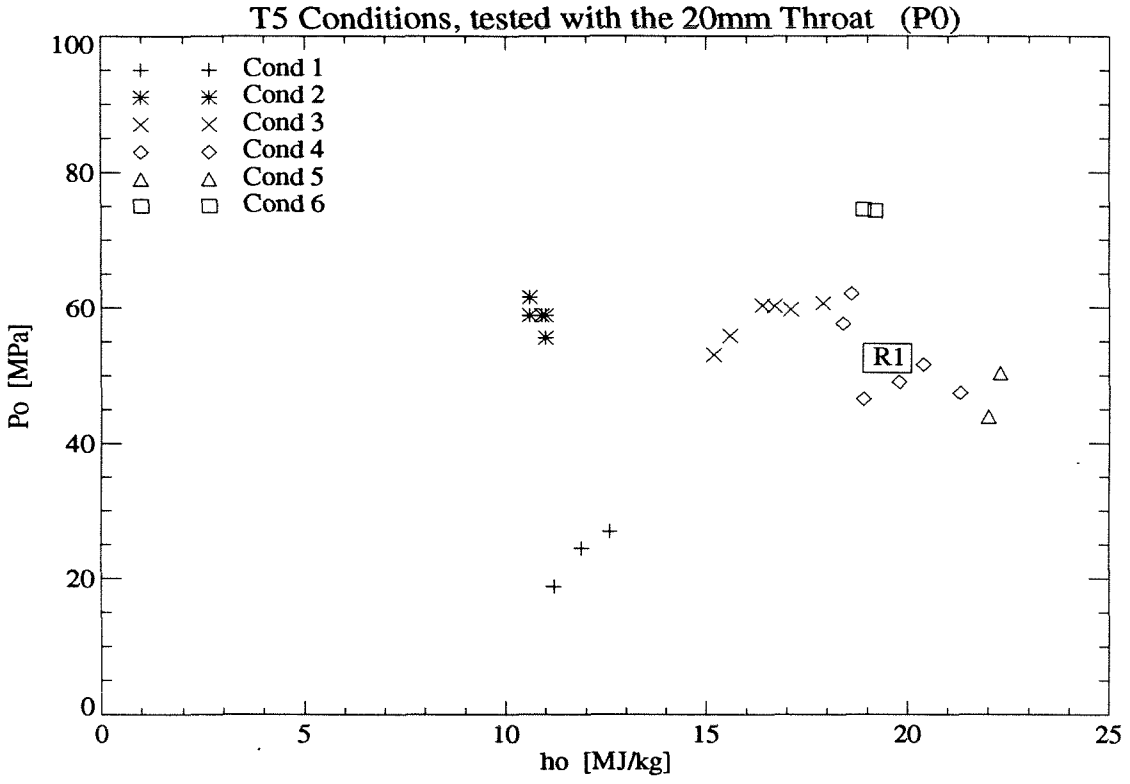

Figure 4.2. Nozzle Reservoir Pressures p_0 vs h_0.

This plot is representative of the envelope of the common conditions performed in T5, with air as the test gas, in terms of the two reservoir parameters. The nozzle reservoir pressure p_0 ranges from some 20 MPa to about 80 MPa, while the specific reservoir enthalpy h_0 ranges from about 10 MJ/kg to some 23 MJ/kg.

Naturally, the denominations of the 6 conditions apply here in the same way as in figure 4.1. Only the values and variations (deviations around an averaged values) differ.

Condition 1 gets more scattered, while conditions 2 & 6 get more grouped. For the other conditions (3, 4, &5), the p_0 distribution follows the p_4 one.

The scattering of condition 4 is essentially due to the multiple modifications, varying the filling pressures among other things, made in order to manage the buffers designed to stop the piston. Again, the "R1 box" stands in the middle of condition 4, showing, as expected, good repeatability between the two different series.

It seems that, for high enthalpies ($h_0 > 19$ MJ/kg), the nozzle reservoir pressure p_0 cannot reach the theoretical 60 MPa (with a 90 MPa burst pressure), at least with the way the conditions were performed during this series.

4.3 Nozzle Calibration Results

4.3.1. Tables of Calibration Results

Following are the tables of the calibration parameters obtained from the parabola fits. When that fit was not satisfactory (curve too flat, not enough points to fit, etc...), the averages from the traces were directly used.

Included in these tables, are the time periods used for the averages, i.e. "test times", the ranges of fitted transducers, the ones modified in order to make the fit easier, the 3 parameters extracted from the parabolas, and some comments related to the fits.

The abbreviation "cfe*" stands for centerline focusing effect. It means that the closest point to the symmetry axis, when (usually) higher than its neighbors, has been corrected relative to its two neighbors, i.e. replaced by a linear interpolation for helping the parabola fit.

Table 4.3 lists results by shot number (#), while table 4.4 by conditions (next two pages).

Recall that (notation) :

$$p_t(x - center) = p_{min} + a.\, x^2 , \qquad p_* \; in \; [MPa] , \; x \; in \; [m]$$

The *center* represents the location of the symmetry axis of the parabola, with respect to the nozzle centerline. Despite the use of meters, centimeters are used in the table, only to respect the order of magnitude.

4.3.2. Minimum Pitot Pressure (vs h_0, vs p_0, & scaled)

One of the more interesting calibration parameters is certainly the minimum pitot pressure value around the symmetry axis of the nozzle. Following are the plots of that derived value for each shot, according to its condition, raw and scaled by p_0, versus the reservoir specific enthalpy h_0, versus the nozzle reservoir pressure p_0.

(To be continued after the two following tables)

Shot #	Case #	Test time ms	Transducers fitted	Transducers replaced	P_{min} MPa	a MPa/m^2	Center cm	Comments
581	3	[1.10, 1.70]	1 - 10	cfe*	0.457	flat	0.0	Curve quasi flat
582	3	[1.10, 1.70]	1 - 5 !	none	0.453	****	***	Huge BL, non fittable
583	3	[1.10, 1.70]	1 - 10	none	0.385	5.73	-3.3	No correction
583	3	[1.10, 1.70]	1 - 10	cfe*	0.383	6.59	-2.4	2 pts replaced
584	3	[1.10, 1.70]	1 - 8 !	none	0.400	****	****	Non fittable, from averages
585	2	[1.35, 2.15]	1 - 8 !	# 3	0.380	11.6	-2.0	From averages and fit
586	4	[0.80, 1.30]	1 - 8 !	????	0.370	****	****	Non fittable, from averages
588	6	[0.85, 1.35]	1 - 11	none	0.484	3.14	-2.8	No correction
588	6	[0.85, 1.35]	1 - 11	cfe*	0.483	3.14	-2.2	2 pts replaced
589	1	[1.40, 2.20]	1 - 11	none	0.167	1.86	-0.3	Good uniformity
590	2	[1.35, 2.15]	1 - 11	none	0.407	6.47	-0.6	
591	4	[0.80, 1.30]	1 - 10	none	0.393	4.96	-2.2	
592	5	[0.80, 1.30]	1 - 11	none	0.362	2.98	****	Too flat to know the center
593	4	[0.80, 1.30]	1 - 10	none	0.347	5.37	-2.4	No correction, 10 pts
593	4	[0.80, 1.30]	1 - 11	none	0.349	4.41	-2.5	No correction, 11 pts
594	4	[0.80, 1.30]	1 - 11	none	0.331	5.03	-1.9	
595	2	[1.35, 2.15]	1 - 11	cfe*	0.389	6.97	-1.6	
596	2	[1.35, 2.15]	1 - 11	none	0.408	6.34	-1.9	No correction
596	2	[1.35, 2.15]	1 - 11	cfe*	0.402	7.38	-1.5	2 pts replaced
597	1	[1.40, 2.20]	1 - 11	cfe*	0.160	3.64	-1.5	2 pts replaced
598	6	[0.85, 1.35]	1 - 11	none	0.500	6.62	-2.1	No correction
598	6	[0.85, 1.35]	1 - 11	cfe*	0.497	7.23	-1.9	2 pts replaced
599	3	[1.10, 1.70]	1 - 11	none	0.382	5.90	-1.5	
600	5	[0.80, 1.30]	1 - 11	none	0.294	3.28	-2.5	No correction
600	5	[0.80, 1.30]	1 - 11	cfe*	0.293	3.54	-2.3	1 pt replaced
601	4	[0.80, 1.30]	1 - 11	none	0.299	4.63	-2.5	No correction
601	4	[0.80, 1.30]	1 - 11	cfe*	0.296	5.02	-2.3	1 pt replaced
602	4	[0.80, 1.30]	1 - 13	none	0.389	6.00	-0.7	All 13 pts, no correction
603	3	[1.10, 1.70]	1 - 13	none	0.329	9.55	-0.8	All 13 pts, no correction
603	3	[1.10, 1.70]	1 - 13	#4, 7	0.335	9.06	-0.7	2 pts replaced
604	1	[1.40, 2.20]	1 - 13	none	0.143	8.29	-0.9	All 13 pts, no correction
604	1	[1.40, 2.20]	1 - 13	#6, 7	0.156	7.59	-0.9	2 pts replaced
605	2	[1.35, 2.15]	1 - 13	none	0.393	11.2	-0.8	All 13 pts, no correction

Table 4.3 - Nozzle Parameters by Parabola Fits (Shots 581-605)

Shot #	Case #	Test time ms	Transducers fitted	Transducers replaced	P_{min} MPa	a MPa/m^2	Center cm	Comments
589	1	[1.40, 2.20]	1 - 11	none	0.167	1.86	-0.3	Good uniformity
597	1	[1.40, 2.20]	1 - 11	cfe*	0.160	3.64	-1.5	2 pts replaced
604	1	[1.40, 2.20]	1 - 13	none	0.143	8.29	-0.9	All 13 pts, no correction
604	1	[1.40, 2.20]	1 - 13	#6, 7	0.156	7.59	-0.9	2 pts replaced
585	2	[1.35, 2.15]	1 - 8 !	# 3	0.380	11.6	-2.0	From averages and fit
590	2	[1.35, 2.15]	1 - 11	none	0.407	6.47	-0.6	
595	2	[1.35, 2.15]	1 - 11	cfe*	0.389	6.97	-1.6	
596	2	[1.35, 2.15]	1 - 11	none	0.408	6.34	-1.9	No correction
596	2	[1.35, 2.15]	1 - 11	cfe*	0.402	7.38	-1.5	2 pts replaced
605	2	[1.35, 2.15]	1 - 13	none	0.393	11.2	-0.8	All 13 pts, no correction
581	3	[1.10, 1.70]	1 - 10	cfe*	0.457	flat	***	Curve quasi flat
582	3	[1.10, 1.70]	1 - 5 !	none	0.453	****	***	Huge BL, non fittable
583	3	[1.10, 1.70]	1 - 10	none	0.385	5.73	-3.3	No correction
583	3	[1.10, 1.70]	1 - 10	cfe*	0.383	6.59	-2.4	2 pts replaced
584	3	[1.10, 1.70]	1 - 8 !	none	0.400	****	****	Non fittable, from averages
599	3	[1.10, 1.70]	1 - 11	none	0.382	5.90	-1.5	
603	3	[1.10, 1.70]	1 - 13	none	0.329	9.55	-0.8	All 13 pts, no correction
603	3	[1.10, 1.70]	1 - 13	#4, 7	0.335	9.06	-0.7	2 pts replaced
586	4	[0.80, 1.30]	1 - 8 !	????	0.370	****	****	Non fittable, from averages
591	4	[0.80, 1.30]	1 - 10	none	0.393	4.96	-2.2	
593	4	[0.80, 1.30]	1 - 10	none	0.347	5.37	-2.4	No correction, 10 pts
593	4	[0.80, 1.30]	1 - 11	none	0.349	4.41	-2.5	No correction, 11 pts
594	4	[0.80, 1.30]	1 - 11	none	0.331	5.03	-1.9	
601	4	[0.80, 1.30]	1 - 11	none	0.299	4.63	-2.5	No correction
601	4	[0.80, 1.30]	1 - 11	cfe*	0.296	5.02	-2.3	1 pt replaced
602	4	[0.80, 1.30]	1 - 13	none	0.389	6.00	-0.7	All 13 pts, no correction
592	5	[0.80, 1.30]	1 - 11	none	0.362	2.98	****	Too flat to know the center
600	5	[0.80, 1.30]	1 - 11	none	0.294	3.28	-2.5	No correction
600	5	[0.80, 1.30]	1 - 11	cfe*	0.293	3.54	-2.3	1 pt replaced
588	6	[0.85, 1.35]	1 - 11	none	0.484	3.14	-2.8	No correction
588	6	[0.85, 1.35]	1 - 11	cfe*	0.483	3.14	-2.2	2 pts replaced
598	6	[0.85, 1.35]	1 - 11	none	0.500	6.62	-2.1	No correction
598	6	[0.85, 1.35]	1 - 11	cfe*	0.497	7.23	-1.9	2 pts replaced

Table 4.4 - Nozzle Parameters by Parabola Fits (Conditions 1 to 6)

p_{min} vs h_0

The first step is obviously to plot the minimum pitot pressure p_{min} versus the reservoir specific enthalpy h_0, in order to compare with the "plots of conditions" (figures 4.1 and 4.2, in chapter 4.2), and to check if the classification by conditions is still valid, as far as the test section is concerned.

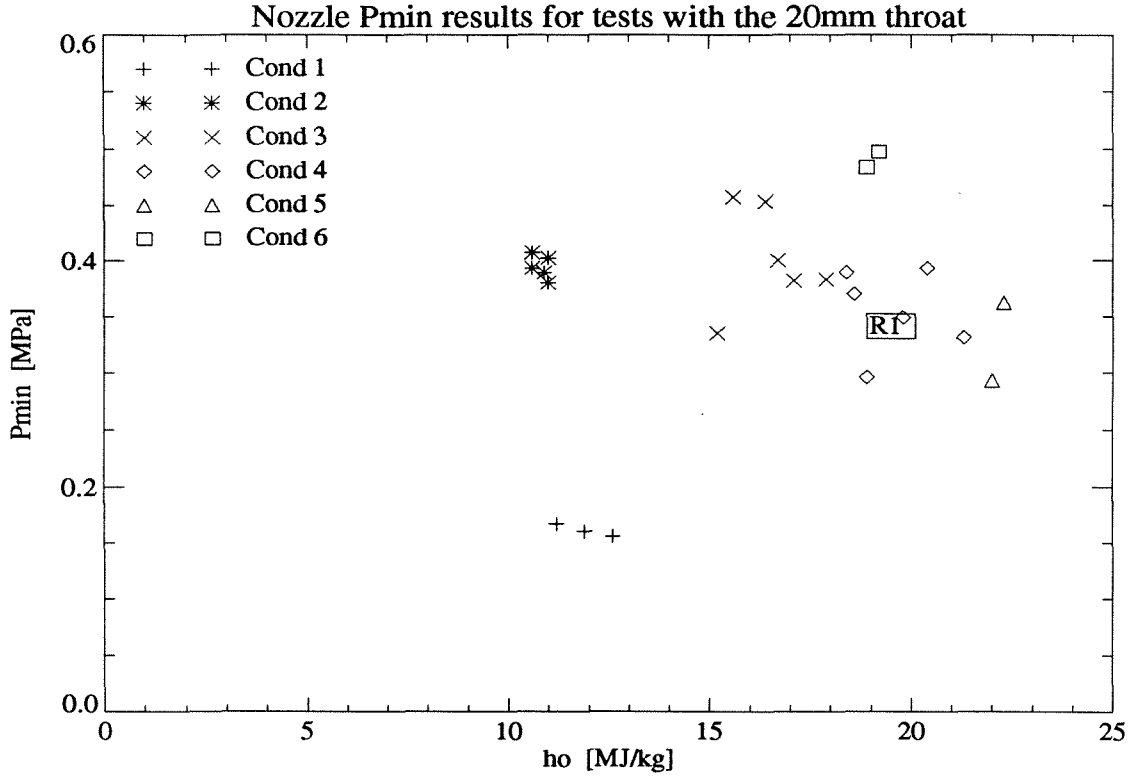

Figure 4.3. Minimum Pitot Pressure p_{min} vs h_0.

Successfully, the minimum pitot pressure follows the same partition (grouping), and thus the classification into conditions is indeed valid.

On one hand, some conditions (1, 2, 6) are visibly grouped, which is truly encouraging. On the other hand, the scatter of conditions 3 and 4 is quite large, but may be explained by the different filling pressures needed to reach these conditions, the burst pressures, and/or the recovery factors. The "R1 box" still stands in the middle of condition 4, meaning that the repeat series can be combined with the general 20mm throat one.

Since this plot (figure 4.3) looks very similar to the "plot of condition" p_0 *vs* h_0 (figure 4.2), except obviously for the pressure scales, it seems natural to want to investigate the scaling of p_{min} by p_0.

There is no obvious trend between the raw p_{min} and h_0, that can be inferred from the above plot.
Furthermore, some other studies (not included in this thesis) show no sensible variations of p_{min} with the axial position z, over the covered (limited) range.

p_{min} vs p_0

The following plot was therefore drawn in order to verify the scaling by p_0, and to point out some useful correlation between a test section parameter (p_{min}) and a T5 reservoir parameter (p_0).

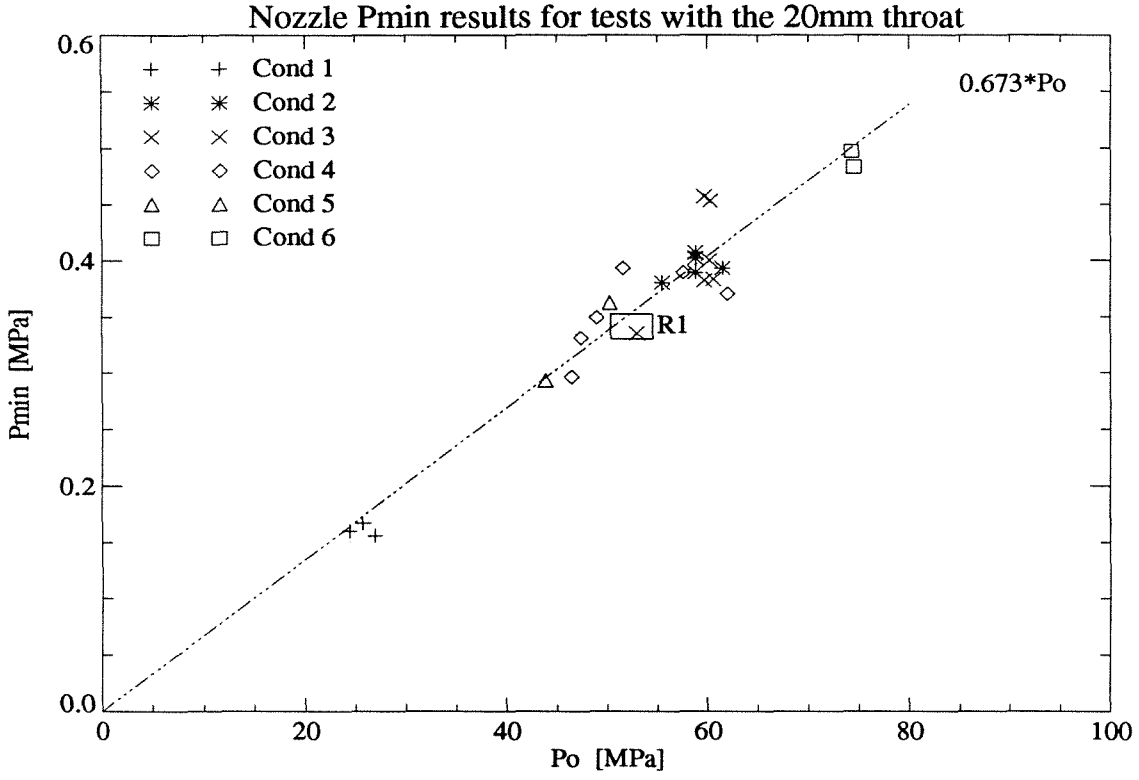

Figure 4.4. Minimum Pitot Pressure p_{min} vs p_0.

The following table presents some results on a linear and proportional correlation. In all cases, a least square fit was computed, and the standard deviation is around 0.02 MPa.

Notation : $p_{min} * 100 = a_0 + a_1 * p_0$

p_{min}, p_0, *and* a_0 *in* $[MPa]$, a_1 *dimensionless*

Constraint	a_0	a_1
24 pts & R1 free	-0.279	0.678
adding (0,0) as a pt	-0.157	0.676
(0,0) weighted 25	-0.014	0.673
passing through (0,0)	-0.000	0.673

Coefficients for different least-square fits

That is to confirm that these two parameters are indeed proportionally correlated, and therefore one is justified in studying the ratio p_{min}/p_0.

p_{min}/p_0 vs h_0

So was the minimum pitot pressure scaled by the nozzle reservoir pressure, and the ratio p_{min}/p_0 studied, versus the two reservoir parameters h_0 and p_0, in search of some secondary correlations or trends.

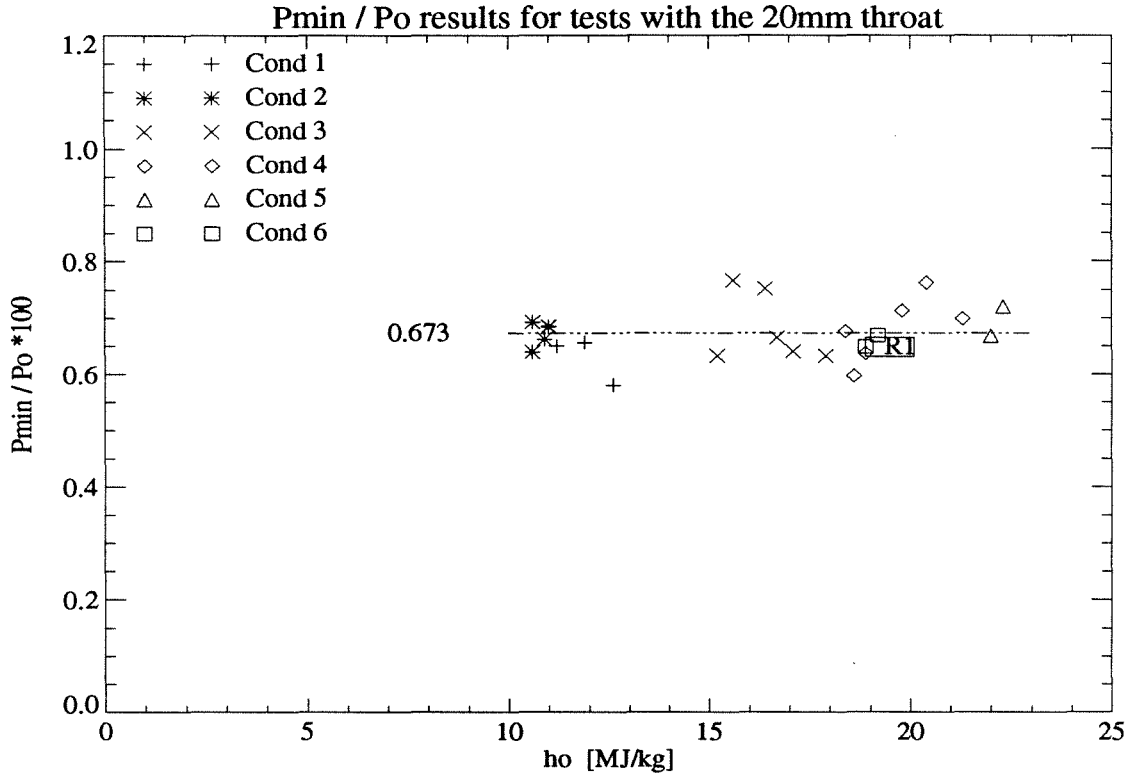

Figure 4.5. Scaled Minimum Pitot Pressure p_{min}/p_0 vs h_0.

According to this plot, the ratio p_{min}/p_0 appears to be quite constant. On one hand, it means that the two parameters p_{min} and p_0 can indeed be considered as proportional - in other terms, the correlation line (on figure 4.4) can be considered as going through the origin. On the other hand, it shows that this ratio is independent of h_0, at least on the covered range.

Constraint	average,	deviation
avg of 24 pts & R1	0.671	6.9 %
least-square fit	0.673	6.8 %

Average & least-square fit, of p_{min} / p_0

Note that it is not what one should expect from computational grounds. Actually, according to SURF simulations, this ratio $p_t(0)/p_0$ should increase with h_0 (see figure 7.3 in section 7).

p_{min}/p_0 vs p_0

Finally, the ratio p_{min}/p_0 was plotted versus the nozzle reservoir pressure itself, in order to check if there were some higher order dependence.

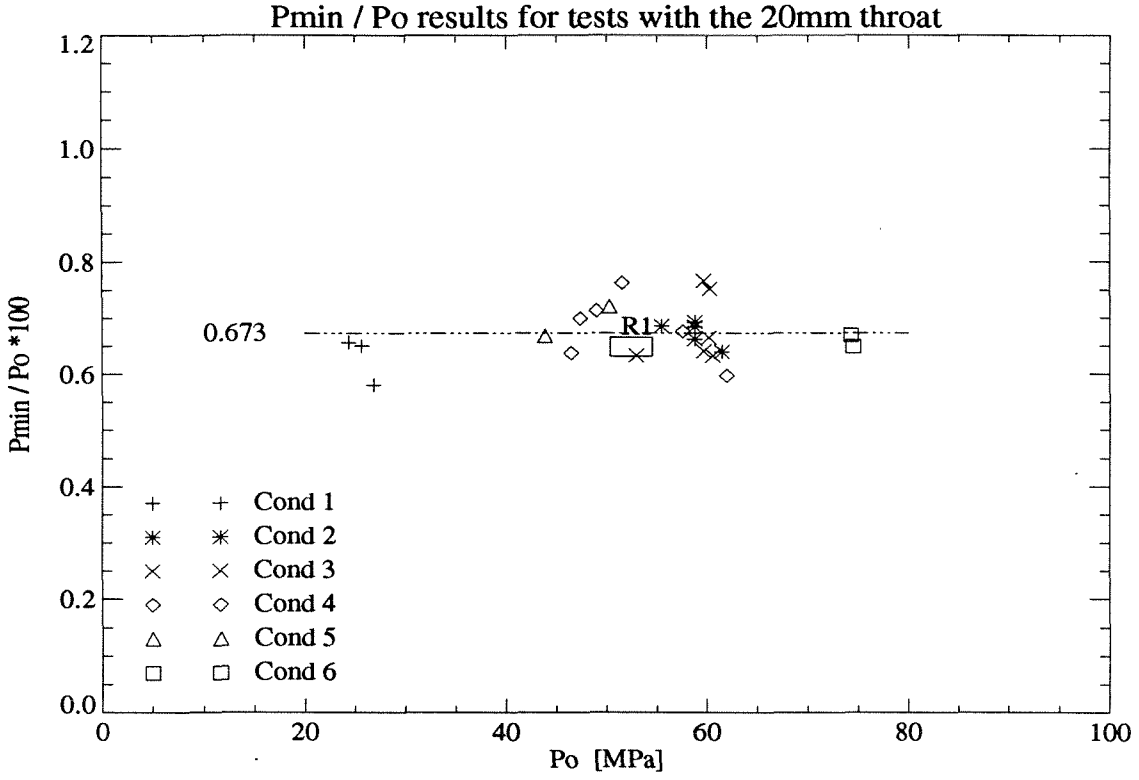

Figure 4.6. Scaled Minimum Pitot Pressure p_{min}/p_0 vs p_0.

The above figure clearly shows that there is no other major dependence of the ratio on p_0, in the range considered.

Conclusion on p_{min}

From the preceeding study, it seems clear that the nozzle parameter p_{min} has to be scaled by the T5 reservoir parameter p_0, and that ratio is independent of h_0 and p_0, at least over the envelope covered by the common conditions in T5, with the 20mm throat (area ratio of around 225), and for air as the test gas.

So, in a first approximation (7%), one can apply :

$$\frac{p_{min}}{p_0} = \frac{0.673}{100}$$

for p_0 = [20, 80] MPa, h_0 = [10, 23] MJ/kg, and with the 20mm throat (area ratio of 225). The above result holds only for air as the test gas and for the present T5 contoured nozzle.

4.3.3. Curvature "a" along the Radius (vs h_0, vs p_0, & scaled)

Recall that, what is called "curvature" is in fact only the coefficient "a" of the second order term in the parabola development, defined as follows :

$$p_t(r) - p_{min} = a.\, r^2 , \qquad a \text{ in } [MPa/m^2]$$

It has not been scaled by a (squared) distance for three main reasons. First, the exit radius could be a good candidate, but anyway, it is a constant for the present T5 nozzle (fixed exit radius of 15.7cm). Also, it is not clear at this time, which (or how) characteristic lengths of the contoured nozzle influence the curvature "a", and would be more appropriate for the scaling. Finally, the above formula, with the raw curvature, gives directly the maximum deviation of the pitot pressure distribution for a given model radius. Since it corresponds to the deviation between the model nose on the centerline and the edges, it relates the maximum size of the model to the maximum allowed deflection of the upstream flow.

Since this coefficient "a" is at the same algebraic level as p_{min} (keeping the radius position independent), a similar scheme was followed, studying the curvature versus the two reservoir parameters, first raw and then scaled by p_0.

"a" vs h_0

Just as was first done for the minimum pitot pressure p_{min}, the first plot shows the curvature "a" versus the reservoir specific enthalpy h_0.

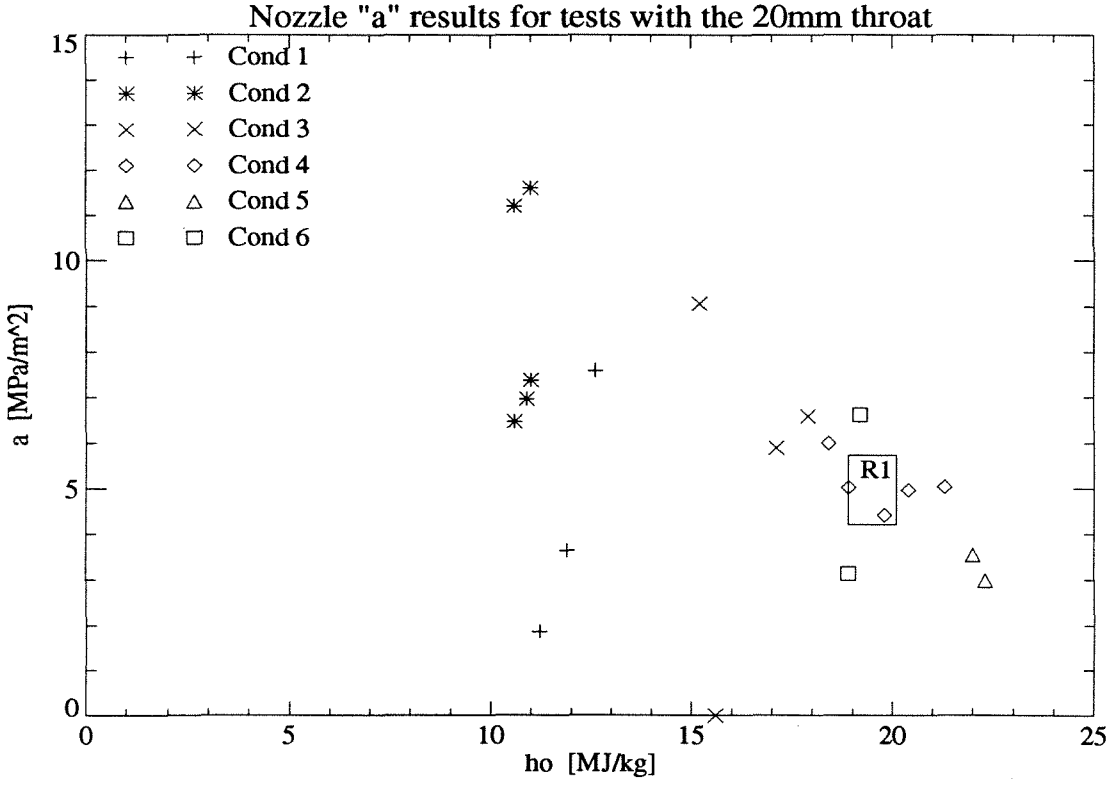

Figure 4.7. Curvature "a" vs h_0.

Some first remarks can be pointed out from this plot (figure 4.7). A large scattering can be observed for low values of h_0 (10-12 MJ/kg), but the opposite is true for high values ($h_0 > 17$ MJ/kg). Despite this scattering, the plot exhibits a clear decreasing trend of the raw curvature "a" with h_0. In other words, the pitot pressure distribution is more uniform for high enthalpies. Note that the contoured nozzle was designed for high h_0 ! Also, the R1 box lies again in the middle of the other points from condition 4.

"a"/p_0 vs h_0

The scaling of the minimum p_{min} by the nozzle reservoir p_0, and more generally of the pitot pressure distribution, applies also to the curvature "a", as follows :

$$\frac{p_t(r)}{p_0} - \frac{p_{min}}{p_0} = \frac{a}{p_0} . r^2$$

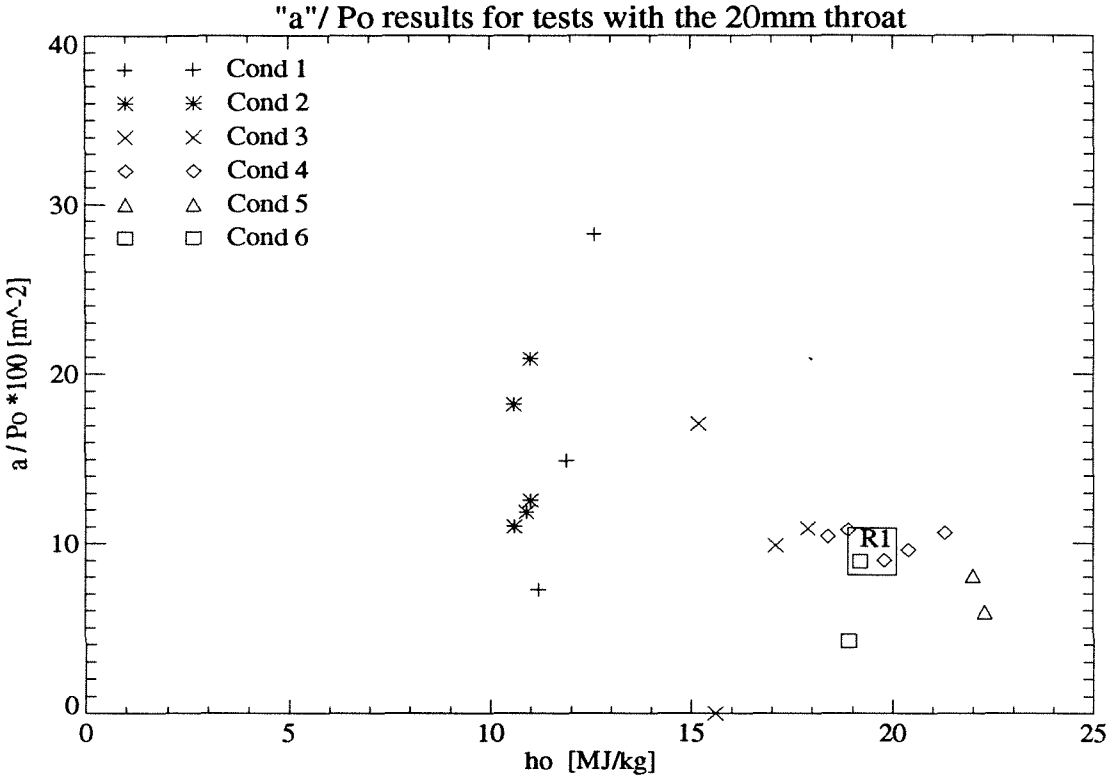

Figure 4.8. Scaled Curvature "a"/p_0 vs h_0.

As expected, this plot (figure 4.8) is similar to the previous one. The same remarks still apply for the scaled curvature, especially the decreasing trend with enthalpy.

This ratio $a/p_0 * 100$ in [m^{-2}] is easily related to the deviation (in %) of the pitot pressure distribution with respect to the minimum, at a radius of 10cm (order of magnitude of the maximum size of a model), by the following derivation :

$$\Delta = \frac{p_t(r = \pm 10cm) - p_{min}}{p_{min}} = \frac{a.\, r^2}{p_{min}} = \frac{\frac{a}{p_0}}{\frac{p_{min}}{p_0}} . r^2 = \frac{\frac{a}{p_0} * 100}{\frac{p_{min}}{p_0} * 100} . 10^{-2} = \frac{\frac{a}{p_0} * 100}{constant} . \%$$

For shots using the 20mm throat, and air as the test gas, the constant is 0.673 .

"a" & "a"/p_0, vs p_0

The curvature (raw and scaled by p_0) is then studied versus the other T5 reservoir parameter p_0.

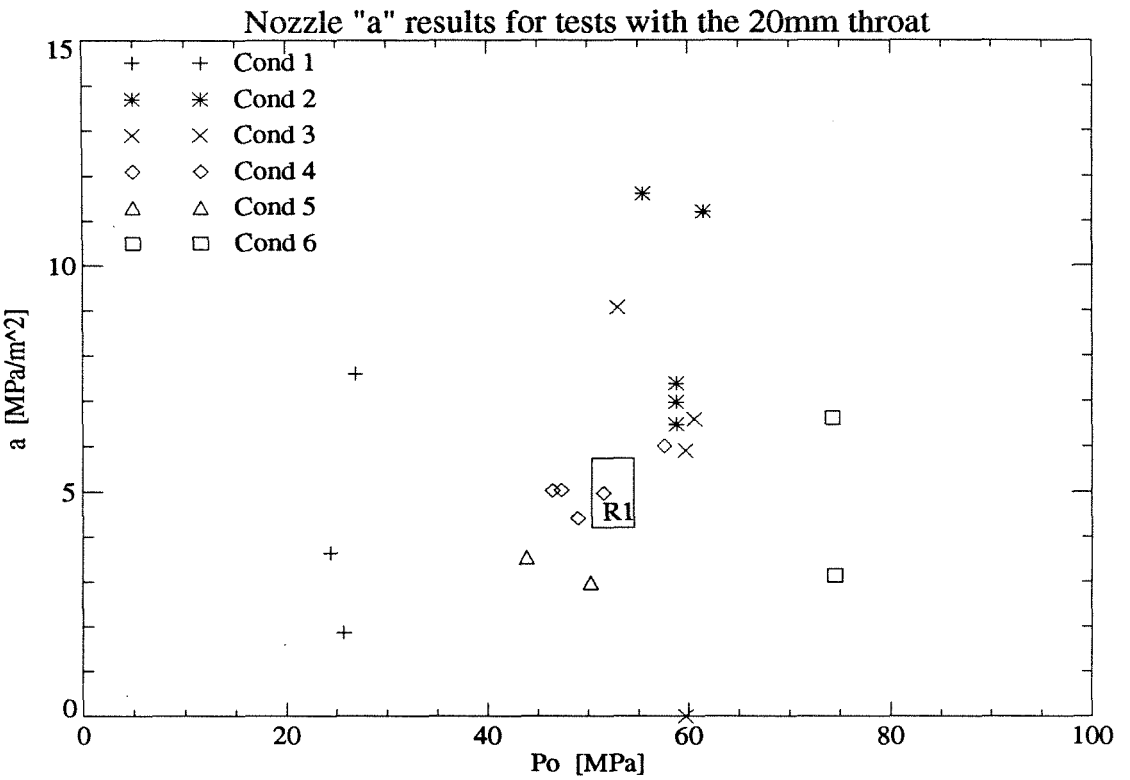

Figure 4.9. Curvature "a" vs p_0.

No obvious trend depending on p_0 appears for the raw curvature on the above plot (figure 4.9). A large scattering is present for all pressures. The discrete p_0 range is due to discrete diaphragm burst pressures.

When non-dimensionalized (see next plot, figure 4.10), despite the scattering that is still present, the curvature a/p_0 seems to slightly decrease with p_0. But this last remark should be taken with caution, since there are very few points for low p_0 (three points around 25 MPa) or for high p_0 (two points around 75 MPa), and furthermore these points are quite different, leading to large standard deviation (especially for low pressure).

Overall, except for condition 1 (low pressure, low enthalpy), the scaled curvature $a/p_0 * 100$ is on the order of 10, which means that the maximum deviation of the pitot pressure distribution with respect to the minimum value (located on the symmetry axis close to the nozzle centerline) is on the order of [10/0.67]%, i.e. 15%.

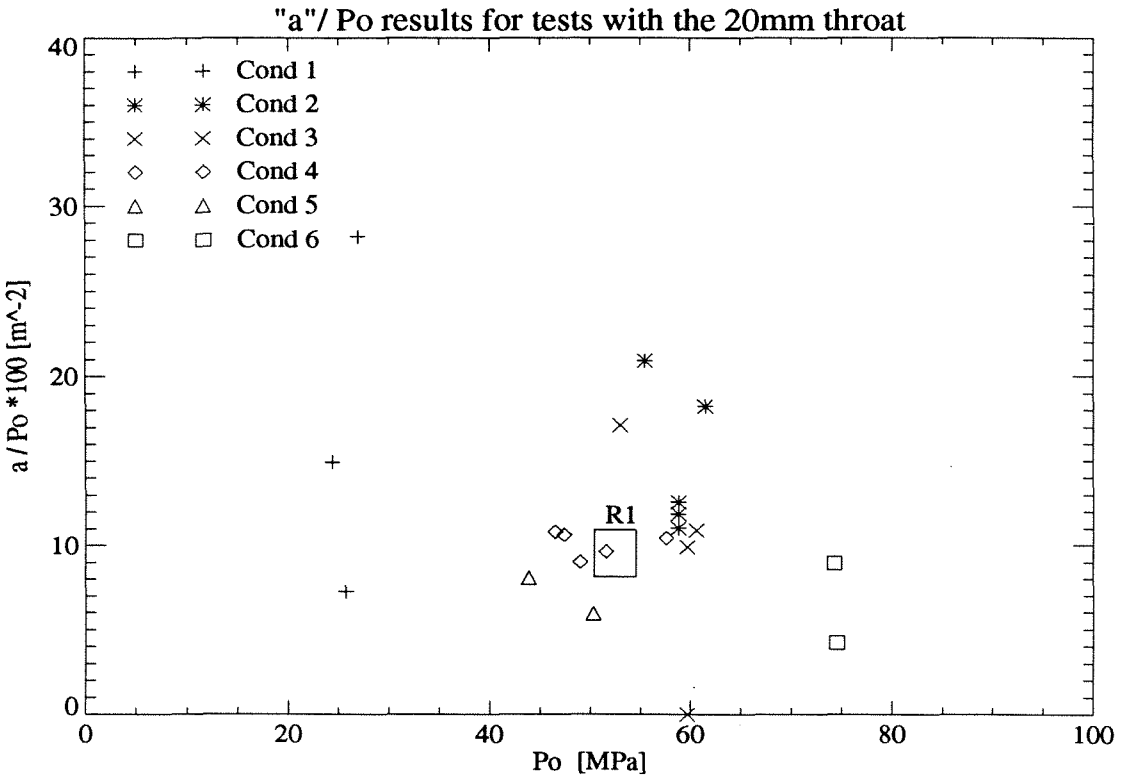

Figure 4.10. Scaled Curvature "a"/p_0 vs p_0.

Conclusions on "a"

Because of a large scattering in the curvature "a" for a given condition (h_0, p_0), it is difficult to set out definitive and precise conclusions. However, certain trends have been pointed out.

When using the 20mm throat (area ratio around 225), and air as the test gas, the curvature of the pitot pressure distribution, raw "a" or scaled a/p_0, is decreasing with the reservoir specific enthalpy h_0. Also, it seems that a/p_0, is slightly decreasing with p_0. As a lower curvature corresponds to a more uniform pitot distribution, the nozzle, which is designed for high enthalpy and an area ratio of 100, seems to perform quite well even at the off-design area ratio of 225 specifically at high pressure, high enthalpy.

After the multiple explanations (through the preceding study) on the role of the so-called curvature "a", and the properties of the scaled parameter a/p_0, it should be clear that this parameter is a quite good and simple way to describe the parabolic-shaped pitot pressure distribution with respect to the minimum p_{min}.

Finally, it is thought that the boundary layer (BL) thickness may influence the curvature. The very slight trend with p_0 may be evidence of this effect. A higher p_0 may decrease the boundary layer thickness (Reynolds number effect), and thus, may decrease the scaled curvature a/p_0.

4.3.4. Symmetry Axis X_s

The following plots (including those in the next paragraph 4.3.5) use the axial position "z" [cm]. It is the distance from the nozzle exit plane to the level of the pitot tips of the rake during the test time. To derive this value for a given shot, one needs to know the nozzle recoil (with respect to the fixed test section), which is studied in the next section 4.3.6.

For a given shot, the parabola fit gives a third parameter, the distribution symmetry axis, which surprisingly does not always correspond to the nozzle centerline. Following is the plot of these gaps (between the two axes) versus the axial position Z. Negative X_S means that the flow symmetry axis (in terms of the pitot pressure distribution) is above the geometric center of the nozzle (centerline). Negative values of Z mean that the pitot tips were inside the nozzle (even during the test time).

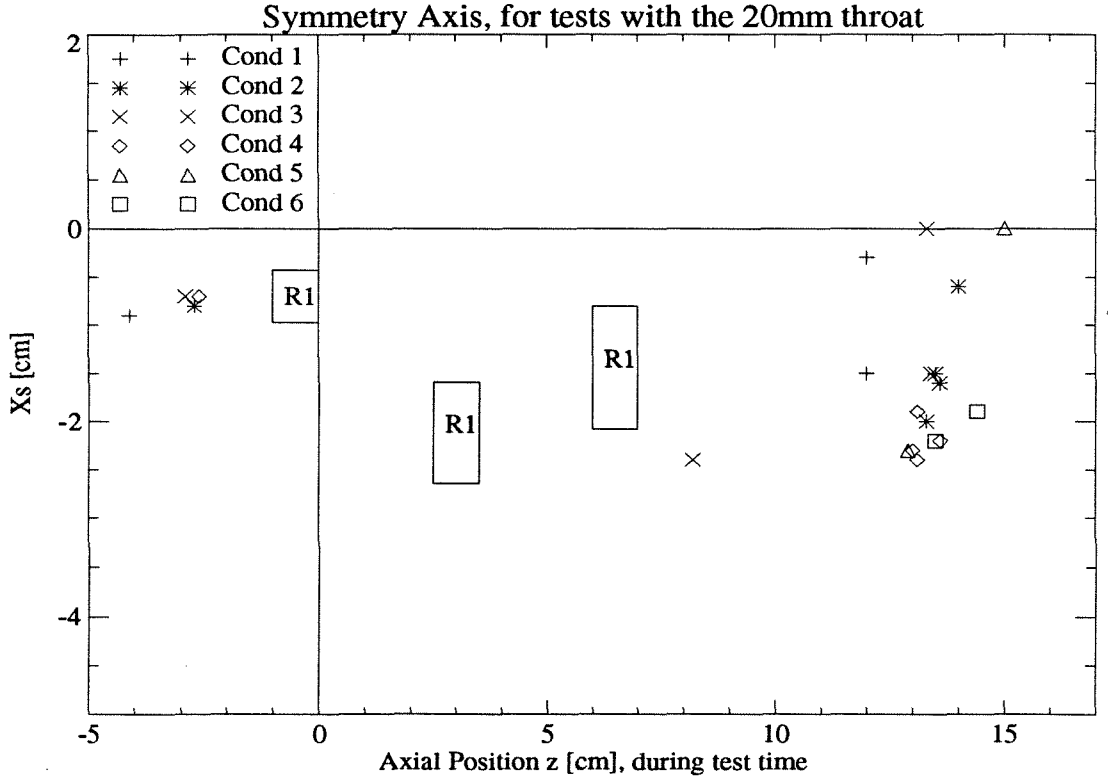

Figure 4.11. Symmetry Axis X_S vs Axial Position Z.

No definite explanation about this notable gap between the two axes, which should obviously match in theory, can be presently proposed. The error bar is considered to be of the order of half the spacing between two pitot tips, i.e. 1 cm. While in few cases the two axes match almost perfectly, most of the time the gap is on the order of 2 cm. The rake center level with respect to the nozzle centerline, has been checked several times, and furthermore, for almost every shot, the distribution symmetry axis converges to the nozzle centerline after the steady period.

Apparently, the problem may be related to the non uniform boundary layer thickness. It seems that the boundary layer (or expansion fan) is thicker at the bottom than at the top. However, it has been impossible to check if the bottom part of the nozzle (never rotated) was indeed rougher than the top part.

It was also thought that poor initial vacuum levels may be the cause. Due to some leaks in the dump tank, and therefore the test section, this may prevent proper nozzle starting. Recall that the rake R13 is fixed to the test section by the bottom, in a quite blocking way for the coming flow. It also covers the whole bottom radius, but only a part of the top one (depending the number of spacers). There is nothing stopping the flow on the top of the pitot rake.

But comparing some shots performed during the fourth series, one with an excellent vacuum level free of leaks and one with about one tenth of an atmosphere, shows indeed a completely different initialization process (worse for the "bad" vacuum level), but no significant change as far as the flow symmetry is concerned. Also, the flow photographs show clean shock wave on the pitot probes during the test time.

Finally, one has to be aware that the contoured nozzle has not been designed for use with the 20mm throat (area ratio of 225) but the 30mm throat (area ratio of 100). In other terms, the conditions presented in the present section are performed off-design and there is indeed a better match between these two axes when using the 30mm throat (see section 5).

4.3.5. Boundary Layer - External Layer - Core

When calibrating the pitot pressure distribution and its deviation (along the radius), another concern, that arises immediately after, is the extent of this distribution. In other terms, it is also important to know the core diameter, the boundary layer thickness, and the extent of the expansion fan, in order to properly size a model.

Even though it was not of prime concern, it is possible to evaluate these dimensions with the available data. In fact, these measurements are only based on the bottom part, since the lowest part of the rake was under the nozzle for several shots. Both the distributions and corresponding fits, as well as the contour plots, have been used to determine the core radius within 1 cm.

All these dimensions, characterizing the flow in general, are based only on the available pitot pressure distributions. For a given distribution, a "limit" is estimated where the pitot pressure drops quite suddenly (after the general curved increase). The "inside" part (toward the centerline) is called the core or flow layer. The "external" part is called, in a general way, the external layer, and more precisely, boundary layer if the rake is still inside the nozzle, and expansion fan if outside. The boundary layer thickness is simply computed as the nozzle (inside) radius (15.7 cm) minus the core radius.

Core - "Flow Layer"

As explained above, the only dimension one may obtain from the data contour plots, is the bottom core radius with respect to the nozzle centerline. It is plotted versus the axial position Z of the rake, with respect to the nozzle exit plane during the test time.

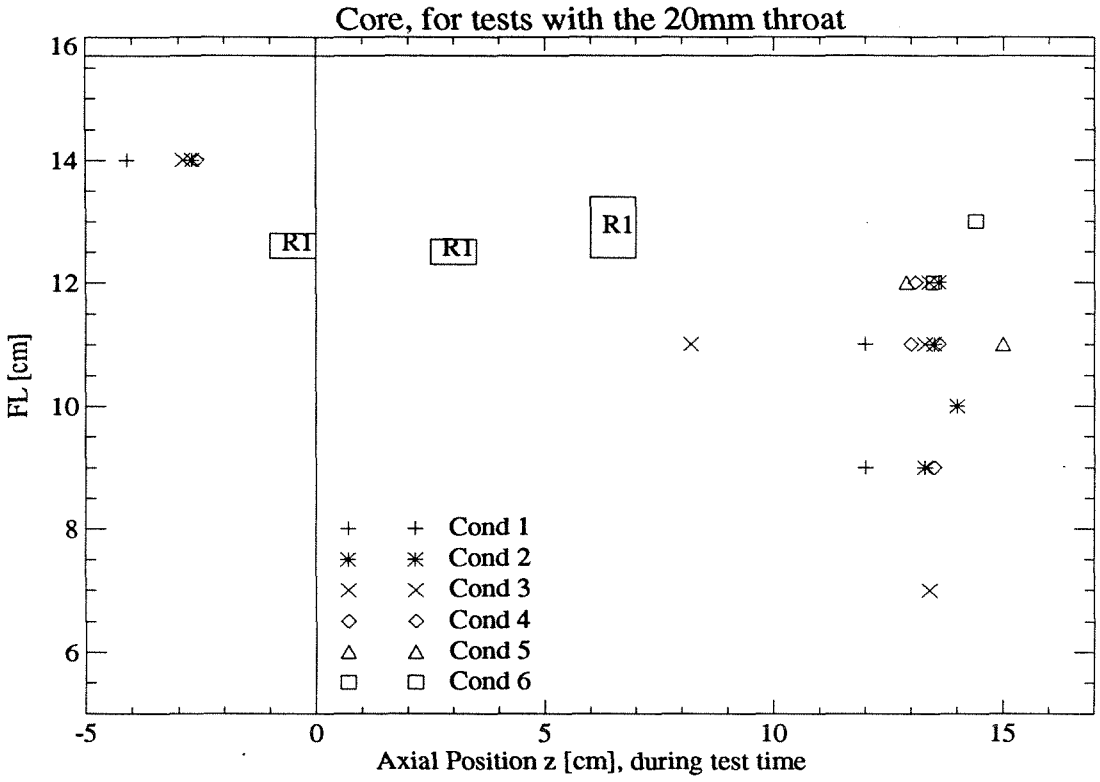

Figure 4.12. Core FL vs Axial Position Z.

Actually, when the rake is inside the nozzle ($Z < 0$), there is no notable limit (boundary layer not resolved) on the contour plots, so the core radius had to be roughly estimated somewhere between 12 cm (lowest pitot tip) and 15.7 cm (nozzle radius). It is represented arbitrarily by a 14 cm value.

The large scatter for the different conditions further downstream (at large Z) prevents any precise conclusion. It is associated, to some extent, with the flatter pitot pressure distribution observed there, and the consequently less well-defined limit. However, one can observe that the expansion fan reduces the core when going away from the nozzle exit. For Z between 12 and 15 cm, which is the usual location for a model during the recoil, the core is roughly 10 cm ($\pm$ 2 cm), thereby limiting severely the model diameter.

Boundary Layer

As show on the above plot (figure 4.12), there is no significant value characterizing the boundary layer thickness, except for a few points from the "R1" condition. When using the 20mm throat, and air as the test gas, the boundary layer (BL) is roughly on the order of 2 to 3 cm thick.

4.4. Conclusions on the Calibration and Use of the 20mm Throat, with Air as the Test Gas

Through the second series of tests, performed during the summer of 1993, the major part of the common T5 envelope of conditions has been calibrated in terms of pitot pressure. Furthermore, the results from the repeat series (presented in the previous section) have been included without any difficulty.

The new way of describing the pitot pressure distribution, using a parabola fit instead of the usual average and standard deviation, has turned out to be quite effective.

The minimum pressure p_{min} was found to be highly correlated, and even proportional to the nozzle reservoir pressure p_0. The ratio p_{min}/p_0 appears to be also independent of the reservoir specific enthalpy h_0. On the covered envelope, which extends over the same area as the common T5 envelope, using the contoured nozzle with the 20mm throat (off-design area ratio around 225), and air as the test gas, this ratio can be considered as independent of the reservoir condition, and is approximated by the constant 0.67/100 (within ± 7%).

The so-called "curvature a", in fact the second order coefficient of the parabola, is in a first approximation, half of the true curvature. It was introduced in order to better characterize the deviation of the pitot pressure distribution with respect to the minimum. It was studied both raw and scaled by p_0, following the study of the minimum p_{min}. In both cases, a large scatter is present, especially for low h_0 and low p_0. However, some major trends are noticeable. The raw curvature (a) or scaled (a/p_0), is decreasing with h_0. The scaled a/p_0 is also slightly decreasing with p_0. With the 20mm throat (area ratio around 225), and using air as the test gas, the order of magnitude of a/p_0 is 10/100 m^{-2}.

The study of the third parabola parameter, i.e. the location of the symmetry axis, is more controversial. The symmetry axis of the pitot pressure distribution, which is considered to be the flow symmetry axis, does not match the nozzle centerline. The difference is about 2 cm. In all the cases, the flow symmetry axis is above the nozzle one. This "shift" still remains unexplained.

Finally, it has also been possible to evaluate the core diameter, and the extent of the expansion fan, still in terms of pitot pressure distribution. Also, an upper limit of the boundary layer thickness has been roughly estimated.

SECTION 5 :

Calibration of the T5 Nozzle

with the 30mm Throat

(Area Ratio of 100),

using Air as the Test Gas.

5.0. Outline of Tests

The 20mm throat was mostly used for some of the ESA tests investigating lower densities, and calibrated mainly for that purpose. However, the nominal design of the T5 contoured nozzle is based on an area ratio of 100. In fact, the common conditions performed on T5 require the use of the 30mm throat. Therefore, the prime concern of this research is to calibrate that particular nozzle in such a configuration.

Shots have been performed during two different series, one year apart, referred to as the first and fourth series. The first series, in April 93 (shots 447 to 465), was the first ever made, using the new R13 rake. This gave a first general idea about the flow quality at the nozzle exit, where models are usually located. However, during the two following series using the 20mm throat (second and third series, presented in the previous sections), additional questions were raised about centerline focusing effects and flow symmetry. It was decided consequently to run a new series to study these new points, and at the same time, to check previous results from the first series.

This fourth series was performed in April 94 (shots 691 to 717). Obviously, there are some differences with the first series. The fourth one was carried out more carefully, as far as the vacuum levels are concerned, and how the conditions were set up. The shots were also much closer to the "tailored interface" condition. The piston motion had also been improved [Bélanger, 1994], leading to better recovery factors. Furthermore, for the fourth series, all the electrical connections, and especially the ones linked with the rake, were greatly improved.

Between these two series, new techniques to reduce the data and new visualizations were developed in order to better understand and characterize the flow at the nozzle exit. The data from the first series were reworked accordingly.

No series was dedicated to specifically studying the repeatability of a given condition, using the 30mm throat. The series conducted with the 20mm throat is thought to be enough to prove the good repeatability of T5. Nevertheless, the repeatability with the 30mm throat can be visualized on the following plots in this section, since for a given condition, the points are grouped together.

In this section, only the shots using air as the test gas are presented. The other test gases are presented in the following section 6.

Finally, it is important to note that "30mm throat" and "area ratio of 100" are only general denominations used in T5. The actual minimum throat diameter is designed at 1.1840 inch, corresponding to 30.074 mm. The nozzle exit diameter is 314 mm, leading to a nominal area ratio of 109. Some variations also occur depending on the number of shots, and their enthalpies, and as a result of crack level of the throat.

5.1. History of Shots and T5 Parameters Results

This section presents the shots tested with the 30mm throat, but exclusively using air as the test gas. Tests with other gases are presented in the following section. These shots were performed during the first series (shots 447 to 465) and the fourth series (shots 691 to 717).

A complete history of these two series, shot by shot, can be found in the tables 5.1.1 and 5.2.2 . These tables give information on how the condition was set up, the exact position of the rake before the shot (i.e. before recoil), and some remarks or modifications. Explanations and symbols regarding the following tables can be found in Section 4 (Ch 4.1 History of Shots 581 to 605).

	Positions		Filling Conditions			
Shot	**Axial**	**High**	**ST**	**CT, %He**	**2R**	**Comments**
#	**cm**	***3/4″**	**kPa**	**kPa**	**psig**	
447	1 (Out)	0.0	40, Air	145, 100%	630	As shot 331 & 1cm out before recoil
	New nozzle, piston					
448	no change	0.0	85, Air	116, 85%	1110	As shot 351
449	no change	0.0	85, Air	116, 85%	1110	Tips clean down to 8, dirty on 9.. 13
451	no change	0.0	50, Air	116, 95%	1120	As shot 160
452	no change	0.0	50, Air	116, 95%	1120	Open tips diameter @ .031"
453	no change	0.0	50, Air	116, 95%	1120	
454	no change	0.0	40, Air	116, 100%	1110	NaCl drops
455	no change	0.0	40, Air	116, 100%	1110	
456	no change	+0.5	40, Air	116, 100%	1110	3/8" Rake up
457	no change	+0.5	40, Air	145, 100%	630	3/8" Rake up
	New piston, bearing					
458	no change	0.0	115, Air	143, 90%	1800	No spacer, initial position
459	no change	0.0	40, Air	145, 100%	630	
460	no change	0.0	50, Air	143, 100%	1720	
463	no change	0.0	20, Air	116, 100%	1110	
464	9 (Out)	0.0	50, Air	116, 95%	1120	Dirty tips only 11,12,13
465	11 (In)	+1.5	50, Air	116, 95%	1120	Rake up 3/4" + 3/8"

Table 5.1.1 - History of 30mm Air Shots, 1^{st} series, Shots 447 to 465

Shot #	Positions Axial cm	High *3/4"	Filling Conditions ST kPa	CT, %He kPa	2R psig	Throat mm	Comments
691	0.6 out	2.5	70, Air	116, 90%	**1250**	30	Buffers perfect, Cond. 2/3
692	0.6 out	2.5	30, Air	116, 95%	**1175**	**20**	Buffers OK, Cond. R1
	Piston leaked on 692 —> New front ring on the piston						
693	0.6 out	2.5	30, Air	116, 95%	1175	**20**	as 692, but bad vacuum (50mm Hg)
	Change end-plate and sleeve of the ST, P_0 holder South in Molybdynium, Transd. North #2474						
694	0.6 out	2.5	30, Air	116, 100%	1110	30	Med P_0, $21 < h_0 < 26$, Pb leak of ST
695	0.6 out	2.5	25, Air	116, 100%	**1150**	30	Med P_0, $23 < h_0 < 26$, real "LA" Air
696	0.6 out	2.5	30, Air	116, 100%	1150	30	Med P_0, $21 < h_0 < 24$, Buffers OK
697	0.6 out	2.5	45, Air	112, 100%	**800**	30	P_0 around 40 MPa, $P_4 = 52$ Mpa
698	0.6 out	2.5	**40**, Air	112, 100%	800	30	taylored 697
699	Triggered 200ms earlier, reason unknown, No Data						
700	0.6 out	2.5	**35**, Air	**80, 90%**	**450**	30	New cond. for low P_0, low h_0
701	0.6 out	2.5	35, N_2	80, 90%	**425**	30	As 700 but with N_2
702	0.6 out	2.5	70, N_2	116, 90%	1250	30	As 691 but with N_2
703	0.6 out	2.5	85, N_2	116, 85%	**1350**	30	Cond. 2 new 2R
704	0.6 out	2.5	85, N_2	116, 85%	**1120**	30	Cond. 2 as usual
	Change the 30mm throat, new = 30.20mm in molybdynium ; repear channel 1 cable						
705	0.6 out	2.5	25, N_2	116, 100%	1150	30*	As 695 but with N_2
	Copper on throat and rake -*- Change piston front ring and bearing (for high pressure shots)						
706	0.6 out	2.5	115, Air	**120, 90%**	**1500**	30*	New Cond 7
707	0.6 out	2.5	**90, Air**	120, 90%	1500	30*	Try to taylor 706
708	0.6 out	2.5	30, Air	143, 100%	1650	30*	Philippe's shot, Cond 6+
	New deposition of Copper on throat ; throat really cracked —> changed & stamped						
	North P_0 holder changed by a Molybdenun one ; New 30.05 mm Stainless-Steel-Copper throat						
709	0.6 out	2.5	100, CO_2	116, 80%	**1500**	30	P_4 higher than burst press.
	Change P_0 North transducer & amplifier by SN 2437 / 4768						
710	0.6 out	2.5	100, CO_2	116, 80%	**1300**	30	P_4 still higher than burst press.
711	0.6 out	2.5	65, CO_2	69, 75%	**525**	30	New cond. based on Wen's #509
712	0.6 out	2.5	**25, Air**	82, 100%	**510**	30	New cond. low P_0 high h_0 for JPD
713	0.6 out	2.5	**80, CO_2**	116, 80%	**1400**	30	Try to taylor #709/ 710
714	0.6 out	2.5	100, H_2	**70, 75%**	**360**	**14**	H2 shot for JPD with 14mm
715	0.6 out	2.5	75, CO_2	116, 80%	1400	**20**	20mm to compare with #713
716	0.6 out	2.5	99, H_2	70, 75%	360	**30**	H2 30mm to compare with #714
717	0.6 out	2.5	65, CO_2	69, 75%	525	**20**	20mm to compare with #711

Table 5.1.2 - History of 30mm Air Shots, 4^{th} series, Shots 691 to 717

As explained in section 2, the T5 parameters results were extracted from the data traces. They are listed in the two following tables. The two series have been separated, since they were performed one year apart. The notation is the same.

Notation : "%" $= \frac{P_{4,N}-P_{4,S}}{P_{4,N}+P_{4,S}} * 100$, for P_4 (standing for p_4). Similarly for P_0.

$P_{4,\,(N \text{ or } S)}$ is the maximum of the curve, smoothed on 15 pts, *i.e.* 0.5 ms.

V_S = Shock Speed between station 3 and 4;

h_0 is taken in a first approximation as $(V_S)^2$.

When "North" or "South" replaces the "%", it means that the average is only based on the respective trace. For example, for the first series, all the nozzle reservoir pressures p_0 are based exclusively on the north traces, since the south transducer was judged not to be reliable (this was determined after the tests, comparing the conditions with the ones for the fourth series).

Following are the results for the first series of April 93 :

	Burst Pres. (MPa)		Nozzle Res. (MPa)		(km/s)	(MJ/kg)	Test	Cond.
Shot	$P_{4,avg}$	%	$P_{0,avg}$	%	V_s	h_0	Gas	#
447	34.1	2.8	25.6	North	3.43	11.8	Air	1
448	84.6	2.2	59.0	North	3.31	11.0	Air	2
449	83.0	2.2	60.7	North	3.31	11.0	Air	2
451	81.6	2.5	62.0	North	4.05	16.4	Air	3
452	85.3	3.4	59.3	North	4.05	16.4	Air	3
453	79.5	South	57.9	North	4.05	16.4	Air	3
454	87.7	3.5	56.7	North	4.58	21.0	Air	4
455	87.5	3.0	56.7	North	4.48	20.0	Air	4
456	87.1	2.3	57.9	North	4.55	20.7	Air	4
457	34.6	2.5	25.5	North	3.59	12.9	Air	1
458	106.0	0.7	75.0	North	3.43	11.8	Air	7
459	34.6	0.2	22.9	North	3.59	12.9	Air	1
460	105.5	2.8	77.2	North	4.48	20.0	Air	6
463	84.1	2.9	56.2	North	5.13	26.3	Air	5
464	98.2	3.6	64.6	North	4.29	18.4	Air	3/4
465	88.1	4.1	67.6	North	4.14	17.1	Air	3/4

Table 5.2.1 - T5 Parameters, 30mm throat, Air, 1st series (Shots 447-465)

Following are the results for the fourth series of April 94 :

Shot	Burst Pres. (MPa) $P_{4,avg}$	%	Nozzle Res. (MPa) $P_{0,avg}$	%	(km/s) V_s	(MJ/kg) h_0	Test Gas	Cond. #
691	89.7	0.3	69.5	0.3	3.66	13.4	Air	2/3*
694	87.2	-0.0	56.2	-1.5	4.51	20.4	Air	5, ST leak
695	89.6	-1.0	58.4	-1.1	4.96	24.6	Air	5
696	101.8	-0.3	60.5	-1.0	4.80	23.0	Air	5
697	54.5	0.6	40.5	-1.8	3.87	15.0	Air	Interm P_0
698	53.2	0.5	39.6	-1.9	4.11	16.9	Air	Interm P_0
700	36.6	1.8	22.4	-1.6	3.26	10.6	Air	1*
706	113.4	-0.8	78.9	South	3.43	11.8	Air	7
707	107.4	-1.4	81.6	South	3.59	12.9	Air	7
708	106.9	-1.0	80.0	-0.8	4.88	23.8	Air	6+
712	43.4	1.2	27.3	-1.6	4.20	17.6	Air	New

Table 5.2.2 - T5 Parameters, 30mm throat, Air, 4th series (Shots 691-717)

5.2. Range of Covered Conditions for the Calibration

The burst pressure is not presented anymore in this section and the following ones, since it was seen not to be an important parameter for the calibration. It just represents a mean to obtain the desired nozzle reservoir pressure.

It may be useful to note that there is a slight difference, especially during the fourth series, between the diaphragm burst pressure (controlled by the diaphragm thickness and indentations), and the actual measured and recorded maximum p_4. The latter can be higher than the former, due to a better piston course (obtained by a better setting of the 2R pressure), still compressing after the diaphragm burst, leading to a better recovery factor (up to 75%), i.e. for the same condition, higher nozzle reservoir pressure and usually also slightly higher enthalpy.

Therefore, the tested conditions are hereafter only presented in terms of nozzle reservoir pressure p_0 versus the specific enthalpy h_0. They cover the whole range of common T5 conditions and even extend it, in order to investigate the whole accessible domain. The main constraint is the discrete diaphragm burst pressure values (35, 90, 110, and occasionally 45, and now 55 MPa). The enthalpy can be made between 10 and 25 MJ/kg easily, except for low pressure where the maximum is around 18 MJ/kg.

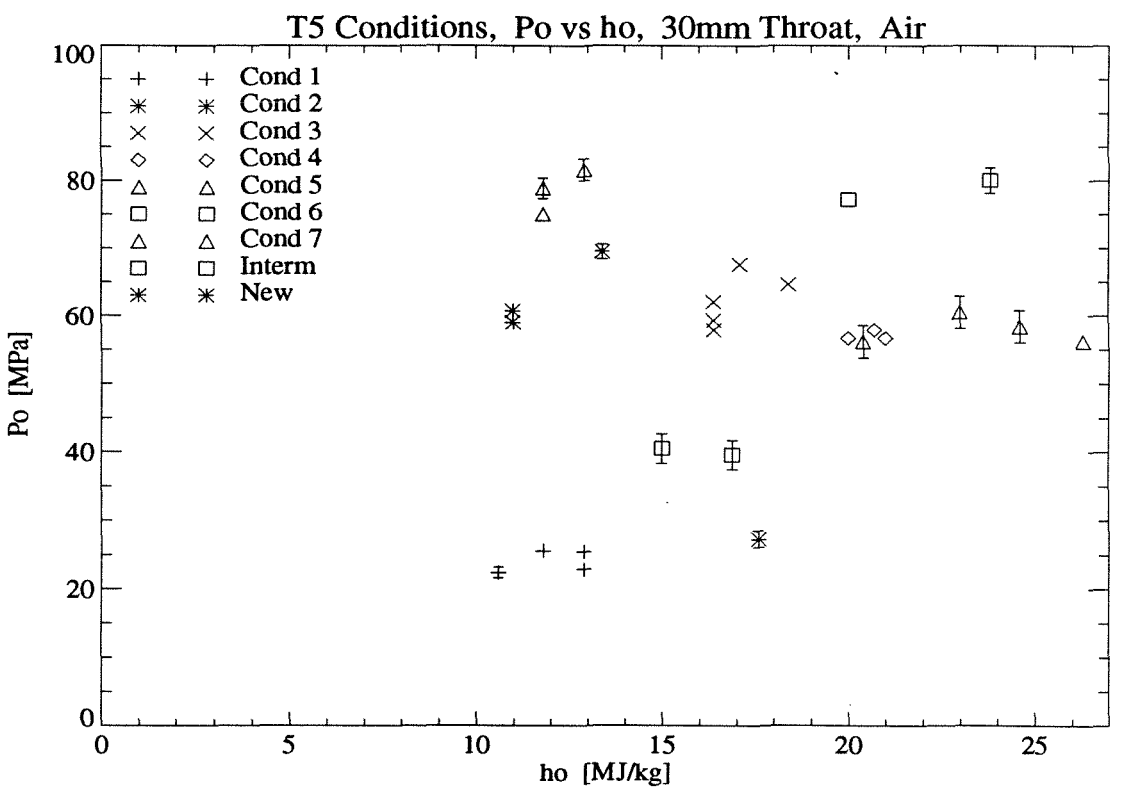

Figure 5.1. Conditions tested with the 30mm Throat, using Air.

The fourth series has been differentiated from the first one, by using error bars for the nozzle reservoir pressure. The enthalpy here is approximated by v_s^2.

5.3. Nozzle Calibration Results

The calibration study followed for the 30mm throat is very similar to the one for the 20mm. The general apparatus -machine, rake, transducers, data acquisition system- is exactly the same. The contents and the logic of this paragraph are therefore similar to the corresponding one of the previous section. The results of the first and fourth series have been grouped together, except when some notable differences appear between them.

5.3.1. Tables of Calibration Coefficients

Using the same techniques, for extracting the averaged steady values, and then fitting them by a parabola (techniques described in the previous sections), one can derive the following calibration results.

Shot #	Case #	Test time ms	Transducers fitted	Transducers replaced	P_{min} MPa	a MPa/m^2	Center cm	Comments
447	1	[1.30, 1.80]	1 - 7 !	2, 4	0.318	10.4	-0.9	(8, 9, 10) non useable
448	2	[1.30, 2.00]	1 - 10	2, 4, 9	0.791	16.5	-0.1	Cf time ave
448	2	[1.35, 2.05]	1 - 10	2, 4, 9	0.791	16.5	+0.1	See "a" anyway
449	2	[1.30, 2.00]	1 - 10	2, 4, 9	0.824	11.6	+0.5	"a" turbulent, see axis
449	2	[1.35, 2.05]	1 - 10	2, 4, 9	0.825	11.4	-0.7	Still pb with sym axis
451	3	[1.00, 1.60]	2 - 10	2, 9	0.821	23.5	-0.7	Pb with #1 non corrected
452	3	[1.00, 1.60]	1 - 10	9	0.812	12.9	-0.4	Good fit, ave a bit before ?
453	3	[1.00, 1.60]	2 - 10	none	0.841	8.32	-1.6	#1 out, curious "a", pb axis
454	4	[0.80, 1.30]	1 - 10	none	0.805	13.4	-0.3	Good fit
455	4	[0.80, 1.30]	1 - 10	none	0.780	13.2	+0.1	Good fit, really steady
456	4	[0.80, 1.30]	1 - 10	none	0.808	7.69	+0.7	Good fit, quite flat
457	1	[1.30, 1.80]	1 - 11	none	0.369	6.64	+0.8	Positive off-center
457	1	[1.30, 1.80]	1 - 10	none	0.368	7.00	+1.0	No real steady period
458	7	[1.10, 1.80]	1 - 10	none	1.059	17.9	+0.4	a & BL thickness almost cst
459	1	[1.30, 1.80]	1 - 10	none	0.334	5.76	-0.1	Nice steady period
460	6	[0.85, 1.35]	1 - 10	none	1.048	12.1	+0.1	flat
463	5	[0.70, 1.20]	1 - 7 !	none	0.765	0.87	-2.6	Big BL, really flat
464	3/4	[0.85, 1.40]	1 - 8 !	none	0.810	21.1	-2.1	Huge BL, jump in "a"
465	3/4	[0.85, 1.40]	1 - 12	none	0.849	13.9	-0.8	Rake inside, ave before ?

Table 5.3.1 - Nozzle Parameters by Parabola Fits, 1st series (Shots 447-465)

Shot #	Case #	Test time ms	Transducers fitted	repl.	P_{min} MPa	a MPa/m^2	Center cm	Comments
691	2/3	[1.15, 1.85]	2 - 13	5	0.903	13.3	-0.3	Pb with #1; #5 higher bc
694	4	[0.70, 1.20]	2 - 12	5	0.730	10.9	-1.7	ST leaking so cond 5 -> 4
695	5	[0.70, 1.20]	2 - 12	5	0.759	7.2	-1.2	LA Air, very high h_0
696	4/5	[0.70, 1.20]	2 - 12	*	0.781	8.8	-2.1	Negative center during test time
697	Int	[1.05, 1.75]	2 - 12	(5)	0.533	6.7	0.0	Really good symmetry
698	Int	[1.05, 1.75]	2 - 12	(5)	0.505	7.0	-0.0	Really good symmetry
700	1*	[1.30, 1.80]	2 - 12	*	0.290	4.5	+0.1	New Cond #1
706	7	[1.10, 1.60]	1 - 13	*	1.093	20.3	-0.8	Not tailored
707	7	[1.10, 1.60]	1 - 13	*	1.100	17.2	-1.0	Above cond. tailored
708	6+	[0.75, 1.20]	2 - 12	*	1.055	20.8	-0.6	Throat really cracked
712	New	[0.80, 1.50]	1 - 13	*	0.344	5.0	-1.1	Real L.A. Air, DT leaking

Table 5.3.2 - Nozzle Parameters by Parabola Fits, 4th series (Shots 691-717)

5.3.2. Minimum Pitot Pressure

Recall that the minimum pitot pressure represents, in a quite good approximation, the value on the centerline of the nozzle. It is the minimum of the parabola fit, lying obviously on the parabola symmetry axis, which is very close to the nozzle centerline (see paragraph on the flow symmetry).

This minimum is better defined for the fourth series (than for the first one), because the rake was positioned in the core, symmetrically around the centerline. Thus, more points are available for the parabola fit, and they exhibit the best balanced distribution for the study of the flow symmetry.

The study of the minimum pitot pressure p_{min} for the 30mm throat using air as the test gas, is similar to the one for the 20mm throat. p_{min} was first plotted versus the specific enthalpy h_0 , in order to check the distribution of the conditions and their repeatability. Then, p_{min} was plotted versus the nozzle reservoir pressure p_0 to check the correlation of these two parameters and to determine the constant of proportionality. Then, the dimensionless ratio p_{min}/p_0 was studied versus p_0 and versus h_0, to check for any other major dependence.

p_{min} vs h_0

As expected, the following plot of the minimum pitot pressure versus the specific enthalpy is similar to the one of the nozzle reservoir pressure (Fig 5.2.). The distribution

in the different conditions is therefore valid. Note that the repeatability, as far as these values are concerned, can be checked on such plots, since for a given condition the points are indeed grouped together.

The two series were not separated, even if the shots were conducted more carefully during the fourth series, leading to slightly different points for a given condition (higher pressure, higher enthalpy). In order to differentiate them, the points from the fourth series have been circled. Also, during the fourth series, new conditions have been investigated, specifically those labeled "interm" (intermediate p_{min}, around 0.5 MPa), and "new" (low pressure, medium enthalpy).

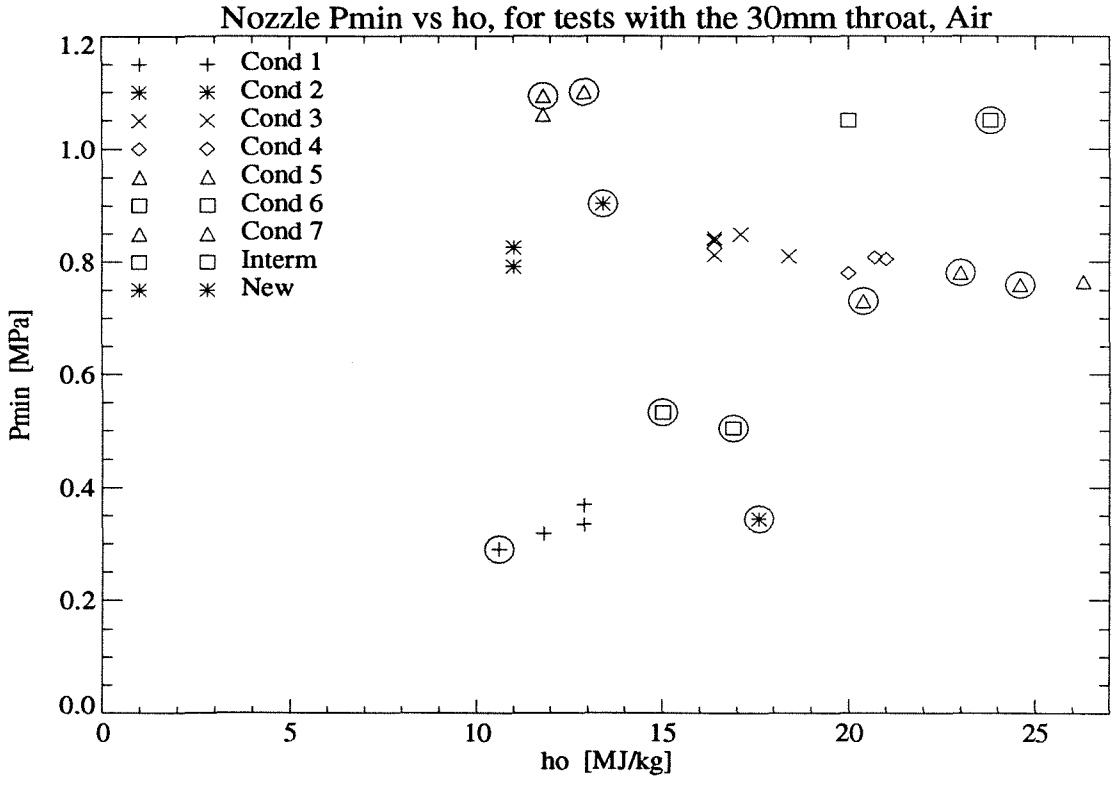

Figure 5.2. p_{min} vs h_0, 30mm Throat, Air.

Correlation plots : p_{min} vs p_0

Then, p_{min} was plotted versus the other reservoir parameter, namely the nozzle reservoir pressure p_0. As expected, these two pressures are highly correlated. For example, for the fourth series, taking into account all the points during the steady periods for all the shots, the correlation factor reaches 0.998.

Furthermore, as revealed on the following plot, they are simply proportional. The constant of proportionality does not seem to depend on the condition, meaning neither on the nozzle reservoir pressure p_0, nor on the specific enthalpy h_0, the only two reservoir parameters (for a given nozzle and test gas).

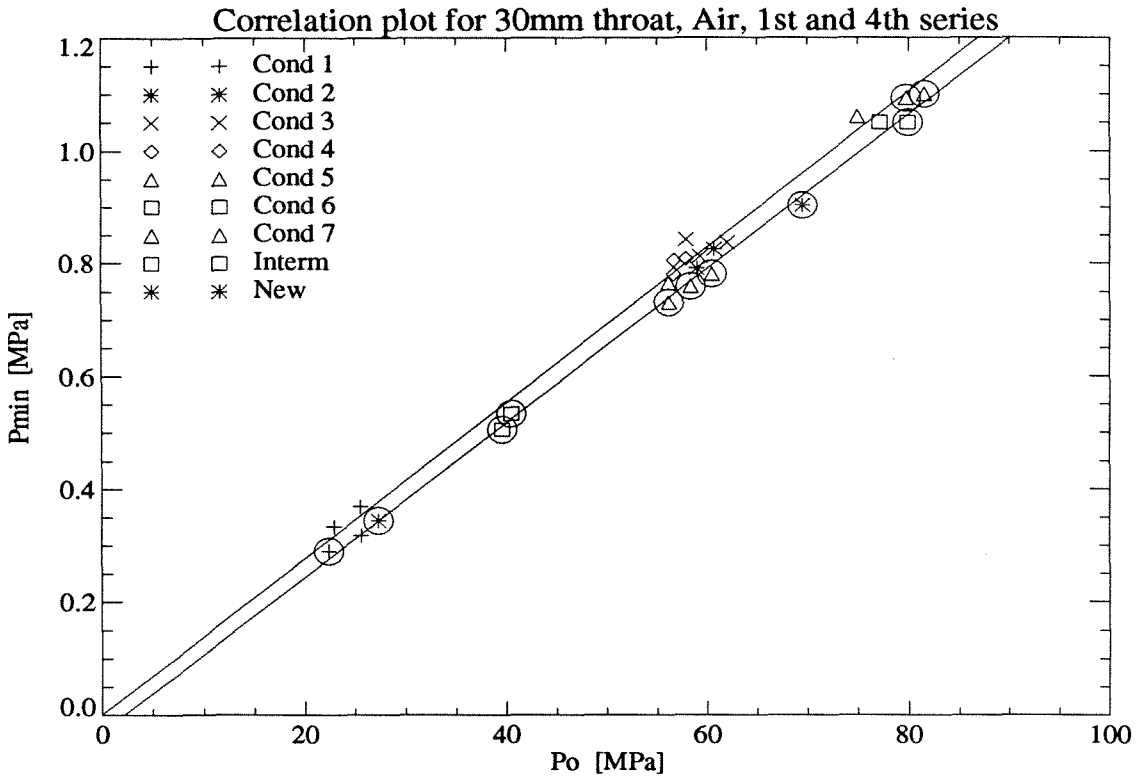

Figure 5.3. p_{min} vs p_0, 30mm Throat, Air.
Points from the fourth series have been circled.

While the points of the two series were not separated, each series was fitted separately.

Following are the equations of the two least squares fits :

For the first series :

$$p_{min} = 0.105\ E-02 + 1.379\ E-02 * p_0\ , \quad (stdev = 0.058)$$

For the fourth series :

$$p_{min} = -2.94\ E-02 + 1.366\ E-02 * p_0\ , \quad (stdev = 0.017)$$

There is obviously a small difference between the two series. While the slopes are identical, the least square fits lies on two different levels. For the first series, the fit can be considered going through the origin. However, for the fourth series, there is a 0.03 MPa shift (in terms of pitot pressure), although the points are more correlated and therefore the fit more accurate.

This shift can be explained in several ways. First, it has to be noted that it is of the order of the error bar of one minimum pitot pressure estimation. Then, the difference may be due to calibration of the nozzle reservoir pressure transducers. Also, only the north one was used for the first series. Finally, the throat design was slightly modified between the two series.

Regarding these results, only the slope is considered to be meaningful for these calibration shots. That allows one to non-dimensionalize the pitot pressure with the nozzle reservoir pressure. It is a constant, 1.37 E-02, with naturally some fluctuations from shot to shot on the order of 5%. The fluctuations do not seem related to the conditions. Actually, the ratio p_{min}/p_0 was studied in the following paragraph, in order to confirm that assumption.

Ratio p_{min} / p_0

The ratio p_{min}/p_0 was therefore studied in order to check for some noticeable dependence. The different value of the averaged ratio between the two series (1.38 and 1.31, respectively) is supposed to be related to the small shift. There is no definite explanation for that 5% difference.

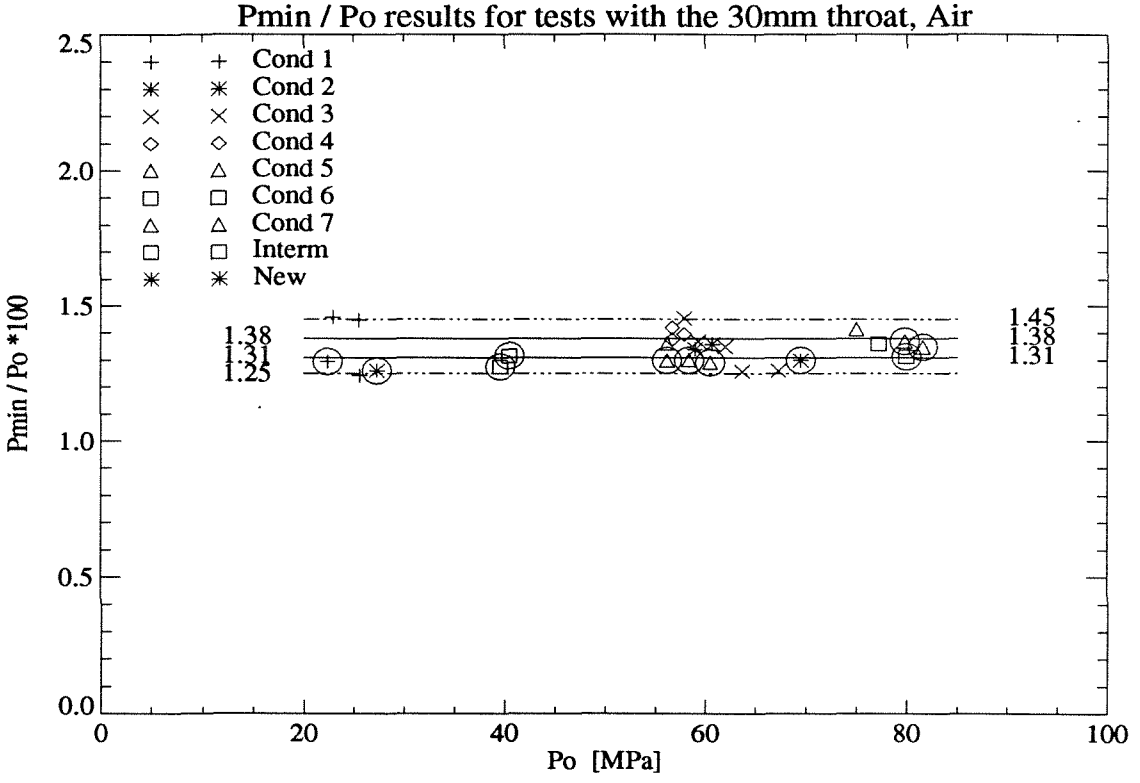

Figure 5.4. Ratio p_{min}/p_0 vs p_0, 30mm Throat, Air.

On figure 5.4, the horizontal lines represent the averaged ratios, and the ± 5% values. The values on the right are for the first series, the ones on the left for the fourth one.

As expected, according to the high correlation coefficient, there is no other notable dependence (higher order) between the minimum pitot pressure and the nozzle reservoir pressure.

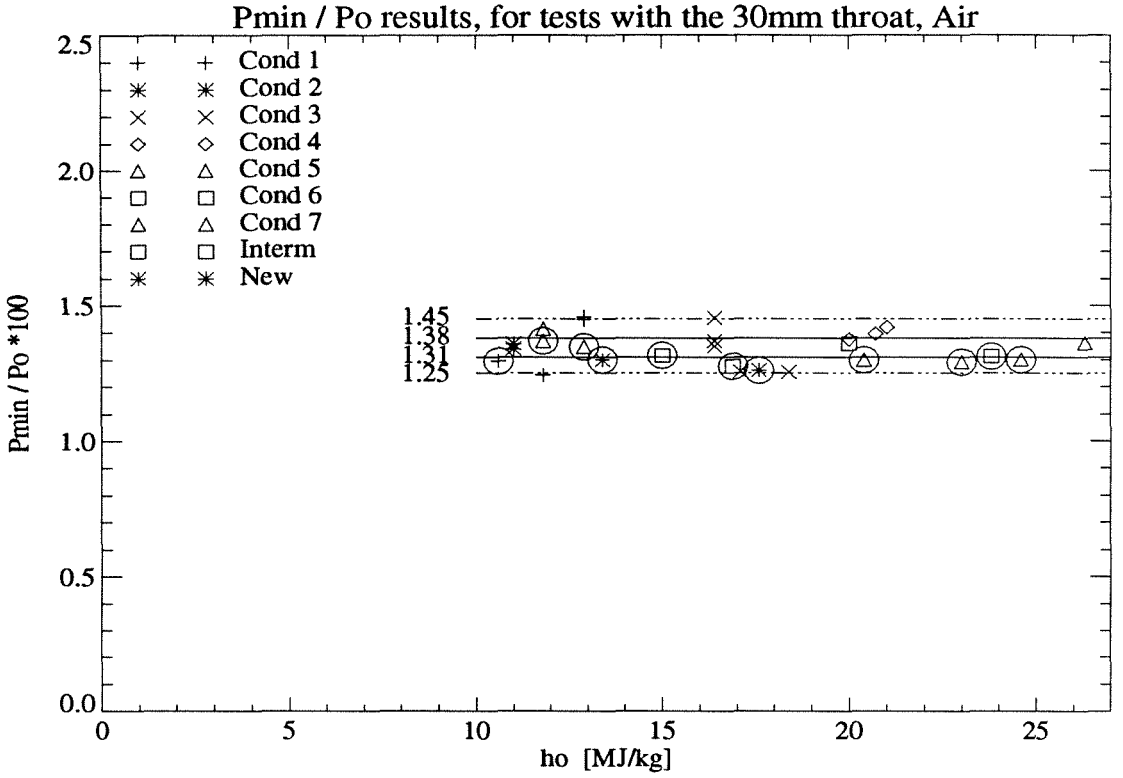

Figure 5.5. Ratio p_{min}/p_0 vs h_0, 30mm Throat, Air.

Surprisingly, there is no significant dependence between the ratio and the specific enthalpy, at least on the studied range, which nevertheless covers the entire T5 envelope.

So, within the T5 envelope and using the 30mm throat, with air as the test gas, the ratio p_{min}/p_0 is a constant. Because of some parameters that cannot be controlled, such as the exact throat radius, the value has slightly changed in one year.

$$\frac{p_{min}}{p_0} = \frac{1.38}{100}\ ,\ stdev = 4\% \qquad (30mm\ throat,\ 1^{st}\ series)$$

$$\frac{p_{min}}{p_0} = \frac{1.31}{100}\ ,\ stdev = 2\% \qquad (30mm\ throat,\ 4^{th}\ series)$$

Again, not that it is not what one may expect from computational grounds. Actually, according to SURF simulations, this ratio $p_t(0)/p_0$ should increase with h_0 (see figure 7.3 in section 7).

Comparison between the Ratios p_{min}/p_0, Using the 30mm and the 20mm Throat.

In section 4, it was seen that, with the 20mm throat, the ratio p_{min}/p_0 is also independent of p_0 and h_0 :

$$\frac{p_{min}}{p_0} = \frac{0.67}{100}\ ,\ stdev = 7\% \qquad (20mm\ throat,\ within\ T5\ envelope)$$

So, the ratio p_{min}/p_0 for the 30mm throat over the 20mm one, ranges between 1.96 (comparing with the fourth series) and 2.06 (with the first series). From another point of view, the ratio of the two slopes of the correlation plots is 1.37 / 0.68 = 2.01, considering the two 30mm series. Even if the combined standard deviations are of the order of 10%, both analysis show that this ratio is close to 2.0 for air.

It is thought that this ratio p_{min}/p_0 should be inversely proportional to the ratio of the area ratios. Since the exit diameter (314mm) has never been modified, the latter ratio is equivalent to the square of the ratio of the throat diameters. In theory, that should be $(30/20)^2$, i.e. 2.25 . But there is a small uncertainty concerning the exact diameters, due essentially to the crack level, and the melting of the nozzle entry. Nevertheless, according to some throat measurements during the fourth series, this ratio cannot be lower than 2.15 (see also the discussion in section 8).

Actually, the so-called 30mm throat is currently designed with a diameter of 30.07 mm (1.184 ± 0.001 inch). Measurements of the diameter of new ones range from 29.80 mm to 30.05 mm. For used ones, they range from 29.68 mm to 30.35 mm. Furthermore, it may happen that a used throat is not perfectly round anymore. For example, a given so-called 30mm throat showed a diameter ranging from 30.12 mm to 30.23 mm. Similar observations apply to the so-called 20mm throat. The designed diameter is 20.04 mm (0.789 ± 0.001 inch). Measurements on used ones range from 20.27 mm to 20.62 mm. On a specific so-called 20mm throat, the diameter ranged from 20.32 mm to 20.62 mm. The respective designs are presented in appendix 5.

5.3.3. Curvature of the Pitot Pressure Distribution

As was the case for the 20mm throat, the pitot pressure distribution along the radius for the tests using the 30mm throat, happens to have the same general parabolic convex shape. It was thus fitted by a second degree polynomial using the same technique. As discussed in the previous section, the coefficient "a" of the second degree term (called hereafter curvature), is in fact half the approximate curvature around the minimum of the parabola. That coefficient therefore expresses the deviation of the pitot pressure distribution with the radius.

The study of this parameter parallels the one developed for the minimum pitot pressure, since they follow one another.

"a" vs h_0

The curvature was first plotted versus the specific enthalpy, in order to visualize the distribution in terms of conditions.

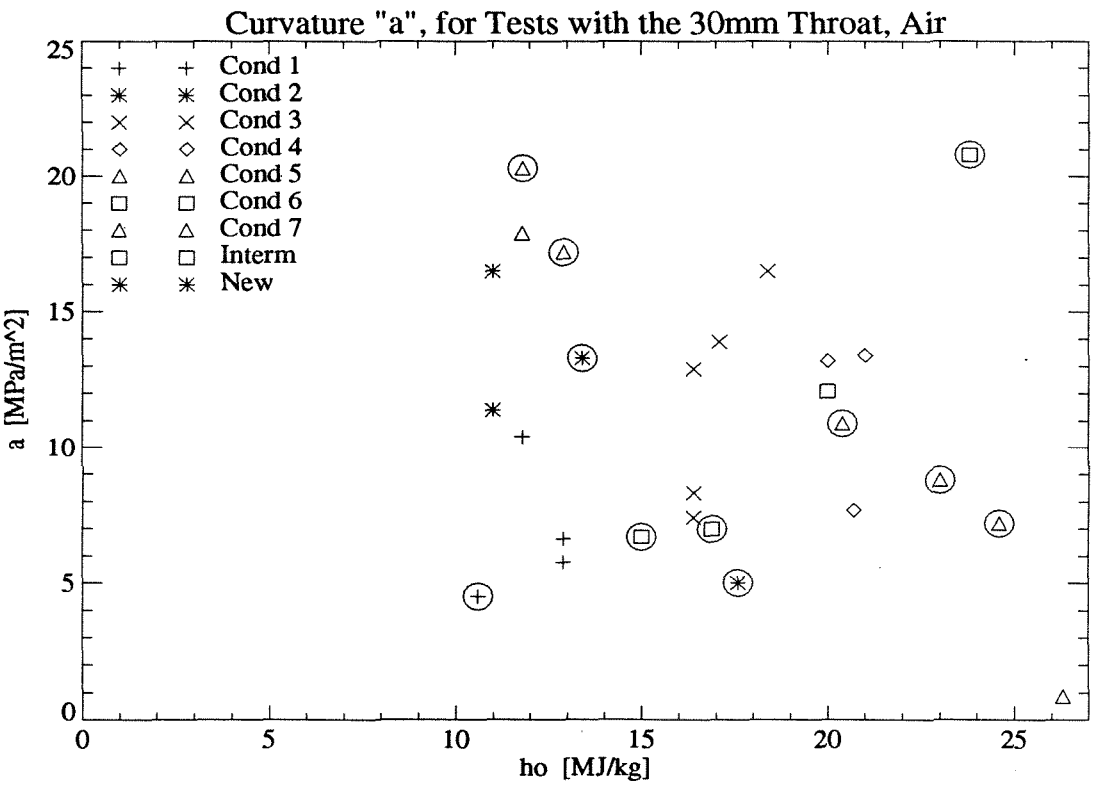

Figure 5.6. Curvature "a" vs h_0, 30mm Throat, Air.
Points from the fourth series have been circled, in order to differentiate them from the ones from the first series.

The error made on the curvature is on the order of 20%. This is due to three main reasons. First, the history of the parameter, for a given shot, shows some large fluctuations, even during the "steady" period. Then, the averaged value depends slightly on

the chosen boundary points, and the number of points under and above the centerline. Finally, it is not implied that the pitot pressure distribution is theoretically a parabola, but only that a second degree polynomial fit is a useful tool giving valuable information on that distribution. Note nevertheless that, most of the time, higher order polynomials (third and fourth) give fits very close to the parabola, within the core.

It appears that the deviation within one condition is much larger than for the minimum pitot pressure. This may be explained by the previous reasons, or by a high sensitivity to some (known or unknown) parameters.

It seems that two points have to be removed for the study of the curvature. From the first series, shot 447 was the very first one, with several bad traces and a large imbalance regarding the symmetry. From the fourth series, shot 708 presents a peculiar behavior, and specifically a curvature too large for its corresponding enthalpy. It is thought to be related to a highly cracked throat that may have generated a poor quality flow - as the throat was extracted to be changed after the shot, it fell apart in two pieces.

The Ratio "a" / p_0

The curvature was then studied versus the nozzle reservoir pressure p_0. Unlike the minimum pitot pressure, it does not exhibit a direct correlation, but a much more diffuse increasing trend. No obvious conclusions were drawn from this study.

Nevertheless, it was continued, investigating the scaled curvature, following the same procedure as for the 20mm throat.

It has to be pointed out that, unlike the minimum pitot pressure p_{min}, scaling by the nozzle reservoir pressure p_0 does not make the curvature dimensionless. The dimension of the "scaled curvature" a/p_0 is $[m^{-2}]$. This could be non-dimensionalized by some characteristic lengths. The exit radius is likely to be a parameter, but so are the length of the nozzle, and the throat diameter. As far as the exit diameter is concerned, it is fixed on T5 by the nozzle to 314 mm and cannot be changed.

As pointed out in the previous section, let us recall that the deviation of the pitot pressure distribution with respect to the minimum, at a given radius, is directly related to the present ratio. For example, at a radius of 10 cm, the deviation can be expressed as follows :

$$\Delta = \frac{P_t(r = \pm 10cm) - P_{min}}{P_{min}} = \frac{a.\, r^2}{P_{min}} = \frac{\frac{a}{P_0}}{\frac{P_{min}}{P_0}}.\, r^2 = \frac{\frac{a}{P_0} * 100}{\frac{P_{min}}{P_0} * 100}.\, 10^{-2} = \frac{\frac{a}{P_0} * 100}{constant}.\, \%$$

The constant for the 30mm throat air shots is roughly 1.4 (see previous paragraph 5.3.2).

"a" / p_0 vs h_0

The ratio a/p_0 was first plotted versus the specific enthalpy h_0.

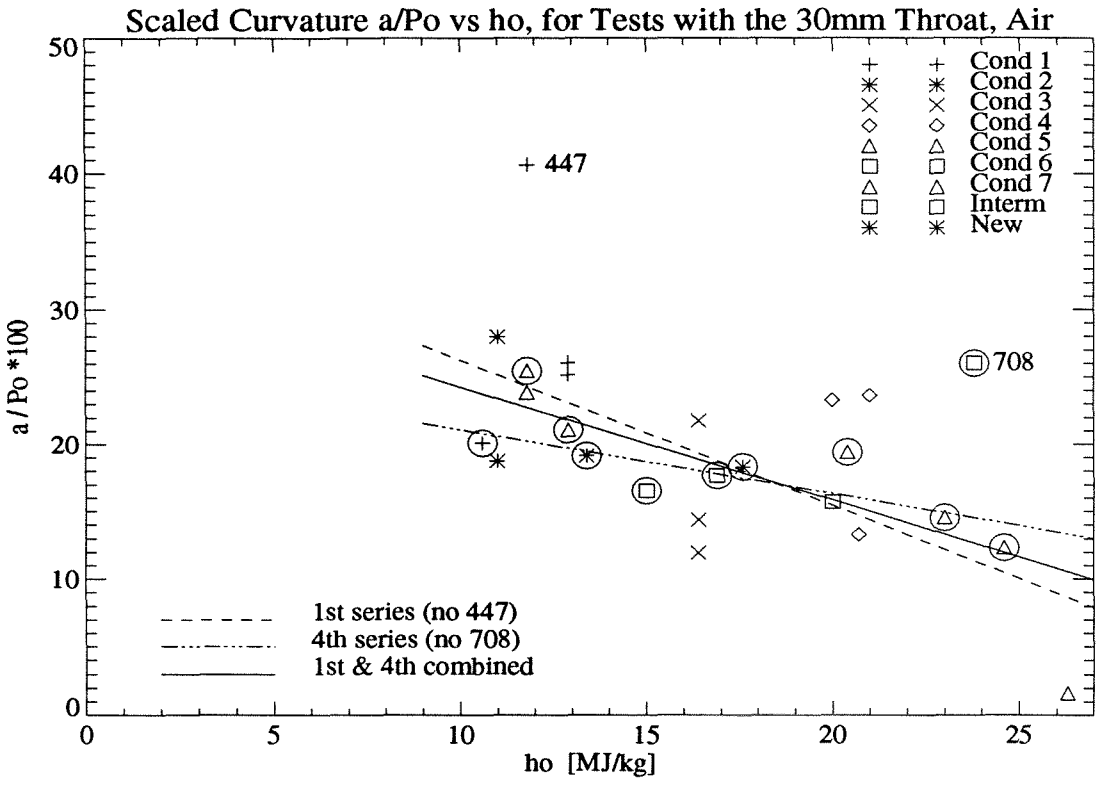

Figure 5.7. Scaled Curvature a/p_0 vs h_0, 30mm Throat, Air.
Again the shots from the fourth series have been circled.

For both series, despite large fluctuations for a given enthalpy, there is a general decreasing trend of the ratio a/p_0 with the enthalpy h_0. The least square fits are only here to visualize that trend, and compare the two series, which are actually similar on the range of interest, i.e. h_0 from 10 MJ/kg to 25 MJ/kg. Shots 447 and 708 were not taken into account for these fits.

The scaled curvature a/p_0 is roughly on the order of 25/100 for low h_0 (on the order of 10 MJ/kg), corresponding to a maximum deviation at the edge of the core of about 18% in the pitot pressure distribution. It decreases to about 10/100 at high h_0 (of the order of 25 MJ/kg), leading to a maximum deviation less than 10%. For an intermediate h_0, a/p_0 can be estimated around 20/100.

"a" / p_0 vs p_0

The ratio a/p_0 was then plotted versus the second known parameter : the nozzle reservoir pressure p_0.

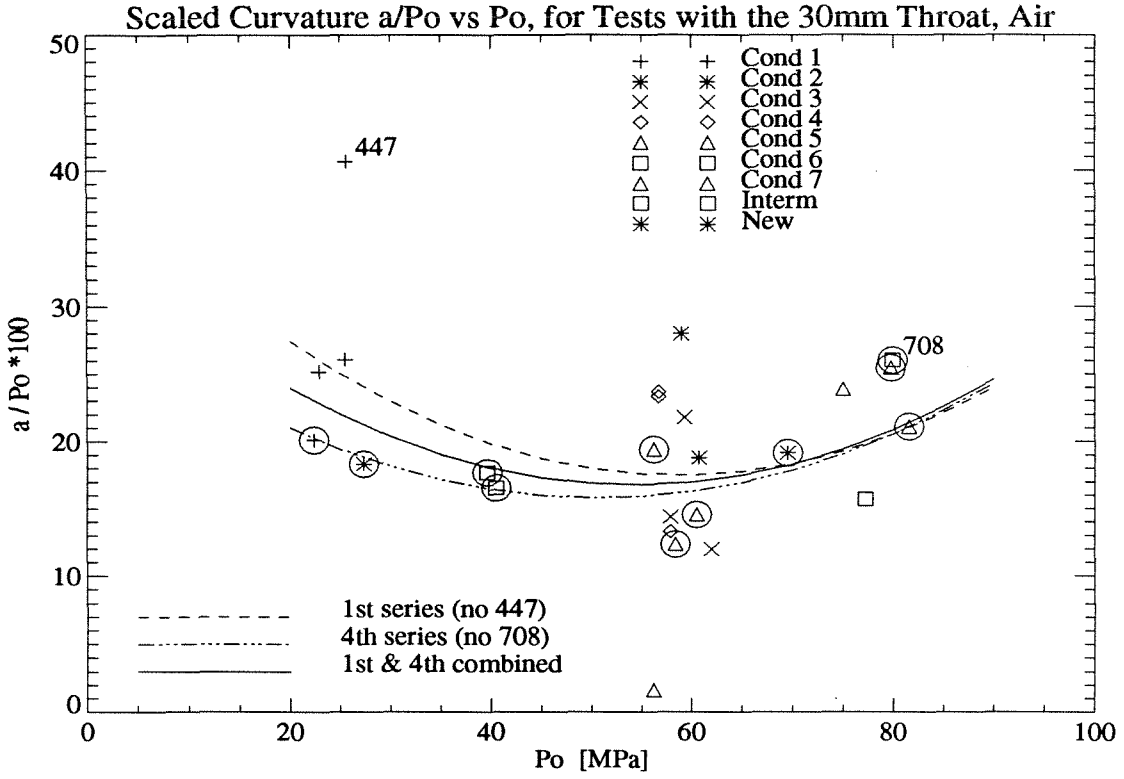

Figure 5.8. Scaled Curvature a/p_0 vs p_0, 30mm Throat, Air.

Again, the shots from the fourth series were circled, and shots 447 and 708 were not taken into account for the fits.

It should be mentioned that the large fluctuation for the 60 MPa p_0, is mainly due to different enthalpies. Besides this fluctuation, the two series exhibit again the same trend. The second order polynomial least squares fits are here only to help visualize that trend and compare the two series. A weak minimum for p_0 appears around 50 - 60 MPa, but because of the discrete range of tested nozzle reservoir pressure, it should be considered in the 60 MPa conditions.

5.3.4. Symmetry of the Pitot Pressure Distribution

From the parabola fit also comes information about the symmetry of the flow, at least as far as the pitot pressure is concerned. In fact, the symmetry axis of the parabola reflects the vertical symmetry of the flow along the calibrated vertical diameter. Since negative coordinates refer to the top of the rake, a negative symmetry axis abscissa x_s means that the pitot pressure distribution is symmetric with respect to an axis laying above the geometric nozzle axis.

Again, this calibration parameter was plotted versus the two known condition parameters : the nozzle reservoir pressure p_0 and the specific enthalpy h_0.

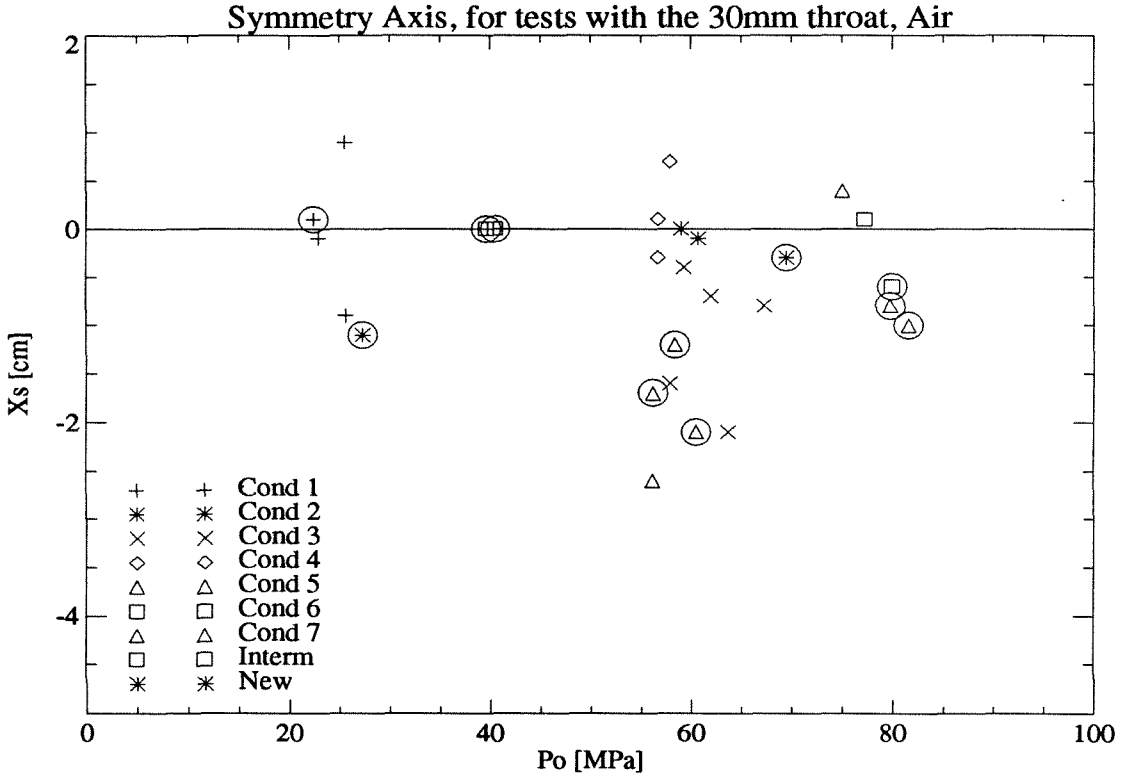

Figure 5.9. Symmetry Axis x_s versus p_0, for Tests with the 30mm Throat, Air.

The behavior of the symmetry axis is obviously different compared to the tests using the 20mm throat (c.f. section 4). First, the values here are closer to zero (figure 5.9). The error made on the position of this axis, after a least-squares fit, is on the order of 1cm. It is due, on one hand, to the spacing between two points and, on the other hand, to the unbalance of the points (at least for the first series). Most of the values are indeed in that error range. Secondly, the values here are both negative and positive, contrary to the 20mm throat case where they were all negative.

This supports the idea that all the derivations and techniques used to find this symmetry axis are suitable, and this axis should be the geometric nozzle axis. Actually, other studies (for example, the history of the parabola fit for a given shot) show that the

programs and the adjustments to know exactly where the nozzle axis projects onto the rake, are correct, since the symmetry axis converges to the nozzle axis after the driver gas contamination for every condition.

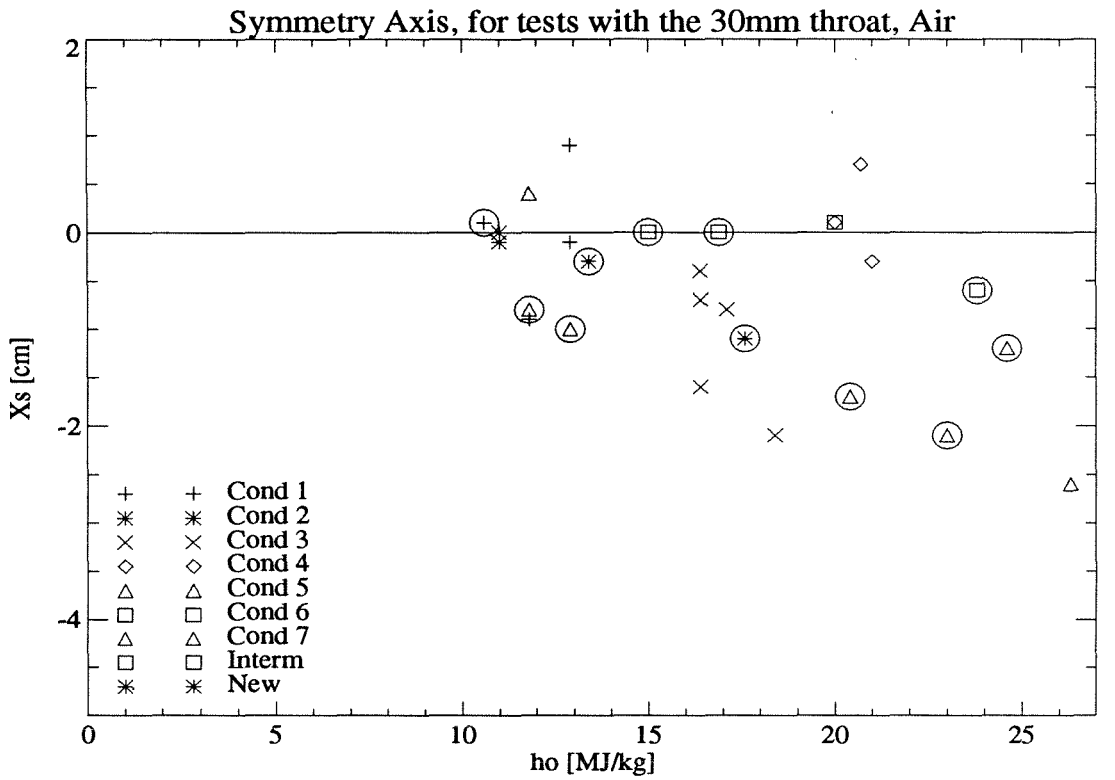

Figure 5.10. Symmetry Axis x_s versus h_0, for Tests with the 30mm Throat, Air.

While it seems that the nozzle reservoir pressure does not influence the symmetry axis behavior, the specific enthalpy h_0 does seem to have an effect. According to the above figure, it seems that the shift between the symmetry axis and the nozzle axis gets larger with an increasing enthalpy. But there are too few points at high enthalpy - h_0 above 22 MJ/kg - to make a definite conclusion. However, the circled points come from the fourth series for which the rake was centered with respect to the nozzle, which means that the symmetry axis can be best estimated at these conditions. Finally, the very high h_0 shot (#463) presents some very peculiar behavior, and therefore should be taken into account with extreme precaution.

5.3.5. The Core and Boundary Layer

An example of a distribution with several points in the boundary layer (BL) is shown in figure 5.11.

On the pitot pressure distributions, it is possible to locate where the core finishes, and therefore to get an estimate of the maximum useful radius for a model. In fact, this is true only for the first series, when the rake was covering the whole lower radius and under. But for the fourth series, the covered range lies inside the core. Therefore from the fourth series, it can be only said that the core is at least 12cm wide in radius, both at the top and at the bottom, for all the calibrated conditions.

For the first series, the edge of the core was estimated from the contour plots. It was always based only on the bottom part of the nozzle. The error bar is on the order of 1cm, essentially because of the spacing between two tips.

It results from the study on the first series that the core ranges between 12cm and 13cm, independently of the condition. Again, shot 463 presents a peculiar behavior, with a smaller core on the order of 10-11cm. Except for the two last shots (464-465), the rake position was not changed during the first series, and the recoil was not significantly different. During the tests, the rake was approximately 10cm downstream of the nozzle exit plane.

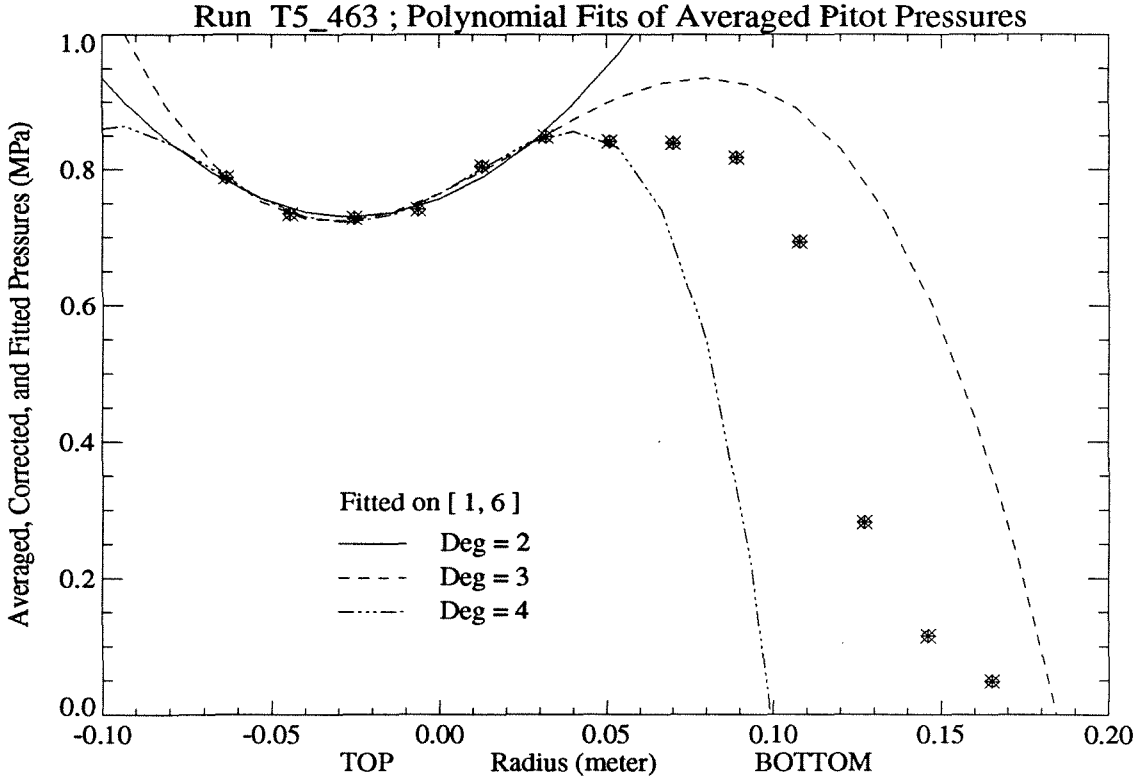

Figure 5.11. Example of Distribution with Several Points in the Boundary Layer.

5.4. Conclusion on the Calibration and the Use of the 30mm Throat, with Air as the Test Gas

We have just seen in this section that the calibration results, using the 30mm throat, and air as the test gas, are better than the ones using the 20mm throat (presented in section 4).

Even though the pitot pressure in the test section still presents a parabolic behavior (instead of a more uniform expected one), a given condition is truly repeatable. The study on the 30mm throat reveals good flow quality, considering a low deviation around the main parabolic profile, no notable centerline focusing effects, and thinner external layers (boundary layer, and expansion fan thickness).

Knowing the two main T5 reservoir parameters, namely the nozzle reservoir pressure and the specific enthalpy, one can predict within a good estimation, the pitot pressure distribution at the level where models are tested. The ratio of the minimum pitot pressure on the centerline over the nozzle reservoir pressure, p_{min}/p_0, was found to be $1.37/100 \pm 5\%$, and it was observed to be independent of the condition (h_0 or p_0) over the calibrated envelope, which covers all the common T5 conditions, i.e. from $h_0 = 10$ MJ/kg to 27 MJ/kg, and from $p_0 = 20$ MPa to 85 MPa. As to the scaled curvature, a/p_0 can be approximated around $20/100$ m^{-2} $\pm$ $10/100$ m^{-2}, with a decreasing trend versus the enthalpy, and a slight minimum for the 60 MPa shots.

Better quality flow (compared to the 20mm throat shots) was also visualized through the study of the symmetry axis of the pitot pressure distribution, which matches better with the nozzle axis, except maybe for some high enthalpy conditions.

Finally, the core, at the level where models are tested, is estimated to range between 12 cm and 13 cm. Trends related to the conditions have not been studied, since not enough data points are available, this having not been one of the principal objectives of the calibration. The conflicting study of the symmetry was considered more important, specially during the fourth series.

According to the pitot pressure distributions in the test section, it seems that the best conditions performed with the 30mm throat (area ratio of the order of 100), using air as the test gas, are for high enthalpies ($h_0 > 20$ MJ/kg) and medium pressures (p_0 around 60 MPa, i.e. for burst pressures p_4 of 90 MPa).

Comparisons with SURF computations are presented in section 7.

SECTION 6 :

Calibration of the T5 Nozzle

With Some Other Test Gases :

N_2 , CO_2 , H_2

6.0. Outline of Tests

Among the previously studied series, a few shots were also performed using test gases other than air : N_2, CO_2, H_2.

Nitrogen was to be compared with air, since it was thought to be similar, and since it would be a lot faster to use nitrogen (instead of air) in computational simulations (SURF for example).

Carbon dioxide is representative of a test gas with high chemical activity, and should help understand the chemical effects (dissociation/recombination) involved in the air calibration. Finally, T5 may be operated with hydrogen at conditions where it behaves as a perfect gas, and therefore the condition in the test section is more easily predictable.

Both throats (20mm and 30mm) were used for N_2 and CO_2. The studies with these gases are similar to the previous ones with air. Comparisons between the two throats, and the different gases, are investigated in the present section.

The H_2 shots went through many iterations to approach a tailored condition. Comments on this kind of shot (highly off-design) are discussed through the presentation of H_2 results, at the end of the present section.

6.1. Nitrogen

A total of 10 shots have been run with nitrogen. The 7 ones calibrated with the 30mm throat, have been performed during different series, with originally different purposes.

Shot 461 was the only test during the first series of April 93, which was dedicated to air. The purpose at that time was to compare solely one condition between air, N_2, and CO_2. Note that, for the first series, only the north p_0 transducer was thought to be reliable. The calibration of the south one was supposed to be wrong, giving a nozzle reservoir pressure higher by approximately 10%. Unfortunately, for shot 461, only the south one was available. Thus, it has been "corrected" by lowering its value by 10%. Comments about that correction are presented along with the study.

Shot 646 was the last one of the third series, dedicated to repeating a given condition with the 20mm throat (see section 3). Its purpose was to provide a quick comparison between the 20mm and the 30mm throat, for that given condition.

Finally, shots 701 to 705 were performed during the fourth series of April 94, in order to investigate different conditions with nitrogen, using the 30mm throat. One of the purposes was to confirm (or eventually to reject) the trends observed with air.

Furthermore, 3 shots (640, 642 and 643) were calibrated with the 20mm throat, during the repeat condition series (see also section 3). They are the only ones available for nitrogen using the 20mm throat.

6.1.1. Envelope of Calibrated T5 Conditions with N_2

Listed hereafter are the T5 parameters for the 10 N_2 shots :

	Burst Pres. (MPa)		Nozzle Res. (MPa)		(km/s)	(MJ/kg)	Throat	Cond.
Shot	$P_{4,avg}$	%	$P_{0,avg}$	%	V_s	h_0	Diam.	#
461	81.4	3.4	70.1x0.9	South*	3.39	11.5	30mm	2
646	83.5	0.9	53.2	North	4.51	20.4	30mm	4, R1
701	36.8	1.8	20.5	-1.9	3.24	10.5	30mm	1
702	87.9	-0.7	66.5	-0.4	3.80	14.4	30mm	3
703	102.8	-0.1	72.3	-0.4	3.47	12.0	30mm	2 new
704	97.1	-1.2	59.1	-0.2	3.26	10.6	30mm	2 as 461
705	90.1	-0.7	58.3	South	4.96	24.6	30mm	5
640	91.3	1.1	52.5	0.1	4.51	20.4	20mm	4, R1
642	91.8	0.6	52.5	(4.6)	4.58	21.0	20mm	4, R1
643	83.1	0.9	55.5	North	4.65	21.6	20mm	4, R1

Table 6.1.1 - T5 Parameters, N_2 shots, 30mm and 20mm Throats

The covered range of conditions can be better visualized on the following plot. The symbols were kept the same as for air conditions. The circled ones identify the 20mm throat shots. p_0 of shot 461 was modified following a rough adjustment (10%) of the south transducer (see the outline).

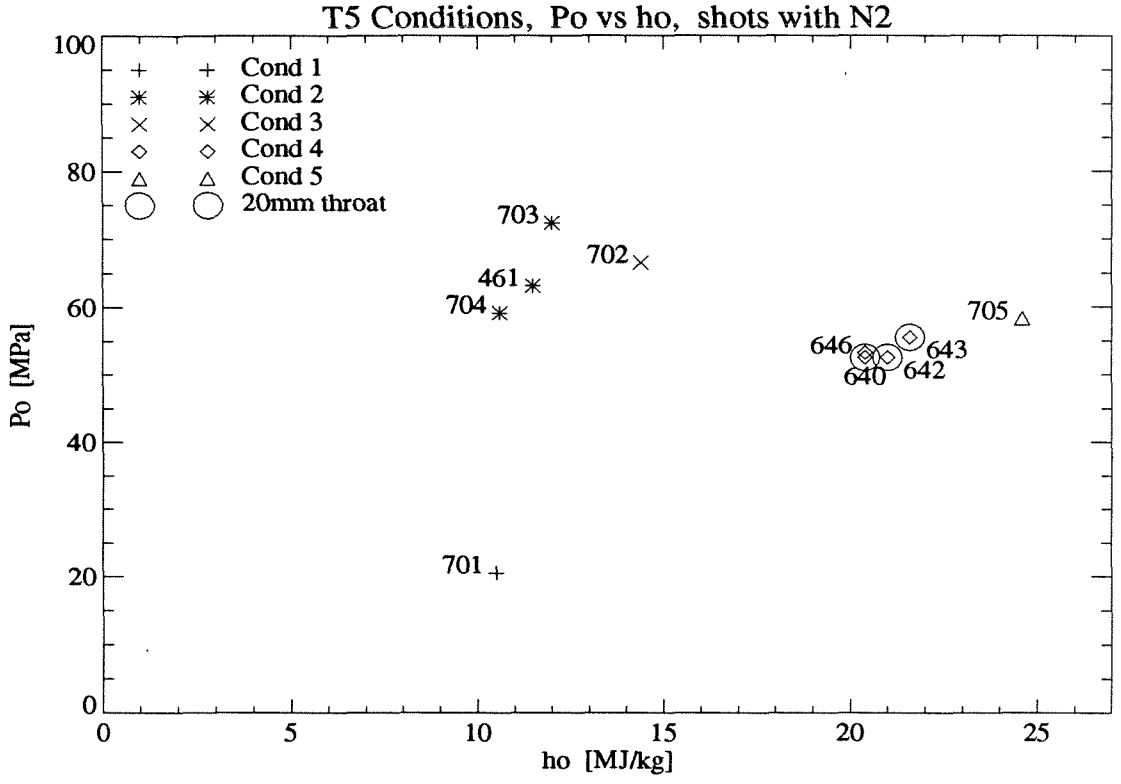

Figure 6.1. Conditions Covered with N_2.

Note : the left upper diamond represents shot 646, with a 30mm throat.

The envelope of conditions is obviously reduced, compared to the one for air shots. Nevertheless, the whole range of enthalpy is covered, for a p_0 around 60 MPa. Actually, except for 701, all the shots were performed with a 90 MPa diaphragm. Note that, despite its high p_0 value, shot 703 is not a high pressure shot, but a modified condition 2, with a better recovery factor, due to a better setting of the 2R pressure (leading to a better trajectory of the piston). Also, condition 4 (during the repeat series) suffered from the use of some weaker diaphragms, and/or poor recovery factors (less than 60%). Thus p_0 ranges from 50 MPa to 75 MPa (not taking into account shot 701), which is wide enough for the present calibration study.

6.1.2. N_2 Calibration Results

Listed hereafter are the calibration parameters from the parabola fits, for the N_2 shots :

Shot #	Cond., Throat	Test time ms	Transd. fitted	P_{min} MPa	a MPa/m^2	Center cm	Comments
461	2, 30mm	[1.35, 2.05]	1 - 10	0.779	17.1	0.1	Long steady period, good sym.
646	4, 30mm	[0.80, 1.30]	1 - 12	0.650	19.4	-2.0	Bad symmetry, high curvature
701	1, 30mm	[1.35, 2.15]	2 - 12	0.256	4.1	-0.7	Tailored cond #1
702	3, 30mm	[1.15, 1.85]	2 - 12	0.812	13.9	0.0	Very good symmetry
703	2, 30mm	[0.85, 1.75]	2 - 12	0.904	14.6	-0.6	Really tailored
704	2, 30mm	[0.85, 1.75]	2 - 12	0.756	9.4	-0.4	To compare with 703
705	5, 30mm	[0.70, 1.20]	2 - 10!	0.737	22.7	-2.6	No #11 trace, new throat
640	4, 20mm	[0.80, 1.30]	1 * 12	0.304	11.4	-0.9	Same fit by higher order poly.
642	4, 20mm	[0.80, 1.30]	1 * 13	0.267	14.1	-0.3	Good symmetry, pb steady
643	4, 20mm	[0.80, 1.30]	1 * 12	0.294	15.4	-0.7	No real steady period

Table 6.1.2 - Nozzle Parameters by Parabola Fits, N_2 Shots

The general study was applied to these N_2 shots, following every step. For convenience, all the intermediate and similar results are mentioned, and only the final results (on the scaled parameters) are presented hereafter.

The Minimum Pitot Pressure p_{min}

The plot of p_{min} versus h_0 is, as expected, similar to figure 6.1 (T5 N_2 conditions). The only exception is related to the 20mm throat shots, which are grouped together, but around a lower value than shot 646 (30mm throat). The classification into the different conditions is still observed, and therefore valid.

In order to check that the scaling by the nozzle reservoir pressure is still meaningful, the correlation plot is drawn for the N_2 shots.

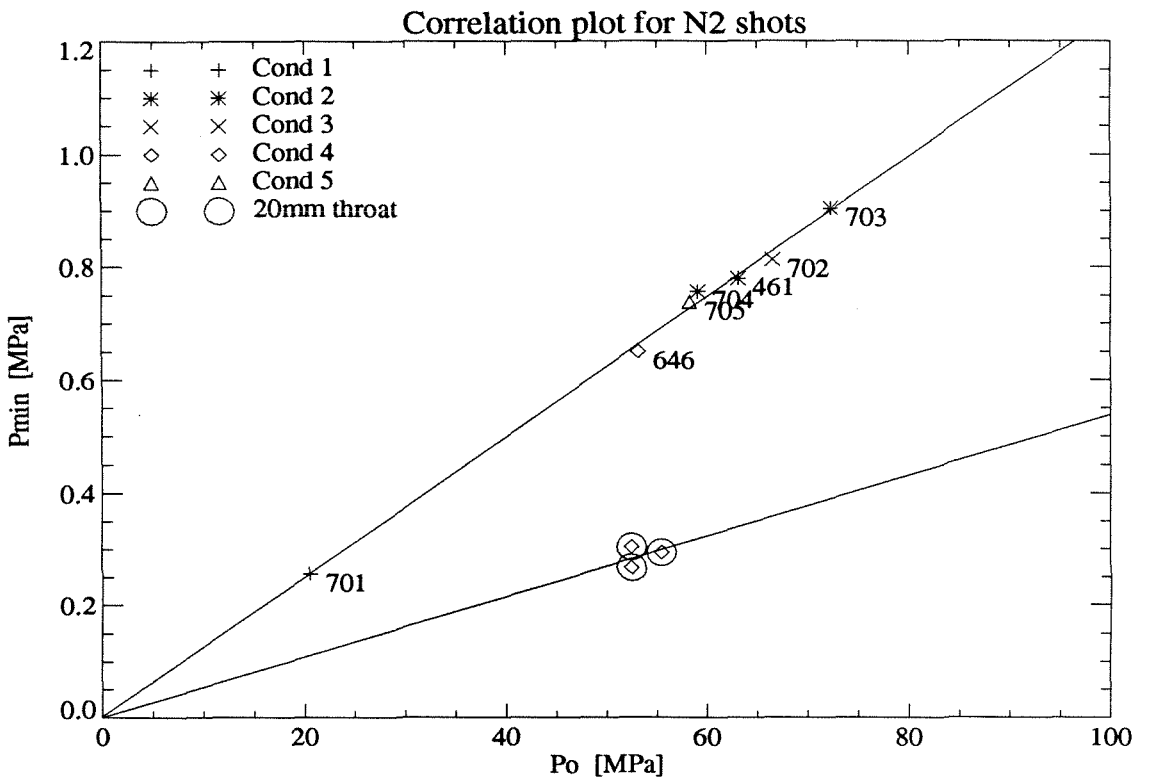

Figure 6.2. Correlation Plot for N_2 Shots.

Note : The numbered points are from the respective shots using the 30mm throat; the circled points represent shots 640, 642, and 643 using the 20mm throat.

The first remark that can be made about the above plot, is that the points representing the shots with the 30mm throat, are impressively correlated, i.e. stand almost perfectly on a straight line. Furthermore, this line goes through the origin, which confirms that the ratio p_{min}/p_0 -and in a more general way, the pitot pressure distribution scaled by the nozzle reservoir pressure- can be studied as such.

There is apparently no notable difference between the different series. This observation, which is in contradiction to what was noticed with air (in the previous section), should be taken really carefully. It is only based on a single point from the first series (461), and an other one from the third series (646). Most of the points (5 out of 7) represent in fact the successive shots from the fourth series (701 to 705).

As to the least square fits, there is a slight difference between the two throats, concerning the origin. For the 30mm throat, the fit depends only on the points representing a shot, and it goes, as a result, close to the origin. But, for the 20mm throat, the three available points are too close together, for a meaningful correlation. Thus, the origin was added as a fourth point, in order to be able to compare the two correlation lines. The results are the following ones :

$$p_{min} = 0.20\ E-02 + 1.242\ E-02 * p_0\ ,\ (stdev = 0.014) \qquad (30mm\ throat,\ N_2)$$

$$p_{min} = 0.03\ E-02 + 0.538\ E-02 * p_0\ ,\ (stdev = 0.019) \qquad (20mm\ throat,\ N_2)$$

Then the ratio p_{min}/p_0 was studied versus p_0 and h_0. As expected from the correlation study, there is no other notable dependence on the two reservoir parameters. The following plot shows the independence regarding h_0. The one versus p_0 (not shown here) is indeed very similar. This plot (figure 6.3) should be compared to the corresponding one for air (figure 5.5). The axes have been kept the same for that purpose.

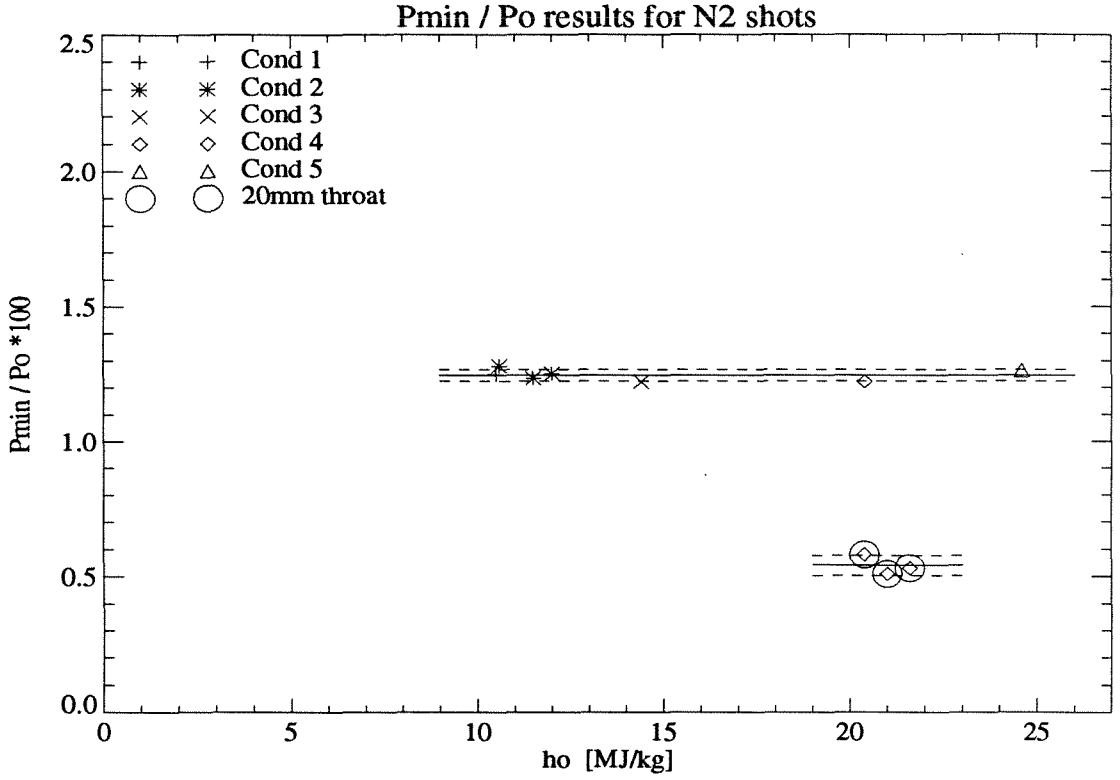

Figure 6.3. Ratios p_{min}/p_0 versus h_0, for N_2 Shots.
Note : The dash lines are one standard deviation apart from the respective average.

Therefore, within the T5 envelope, for a given throat, the ratio p_{min}/p_0 can be considered as a constant, this time using N_2 as the test gas. For both throats, the values have been simply averaged.

$$\frac{p_{min}}{p_0} = \frac{1.246}{100}, \quad stdev = 2\% \qquad (30mm\ throat,\ N_2)$$

$$\frac{p_{min}}{p_0} = \frac{0.539}{100}, \quad stdev = 7\% \qquad (20mm\ throat,\ N_2)$$

Finally, the two throats were compared to each other. The ratio of the two correlation slopes (30mm over 20mm throat) is the same as the ratio of the p_{min}/p_0, i.e. 2.31 . Again, that value should be compared to the 2.25 expected from the ratio of the area ratios. Actually, keeping in mind that there are only three repeated shots available for the 20mm throat, and given all the standard deviations, and the errors on the throat diameters, these two ratios agree quite well. Recall that this was not true when using air as the test gas (paragraph 5.3.2).

The Curvature "a"

As in the study for air shots, the study of the raw (non-scaled) curvature of the pitot pressure distribution for the N_2 shots, exhibits only vague trends : the present curvature "a" is increasing with p_0 and h_0. There is no major difference between the 20mm and the 30mm throat.

Thus, the curvature was scaled by the nozzle reservoir pressure p_0, following the previous studies for air shots (see section 5 for more details).

The ratio a/p_0 was first plotted versus the nozzle reservoir pressure p_0.

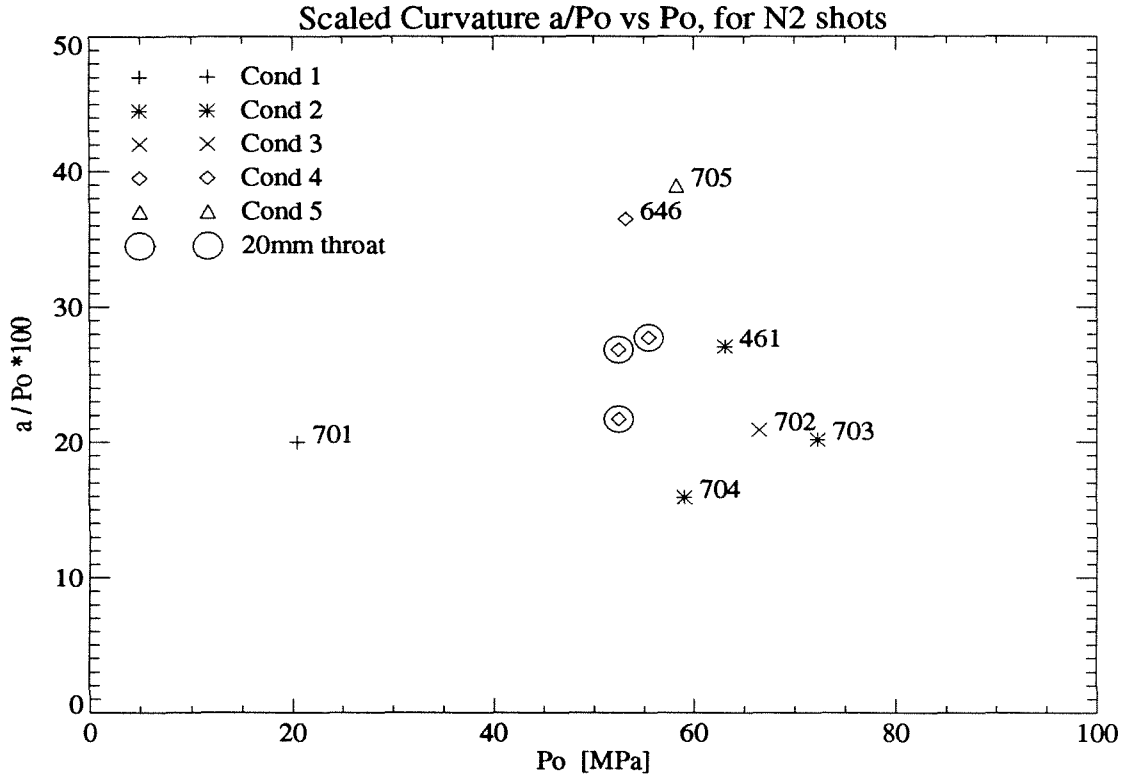

Figure 6.4. Scaled Curvature a/p_0 versus p_0, for N_2 Shots.

Note : The numbered points are from the respective shots using the 30mm throat; the circled points represent shots 640, 642, and 643 using the 20mm throat.

According to these few points, there is no obvious trend of the scaled curvature a/p_0 versus the nozzle reservoir pressure p_0, when using N_2 as the test gas. Also, the points representing the 20mm throat shots are similar to the ones for the 30mm throat. They lie roughly between 20/100 and 30/100, which is the same order of magnitude as with air.

The large fluctuation and the extreme values around p_0 of 60 MPa, are explained by the influence of the enthalpy, as shown in the following plot of a/p_0 versus h_0.

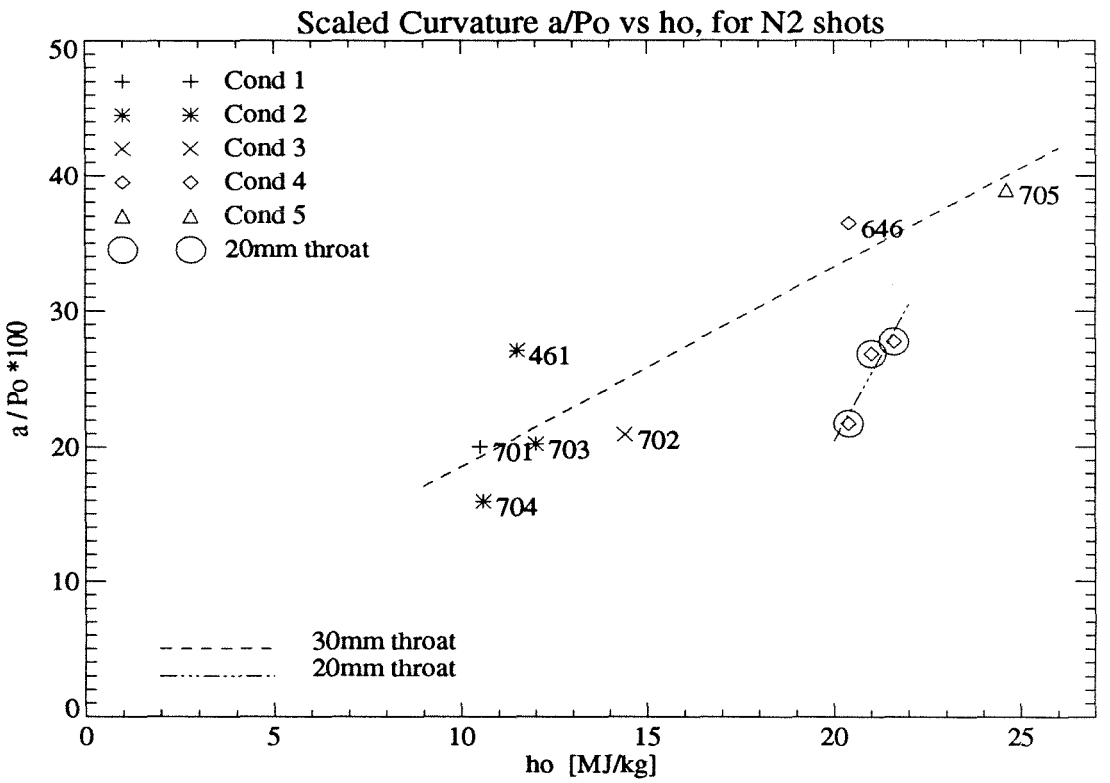

Figure 6.5. Scaled Curvature a/p_0 versus h_0, for N_2 Shots.

Note : The numbered points are from the respective shots using the 30mm throat; the circled points represents shots 640, 642, and 643 using the 20mm throat.

This plot confirms the observation that the curvature (raw or scaled) for the N_2 shots increases with the enthalpy. The least squares fits help visualize that trend. Even if the trend for the 20mm throat, based only on the 3 grouped points, is to be taken into account with extreme precaution, it seems that, for the 30mm throat, the trend can be firmly established.

But this latter result for N_2 is in total disagreement with the corresponding one found for air (see figure 5.7). Again, recall that the results for N_2 shots are based on very few points, and that the curvature of the pitot pressure distribution is a highly fluctuating parameter, according to the study of the air shots.

The Symmetry Axis X_S

For most of the N_2 shots, the symmetry axis of the flow (given as the center of the parabola in table 6.1.2) corresponds to the revolution axis of the nozzle, within 1 cm. But, for shots 646 and 705, on the opposite, there exists a shift between these two axes. In both cases, the large negative values mean that the flow symmetry axis, at the level of the rake, is well above the nozzle axis. Note that these two shots are high enthalpy ones, and show higher curvatures as well. It may also be interesting to know that, for shot 705, the throat was changed just before the run by a new molybdenum one. Some copper

erosion from the shock tube sleeve also occurred during this shot, and was deposited on the throat and on the rake during the shot.

However, the present observation on the large negative shift at high enthalpy, tends to confirm the general trend which was suggested by the 30mm throat air shots (figure 5.10).

6.1.3. Conclusion on the N_2 Shots

Even though few N_2 shots are available, it was seen that some conclusions can be drawn from the above study.

As far as the 30mm throat is concerned, the runs from different series were studied together. That allows to define a sizable envelope, admittedly smaller and less dense than the one for air, but nevertheless covering the common T5 conditions. As to the 20mm throat, the only three repeated shots gave some general information when comparing the two throats.

The ratio p_{min}/p_0, when using N_2 as the test gas, and for a given throat, was again found to be independent of the nozzle reservoir pressure p_0, and of the specific enthalpy h_0, within the T5 envelope. For the 30mm throat, the value of this ratio is 1.24, with a low standard deviation of 2%. For the 20mm throat, the value is of the order of 0.54 . These two values have to be compared with the corresponding ones for air (1.37 and 0.67, respectively). For both throats, the ratios for N_2 are appreciably lower (of the order of 90% and 80%, respectively). Therefore, this is a major difference between these two gases, which should not permit one to assimilate them during any simulation.

As far as the curvature is concerned, there is no major difference between the two throats. The scaled curvature is of the order of 20/100 to 30/100, and it increases with the enthalpy, which is the behavior opposite as the one observed for air.

The flow symmetry axis seems to correspond to the nozzle axis, except for high enthalpy shots, for which an upward slip appears to be quite significant.

No boundary layer study was conducted, since most of the shots were performed during the fourth series, and thus, the pitot pressure distribution covered only the core.

6.2. Carbon Dioxide

Throughout this research program, only 7 shots were performed with CO_2 as the test gas. One of them (462) was run during the first series for the same purpose as shot 461, i.e. a quick comparison with air for a given condition (actually condition 2). But, at the end of the fourth series, it was decided to investigate more carefully CO_2 as a test gas, in order to check if some of the properties found for air or/and N_2, were also applicable to CO_2, or if the latter exhibited some different behaviors.

6 shots were calibrated during this last series, 4 with the 30mm throat, 2 with the 20mm one. They represent the only two common conditions previously used on T5. They correspond approximately to condition 1 and 7 with air or N_2, but it should be noted that they are set up differently. Thus, only very low enthalpy ($h_0 < 10\ MJ/kg$) shots are available for CO_2. The high pressure condition (corresponding to condition 7) was reached using a 90 MPa burst diaphragm (as in shot 462 corresponding to condition 2), but with an improved recovery factor (new setting of the 2R pressure).

Except for the fact that the throat was changed, 717 is an exact repeat of 711, and 715 of 713. It allows a direct comparison between the two throats, at two different conditions.

6.2.1. T5 Covered Conditions

Listed hereafter are the T5 parameters for the 7 CO_2 shots :

	Burst Pres. (MPa)		Nozzle Res. (MPa)		(km/s)	(MJ/kg)	Throat	Cond.
Shot	$P_{4,avg}$	%	$P_{0,avg}$	%	V_s	h_0	Diam.	#
462	88.7	3.1	63.0	North	3.09	9.6	30mm	2
709	115.4	-2.1	80.0	-0.7	2.99	8.9	30mm	2*
710	106.5	-1.2	72.6	-0.6	2.80	7.9	30mm	2*
711	44.6	0.6	29.4	-0.9	2.27	5.2	30mm	New
713	114.6	-2.2	79.0	-1.4	3.00	9.0	30mm	2*
715	106.0	-1.7	84.2	-1.5	2.93	8.6	20mm	as 713
717	45.7	1.6	32.2	-1.2	2.29	5.2	20mm	as 711

Table 6.2.1 - T5 Parameters, CO_2 shots, 30mm and 20mm Throats

Again, the covered range of conditions can be better visualized on the following plot. The symbols have been kept the same as for the corresponding air conditions. The axes ranges have been also kept the same, for the sake of comparison with the other test gases. The circled symbols still identify the 20mm throat shots.

It is obvious on this plot that the envelope of conditions covered with CO_2 as the test gas, is quite limited, specially as far as the specific enthalpies are concerned. Note also that the enthalpies reached during these shots, are all lower than the lowest reached with

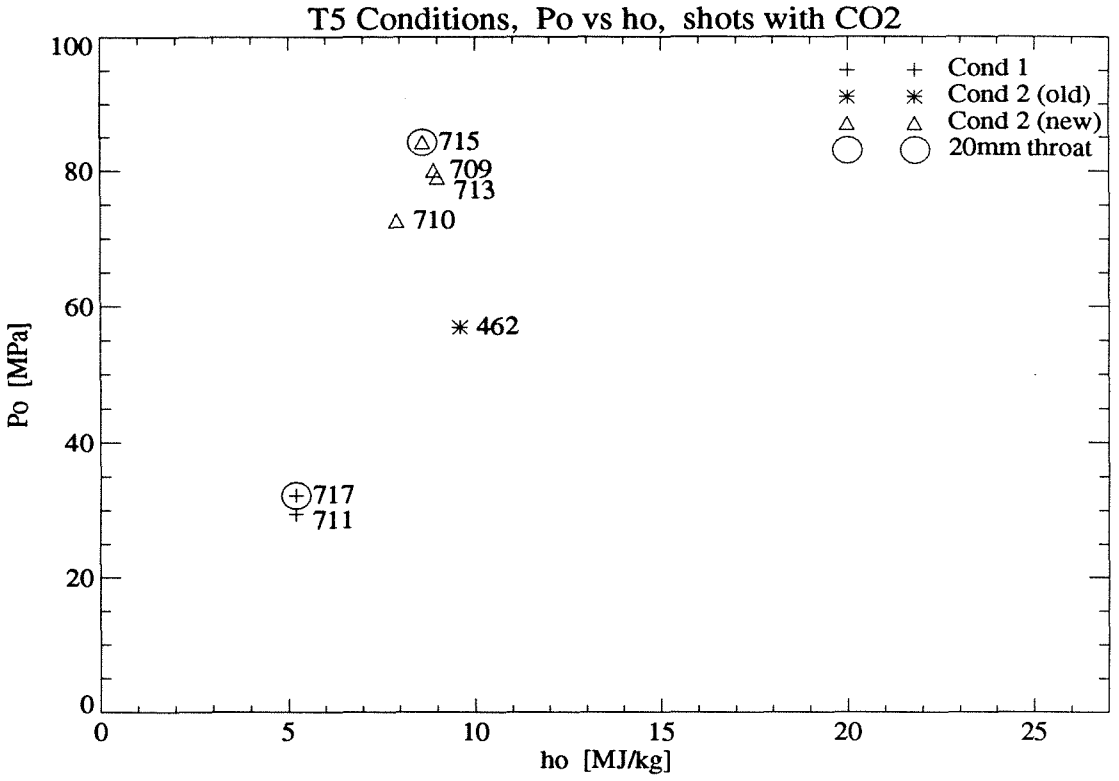

Figure 6.6. Conditions covered with CO_2.

air or N_2, i.e. under 10 MJ/kg. Nevertheless, the nozzle reservoir pressure range is wide enough to allow the usual general calibration study.

6.2.2. CO_2 Calibration Results

Listed hereafter are the calibration parameters, for the CO_2 shots :

Shot #	Cond., Throat	Test time ms	Transd. fitted	P_{min} MPa	a MPa/m^2	Center cm	Comments
462	2, 30mm	[1.30, 1.80]	2 - 10	0.858	5.9	-1.1	Unbalanced, strange #1
709	2*, 30mm	[1.25, 1.85]	1 - 13	1.132	15.1	-0.4	Good symmetry, new throat
710	2*, 30mm	[1.25, 1.85]	1 - 13	0.978	14.4	-0.2	Very good symmetry
711	1, 30mm	[1.50, 2.50]	1 - 13	0.399	5.4	-0.6	Long steady period
713	2*, 30mm	[1.25, 1.85]	1 - 13	1.063	17.6	-0.1	Large overshoot
715	2*, 20mm	[1.25, 1.85]	4 - 10	0.578	18.7	-0.9	Strange distribution
717	1, 20mm	[1.50, 2.50]	1 - 13	0.222	2.1	-1.0	Really flat distribution

Table 6.2.2 - Nozzle Parameters by Parabola Fits, CO_2 Shots

The Minimum Pitot Pressure p_{min}

The plot of p_{min} vs h_0 is omitted again, since it does not present any major interest. As expected, as far as the points representing the shots with the 30mm throat are concerned, this plot is similar to the plots of the covered conditions. As to the circled points (for the 20mm), they present the same behavior, but on a different scale.

However, the plot of p_{min} vs p_0 exhibits once more an interesting correlation between these two parameters, for a given nozzle.

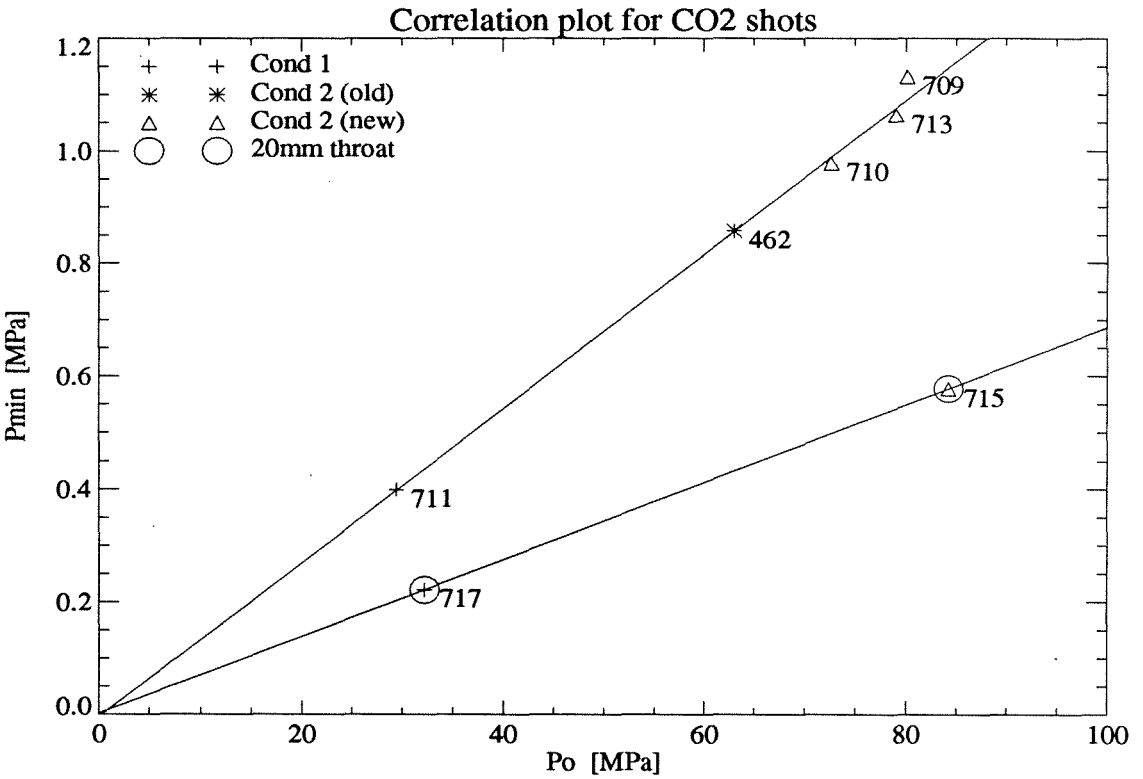

Figure 6.7. Correlation Plot for CO_2 Shots.

For the points representing shots with the 30mm throat, a least squares fit was derived, while, for the two 20mm throat points, it is the simple straight line that goes through. Once more, it is striking that the two lines go through the origin (in a first approximation). That denotes, again for CO_2, that these two parameters, p_{min} and p_0, are proportional for a given throat.

Note that a new throat was installed just before shot 709, and the p_0 north transducer was replaced after the shot, which may explain why the corresponding point is slightly off from the four other ones.

The equations of the two lines are the following :

$p_{min} = -0.45\ E-02 + 1.367\ E-02 * p_0$, $(stdev = 0.026)$ $(30mm\ throat,\ CO_2)$

$p_{min} = 0.16\ E-02 + 0.685\ E-02 * p_0$, $(just\ the\ 2\ points)$ $(20mm\ throat,\ CO_2)$

Contrary to the N_2 correlation, it is notable that the above values of the slopes for CO_2 are quite similar to the ones for air, for both throats (1.37 and 0.68 respectively). So is the ratio of these two slopes (discussion after the presentation of the ratios p_{min}/p_0).

As usual, the ratio p_{min}/p_0 was studied right after, but this time, more in order to get an averaged value (for each throat), rather than to check for any second order dependence. The enthalpy range is indeed too limited (between 5 and 10 MJ/kg) to allow one to draw general conclusions. The ratio p_{min}/p_0 is therefore presented versus p_0 on the following plot.

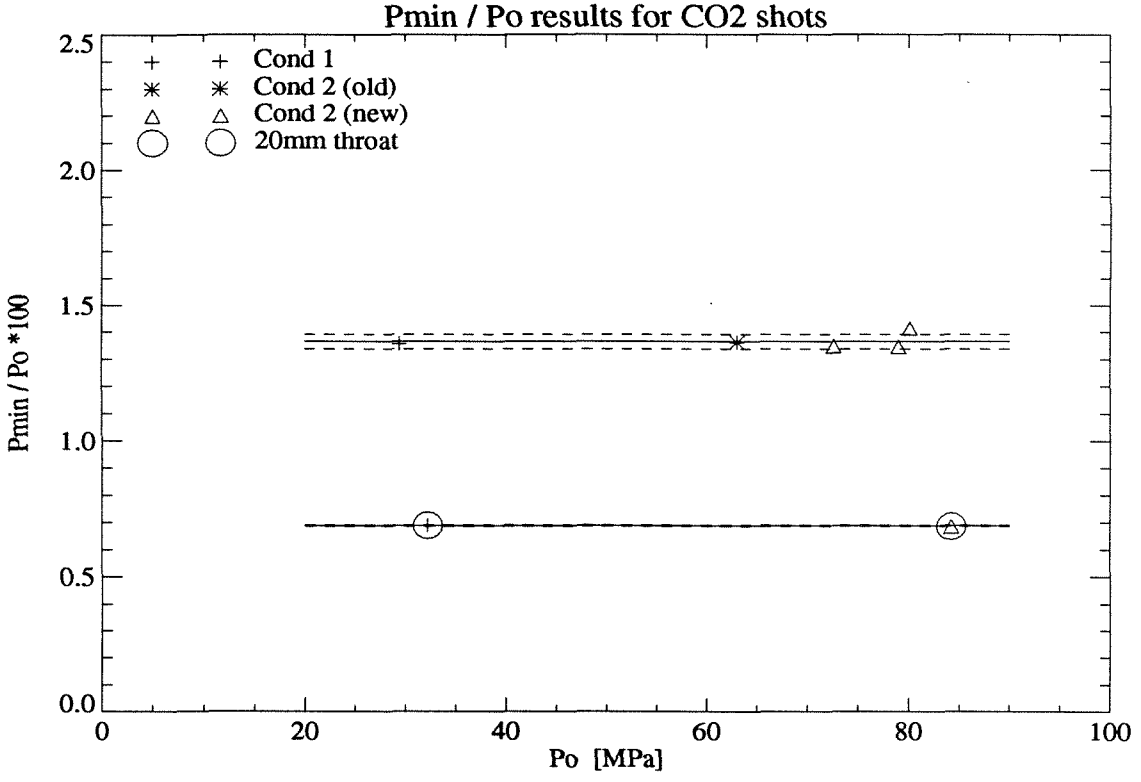

Figure 6.8. Ratios p_{min}/p_0 versus p_0, for CO_2 Shots.

Note : The dashed lines are one standard deviation apart from the respective average.

So, within the T5 envelope and for a given throat, the ratio p_{min}/p_0 can be considered as a constant (at least on the present calibrated envelope), this time using CO_2 as the test gas. For both throats, the values were simply averaged.

$$\frac{p_{min}}{p_0} = \frac{1.365}{100}\ ,\ stdev = 2.0\% \qquad (30mm\ throat,\ CO_2)$$

$$\frac{p_{min}}{p_0} = \frac{0.688}{100}\ ,\ stdev = 0.3\% \qquad (20mm\ throat,\ CO_2)$$

Logically, these values are again quite similar to the ones found for air (between 1.31 and 1.38 for the 30mm throat, and 0.67 for the 20mm, respectively).

Finally, as for the other test gases, the two throats have been compared to each other. The ratio of the correlation slopes is exactly 2.00, and the ratio of the p_{min}/p_0 is 1.98. Therefore, this ratio for CO_2 appears to be the same as for air, i.e. roughly 2.0, but different from the one for N_2 (2.3) and from the expected ratio of the area ratios (2.25).

The Curvature "a"

The curvature "a" was first plotted versus p_0. One can note an increasing trend. There is also no major difference between the points related to the 30mm and the 20mm throat, for a given condition. The curvature was then scaled, as usual, by the nozzle reservoir pressure p_0. Recall that this scaling is directly related to the scaling of the minimum, and more generally the scaling of the whole pitot pressure distribution (see section 2).

Unfortunately, it is not possible to study any trend of the curvature (raw or scaled) with the specific enthalpy, because of its limited calibrated range.

Therefore, only the plot of the scaled curvature a/p_0 versus p_0 is presented.

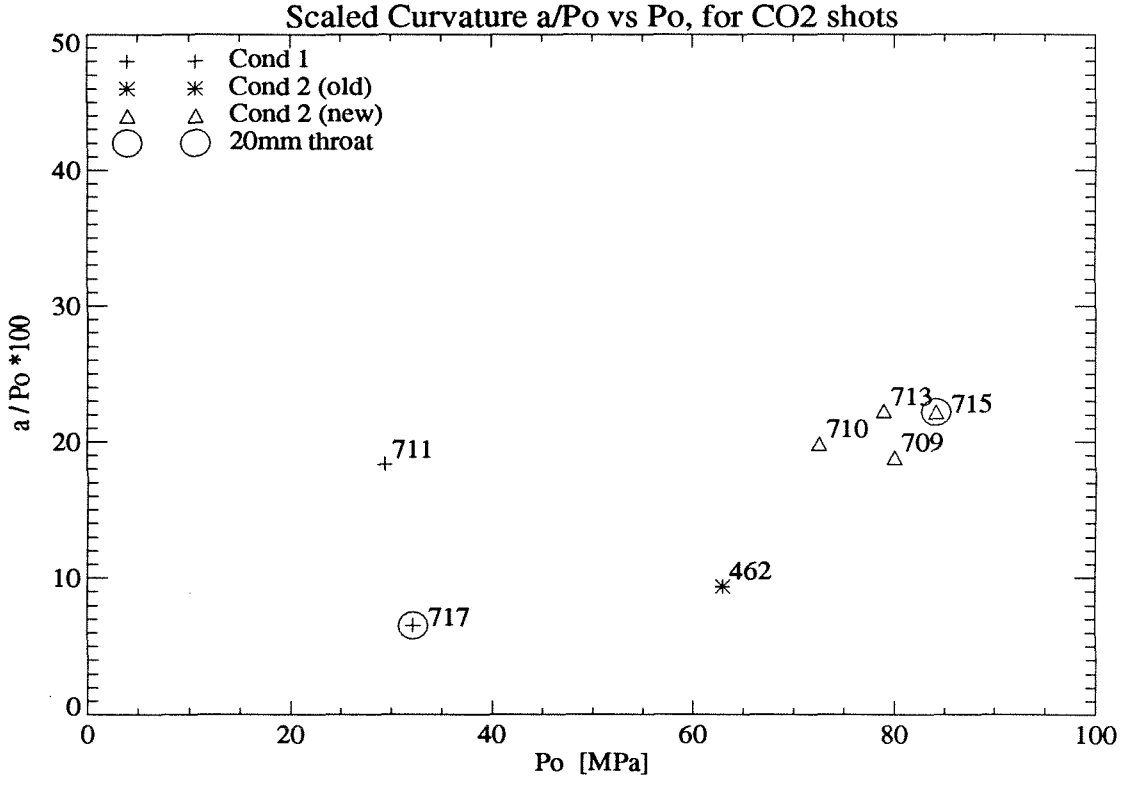

Figure 6.9. Scaled Curvature a/p_0 versus p_0, for CO_2 Shots.

Again, due to the small number of available data points, it is difficult to make any conclusion as far as trends are concerned. The only notable remark is that the values of a/p_0 with CO_2 are on the order of 20/100 and lower, which is, overall, lower than with air or N_2. This means that the distribution is more uniform along the exit diameter. However, this may be due to the fact that only a small enthalpy range has been calibrated.

The Symmetry Axis X_S

For all the CO_2 shots, the difference between the flow symmetry axis and the nozzle axis is less than 1cm (considered as the error bar). However, omitting shot 462 due to its unbalanced distribution of data points, it seems that, with the 30mm throat, there is an almost perfect match between these two axes, as expected. The distribution is quite symmetric around that axis, all along the steady period (and after). However, with the 20mm throat, it seems that the 1cm shift is real, i.e. not due to the fit. Furthermore, the pitot pressure distributions show some unusual behavior (especially shot 715).

6.2.3. Conclusion on the CO_2 Shots

Even though very few CO_2 shots are available, and therefore the calibrated envelope is limited, some preliminary conclusions can be formulated. In fact, only very low enthalpies, between 5 and 10 MJ/kg, have been reached. These values are outside the common T5 range (from 10 to 25 MJ/kg). Nevertheless, the obtained results are satisfactory.

Again, the minimum pitot pressure, whose value is very close to the one on the nozzle centerline, has been found to correlate quite well with the nozzle reservoir pressure, apparently independently once more of the enthalpy. The ratio p_{min}/p_0 appears to be around 1.37 with the 30mm throat, and 0.69 with the 20mm throat. These values are the same as the corresponding ones found for air. So is the ratio of these two values, which is roughly 2.0, again different from the expected 2.25 from the ratio of the area ratios.

The scaled curvature a/p_0 seems to be generally lower with CO_2 than with air or N_2, but again only very low enthalpy shots are considered.

The flow symmetry axis matches the nozzle axis when the 30mm throat is used, while it seems that the distribution is more disturbed when the 20mm throat is used.

Since most of the shots were performed during the fourth series, it was not possible to conduct any boundary layer study.

6.3. Hydrogen

6.3.1. Introduction

The reason for the use of hydrogen as a test gas is that it behaves as a perfect gas at conditions achievable in T5. It should be therefore easy to predict the pitot pressure. Unfortunately, it does not seem possible to reach safely a tailored condition on T5, because of the excessively high ST filling pressure required, even using the weakest diaphragms leading to the lowest burst pressures (between 32 and 35 MPa).

In fact, only 4 shots have been calibrated with H_2 as the test gas. Two of them (shot 714 and 716) were performed at the end of the fourth series (when testing different gases), but respecting the security factor of a maximum of 1 atm as the filling ST pressure, in order to avoid any H_2 leak into the lab. As a result, they are far from being tailored, and when eventually a steady period is reached, the test section may have already been contaminated by the driver gas (a mixture of He and Ar). Furthermore, the 14mm throat was used for shot 714, but the density was then so low that the pitot pressure around the centerline was on the order of the noise. Also, a weak shock wave is clearly present, as a result of using the nozzle far off-design.

After the fourth series, many iterations were tried, increasing the ST filling pressure beyond 1 atm, controlling very closely any possible H_2 leak. Finally, it was decided to limit the filling pressure to 4 atm, and two new calibration shots were performed (shot 744 and 745). The condition is admittedly better (than for 716), but still non tailored. A first steady period is reached after 2.75 ms, for around 1 ms, but the possibility of contamination still holds.

6.3.2. The 4 H_2 Shots

Recall, shot by shot, the different settings, and the main comments about the pitot pressure distribution.

Shot 714 was performed with the 14mm throat, and a ST filling pressure of 1 atm. The driver gas is a mixture of 75% helium and 25% argon. The distribution is U-shaped, and a weak axisymmetric shock wave is noticeable. The center part is quite uniform, but on the order of the noise level (less than 0.01 MPa), which is due to the very low density reached with such an area ratio (around 500). This shot is hereafter omitted, since it is not really useful.

Shot 716 was a repeat of shot 714 but, this time, with the 30mm throat. Again, the condition is far from being tailored, and the steady period seems to take place between 3 and 4 ms. The driver gas may have already contaminated the tested flow. The pitot pressure distribution is V-shaped, with a quite low centered value. Nevertheless, some data can be extracted from this shot by the usual parabola fit technique.

Shots 744 and 745 are an "exact" repeat (as far as the settings are concerned) of the optimum H_2 condition. The ST filling pressure level was raised up to 435 kPa (around 4.4 atm in T5 laboratory), without any apparent leaks. All the other settings were kept the same as for shot 716, i.e. lowest diaphragm burst pressures, same driver mixture (75% He, 25% Ar), same initial CT pressure (70 kPa), same 2R pressure (360 psig), same rake position (centered with respect to the nozzle exit). Surprisingly, the two pitot pressure distributions appear to be quite different. While the distribution for shot 745 looks regular, the one for 744 shows some unexpected behaviors : some quite notable jumps appear on the bottom half pitot traces, characterizing an unexpected non-axisymmetric shock wave (clear on the contour plot), and perturbing significantly the symmetry. Finally, recall that for both shots the steady period is supposed to take place between 2.75 and 3.75 ms (at the nozzle exit), and the flow may have already been partially contaminated.

The pitot pressure traces and contour plots, of shots 744 and 745, are shown in appendix 6.

6.3.3. Some Results for H_2

The results presented hereafter should be considered cautiously, keeping in mind all the previous observations about these shots. They may eventually be taken simply as orders of magnitude. But, for sure, they symbolize the problems faced for conditions far off-tailoring (T5 limits) and far off-design (use of a contoured nozzle).

Shot #	P_0 MPa	V_S km/s	Test time ms	P_{min} MPa	a MPa/m^2	Center cm	Ratio $\frac{P_{min}}{P_0}*100$	Scaled $\frac{a}{P_0}$ $*100$, m^{-2}
716	15.3 ±1.8%	3.92	[3.10, 4.10]	0.095	13.	-0.2	0.62	85.
744	14.6 ±4.3%	3.55	[2.75, 3.75]	0.168	11.	-1.4	1.15	75.
745	14.3 ±3.8%	3.39	[2.75, 3.75]	0.153	10.	-0.3	1.07	70.

Table 6.3 - Main Results for H_2 Shots, 30mm Throat

Note that the ratio p_{min}/p_0 is very different between the three shots, even between the last two repeated ones. The scaled curvatures a/p_0 are also quite different, but all three are very large, an other consequence of being far off-design with the contoured nozzle.

6.3.4. Conclusion on the H_2 Shots

According to these few H_2 shots, it is clear that, with the present contoured nozzle, and the ST filling limitations, it is not worth using H_2 as the test gas in T5. The condition cannot be tailored, and would be far off-design anyway. The distribution, which apparently is not repeatable, may easily present some unexpected characteristics (due to some secondary shock waves), and would be far from being uniform.

6.4 Conclusion on the Use of Test Gases Other than Air

Instead of air, N_2, CO_2 and H_2, were also used as the test gas, mostly during the last (fourth) series. The pitot rake survey reveals interesting results.

Exclude immediately the H_2 case, which has just been discussed in the preceding page (chapter 6.3.4.).

For N_2 and CO_2, it was seen that like with air, the minimum pitot pressure p_{min} around the nozzle centerline is highly correlated with the nozzle reservoir pressure p_0. The correlation line, for every case, comes close enough to the origin, to allow considering the two parameters as proportional, and therefore studying the ratio p_{min}/p_0. Also, with these two test gases, this ratio happens to be, as with air, not only independent on the nozzle reservoir pressure p_0 (as expected from the correlation study), but also on the specific enthalpy h_0, at least in the respective calibrated envelopes (and for a given throat, i.e. a given area ratio). However, while the values of this constant are similar for air and CO_2, the ones for N_2 are lower, with both throats (20mm and 30mm). The ratio of the p_{min}/p_0 with the 30mm throat over that with the 20mm is of the order of 2.0 for air and CO_2, and 2.3 for N_2. These values should be compared with the expected 2.25, ratio of the area ratios. While the two values (measured and expected) agree fairly well for N_2, they are different for air and CO_2. This is probably related to the differences in the chemical activity of the different gases at area ratios larger than 100.

Scaling the minimum necessitates scaling the whole pitot pressure distribution by p_0, and so the curvature a has to be scaled by p_0 as well. The study of the curvature has indeed been proved better once scaled, but there still remain large fluctuations in this parameter for any gas. For N_2, an increasing trend of a/p_0 with the enthalpy h_0 has been noticed (especially with the 30mm throat), contrary to the decreasing trend with air. No major trend versus p_0 can be pointed out. For CO_2, it is unfortunately impossible to see any trend, neither versus p_0, nor h_0, because of the small number of points, and the limited enthalpy range. Overall, the values are lower than with air (or N_2), which means that the distribution is more uniform with CO_2, at least on the performed conditions, which are very low enthalpy ones.

The flow symmetry axis (obtained by the parabola) usually coincide with the nozzle centerline, within 1 cm, which is considered to be on the order of the error bars. Nevertheless, for some cases, there exists a definite shift between these two axes, and surprisingly, it is always in the same direction, that is the flow symmetry axis is clearly above the nozzle centerline. This shift is noticeable for the two high enthalpy, N_2 shots with the 30mm throat, which actually follows the general trend observed with air. For CO_2, the two axes match quite well when using the 30mm throat, but a shift is present when using the 20mm throat.

Since most of the shots with N_2 or CO_2 were performed during the fourth series, with the rake centered with respect to the nozzle exit, the distributions cover only the core, and thus no boundary (or external) layer study was investigated.

SECTION 7 :

Comparison with

S U R F Computations

7.0. SURF : SUpersonic Reacting Flow Code

The program SURF was developed to calculate steady and inviscid SUpersonic Reacting Flows in nozzles [Rein, 1989]. The nozzle geometry can be planar or axisymmetric (2D flows). The gas is considered to be an inviscid non-conducting homogeneous mixture of different species (ions and electrons are also admitted). Chemical reactions in the gas are caused by a change of the equilibrium conditions due to different thermodynamic states in different parts of the flow field. In 1991, the idea of partial chemical equilibrium was introduced to the program [Rein, 1991]. The equation system is solved by the method of lines where the lines are oriented approximately in the flow direction. The finite difference approximations which need to be introduced when applying the method of lines, are obtained via a method of characteristics formulation and a kind of upwind differencing. Since here the method of lines is a space marching method, SURF is limited to supersonic flows where the equation system is always hyperbolic. The initial conditions are approximated using a one-dimensional equilibrium flow solution.

The inputs consist of the nozzle geometry, a list of the different species involved for a given gas, all the expected reactions between them, the respective thermodynamic constants, and the reservoir condition expressed in terms of p_0 and T_0. While p_0 comes directly from the experimental data, T_0 is computed by ESTC (Equilibrium Shock Tube Calculation), given the shock speed v_s, the nozzle reservoir pressure p_0, the shock tube filling pressure, initial shock tube (ambient) temperature, and the gas properties.

The output is the axisymmetric non equilibrium solution within the whole nozzle. The solution is then usually visualized according to three main views : profiles of variables along the nozzle centerline, contour plots of parameters in a longitudinal section, and distributions along a radius in the nozzle exit plane. Available output variables are velocity components, pressure, density, local speed of sound, independent and dependent species concentrations. Additional derived variables are usually the velocity, gamma (ratio of specific heats), temperature, Mach number, and pitot pressure (see example in figure 7.1).

However, what was originally called "pitot pressure" was simply ρU^2, and the computed profiles were far from matching the experimental distributions. Thus, some refinements have been brought to compute the pitot pressure more carefully. They are presented in the next paragraph.

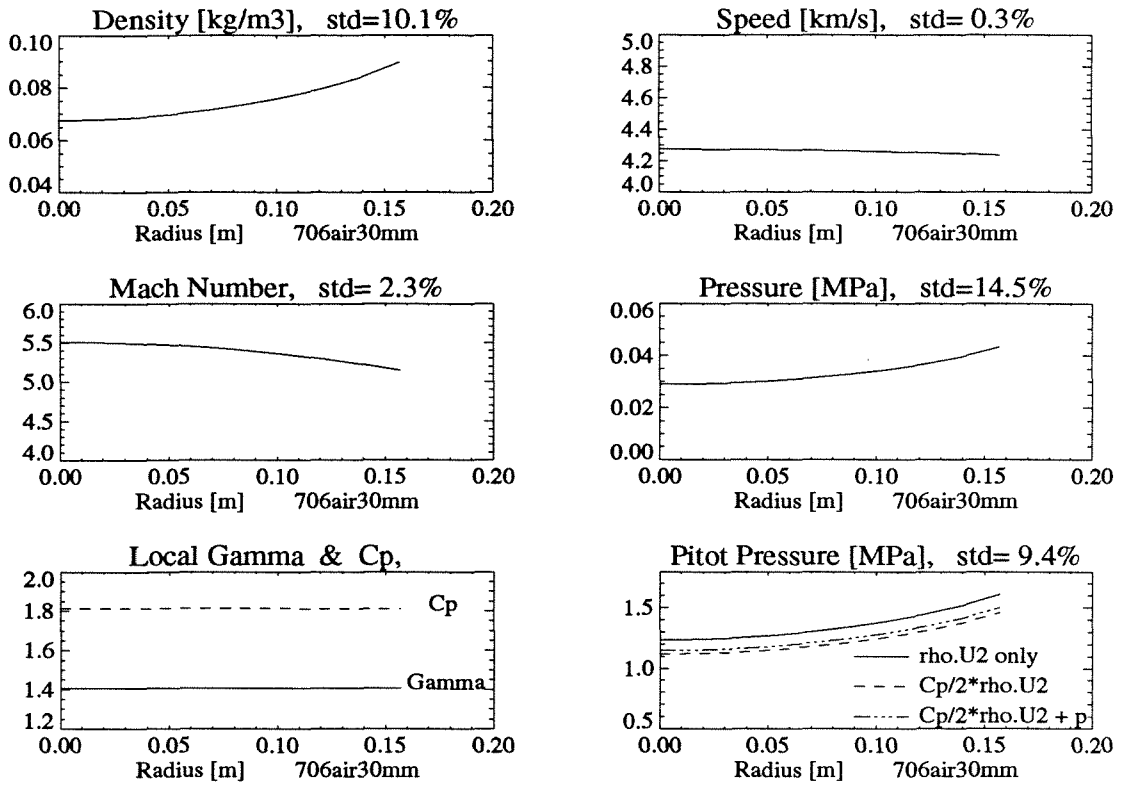

Figure 7.1. Example of SURF Output.

Note that the computed profiles of the pitot pressure present the same characteristic parabolic shape as the experimental distributions (figure 7.1).

7.1. The Computed Pitot Pressure

The main idea behind obtaining a more precise profile of the pitot pressure from the SURF output, comes from the Rayleigh pitot tube formula. It is based on the methods of measurement of total pressure and Mach number from pressure measurements, [Liepmann & Roshko, chapters 6.3 and 6.4], and from the modified Newtonian law for inviscid hypersonic flow [Anderson, chapter 3.3].

Defining $C_p = \dfrac{p_t - p_\infty}{1/2\rho_\infty U_\infty^2}$, and noting that $\rho_\infty U_\infty^2 = \gamma p_\infty M_\infty^2$,

one can rewrite $p_t = \dfrac{C_p}{2}\rho_\infty U_\infty^2 + p_\infty$ leading to $p_t = \left[\dfrac{C_p}{2} + \dfrac{1}{\gamma M_\infty^2}\right]\rho_\infty U_\infty^2$.

Including the Rayleigh pitot tube formula gives

$$C_p = \frac{2}{\gamma M_\infty^2}\left\{\left[\frac{(\gamma+1)^2 M_\infty^2}{4\gamma M_\infty^2 - 2(\gamma-1)}\right]^{\frac{\gamma}{\gamma-1}}\left[\frac{1-\gamma+2\gamma M_\infty^2}{\gamma+1}\right] - 1\right\}$$

or $$p_t = \left\{\frac{1}{\gamma M_\infty^2}\left[\frac{(\gamma+1)^2 M_\infty^2}{4\gamma M_\infty^2 - 2(\gamma-1)}\right]^{\frac{\gamma}{\gamma-1}}\left[\frac{1-\gamma+2\gamma M_\infty^2}{\gamma+1}\right]\right\}\rho_\infty U_\infty^2$$

In other terms, $p_t = coef(\gamma, M_\infty^2) * \rho_\infty U_\infty^2$

In addition to the main assumption required for the Rayleigh pitot tube formula (perfect gas), an approximation on γ has to be made. γ is taken as the local value in front of the shock, and kept constant across the shock. With a γ between 1.34 and 1.43, and a Mach number between 5 and 6, as encountered at the nozzle exit, the corrective coefficient for ρU^2 ranges between 92% and 94%. An example of these corrections is shown on the last plot in figure 7.1.

7.2. Comparison for the 20mm Throat

Some conditions with the 20mm throat have been compared, during a design study for a new contoured nozzle [Nölker, 1994]. The main purpose was to evaluate the accuracy of the program SURF. The compared shots were performed during the third series (repeat of condition 4, with the 20mm throat), both with air and N_2. During the actual shots, the pitot rake was located close to the nozzle exit plane, slightly inside the nozzle.

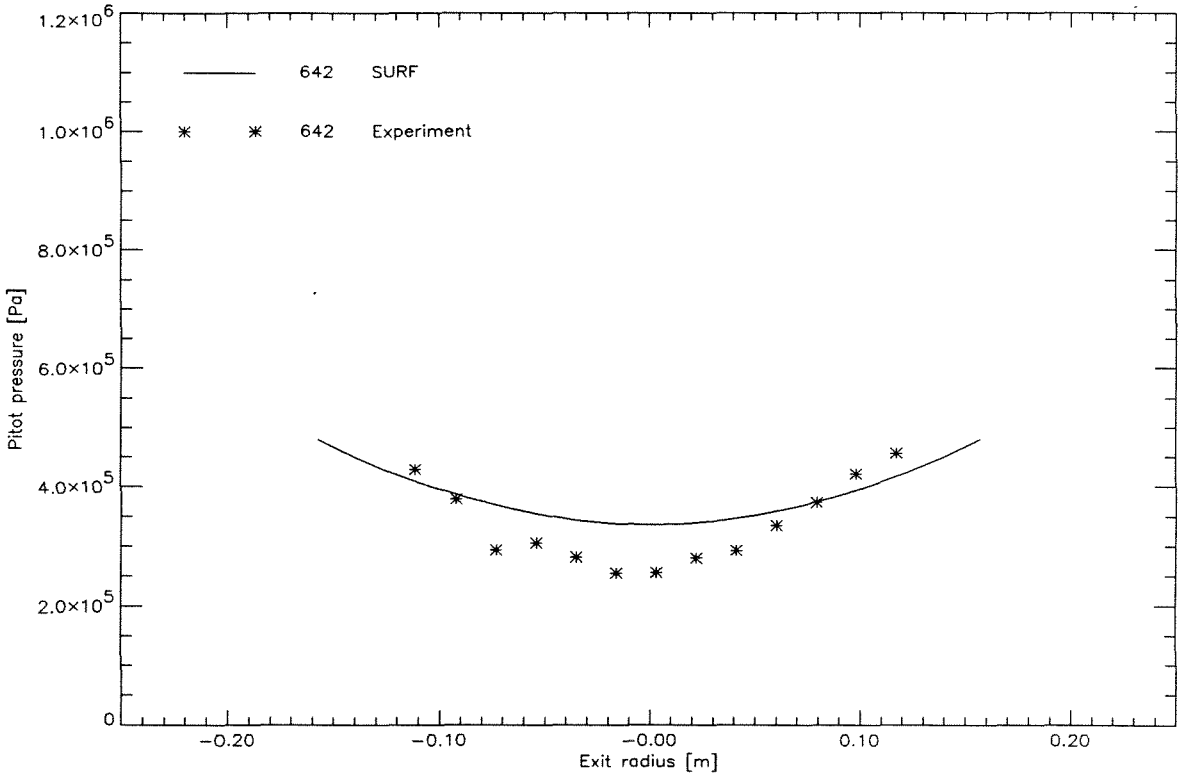

Figure 7.2. Example of Comparison for the 20mm Throat, with N_2 as the test gas.

The main conclusion was that, for some shots, the agreement between the computed profile and the experimental distribution was fairly good, but for most of the cases, it was poor. Indeed, for most of the comparisons, both with air and N_2, the experimental distribution shows a higher curvature, and a lower minimum than the computed profile. An example (from Nölker) is shown in figure 7.2.

7.3. Study of SURF with the 30mm Throat

Despite the disagreement between the experimental distribution and the computed profile, it was decided to investigate different conditions in order to check if SURF was reproducing the general trend observed on the scaled parameters (p_{min}/p_0 and a/p_0). The study was focused on the air, 30mm throat shots from the fourth series.

Shot after shot, one can observe the same general disagreement between the experimental distribution and the computed profile, as with the 20mm throat. The experimental curvature is still higher, and the minimum lower than the computed ones. The first observation may be explained by the boundary layer, not handled by the inviscid code. It may produce higher densities on the edges than computed, which is consistent with the observed behavior.

According to the SURF computations, the velocity profile (along a exit radius) is almost uniform, with a standard deviation (on the whole radius) around 0.3%. The curvature of the pitot pressure distribution is therefore directly related to the density profile. The standard deviation for the density ranges between 7.5% at high enthalpy, and 12% at low enthalpy. This decreasing trend of the curvature with the enthalpy can also be expressed in terms of the scaled pitot pressure curvature $a/p_0 * 100$, in $[m^{-2}]$. It decreases from around 22 for h_0 around 10 MJ/kg, to around 14 for h_0 around 25 MJ/kg. This is in agreement with the observed trend from the experimental points (see figure 5.7). At some enthalpies, a minimum was found for p_0 around 60 MPa, the lowest scaled curvature being on the order of 12 at $h_0 = 20$ MJ/kg and $p_0 = 62$ MPa. This observation is also in agreement with the experimental trend (see figure 5.8).

However, the scaled minimum pitot pressure, which is exactly on the centerline, presents some trends in disagreement with the experimental conclusion of a constant. According to SURF, p_{min}/p_0 should significantly increase with the enthalpy h_0, and slightly with the nozzle reservoir pressure p_0. Values of $p_{min}/p_0 * 100$ range from 1.4 to 1.55, instead of the experimental constant 1.37 (figure 7.3).

The low values of the ratio p_{min}/p_0 at low enthalpies may be explained by respective high values of the curvature. In fact, the ratio $p_t/p_0 * 100$ averaged throughout the whole exit plane is more constant, ranging from 1.65 at low enthalpy to 1.70 at high enthalpy. Note that, given the area ratio of 110, this ratio $p_t/p_0 * 100$ would be 1.45 for a perfect gas.

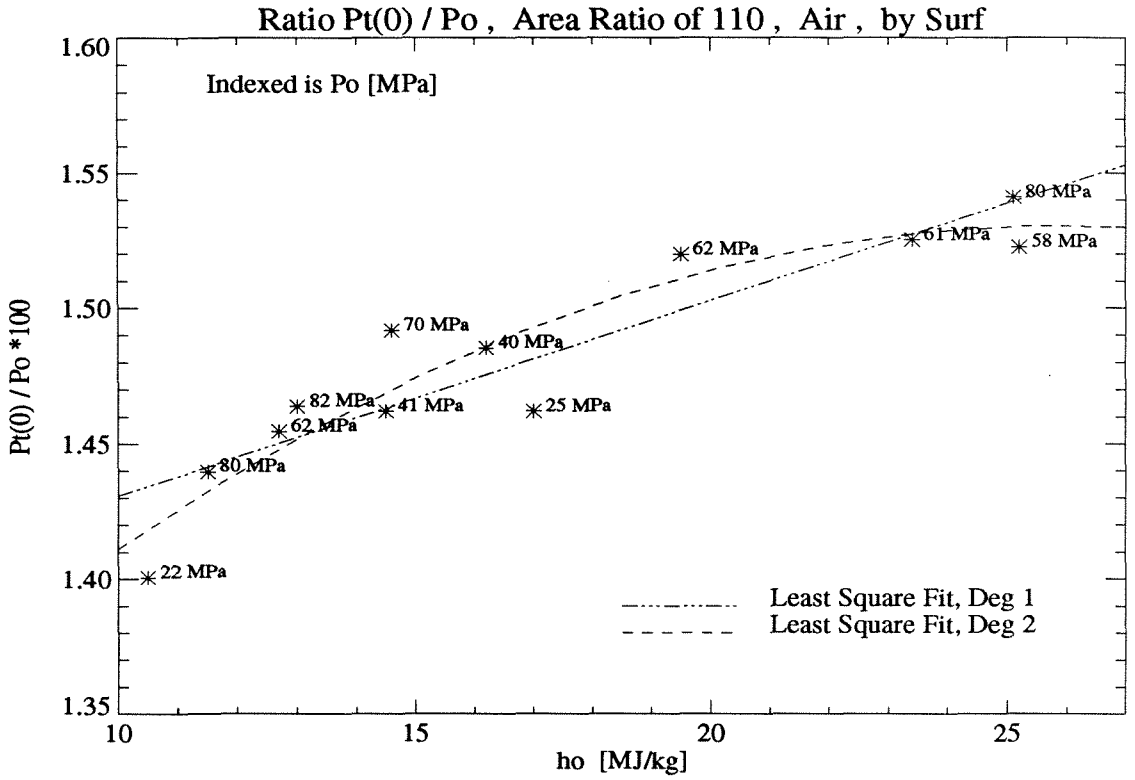

Figure 7.3. Ratio $p_t(0)/p_0$, according to SURF, Area Ratio of 110, with Air.

7.4. Conclusions on SURF

Even though orders of magnitude are often correct, it was seen that the computed pitot pressure profiles do not match the experimental distributions, at least for simulations of air shots, with either the 30mm or the 20mm throat. In most of the cases, the experimental minimum is lower, and the curvature higher, than the computed ones. The latter disagreement may be explained by the lack of boundary layer effects, not handled by SURF, inviscid code. Nevertheless, the trends of the computed scaled curvature agree quite well with the observed ones from the experimental points. However, SURF does not predict a constant value of the scaled minimum pitot pressure p_{min}/p_0 for a given gas and a given area ratio. The disagreement in the values and the trends remain unexplained.

Both the SURF computation, and the pitot pressure derivation, make assumptions. SURF is an inviscid code, does not handle shock waves, and is based on an upstream one-dimensional solution. The pitot pressure derivation is based on the Rayleigh pitot tube formula, for a perfect gas.

SECTION 8 :

General Conclusions,

Discussion,

Recommendations.

8.1. General Conclusions

This research project has extended the understanding of the performance of the T5 nozzle by delineating the limitations of the flow quality in the nozzle exit plane at different conditions.

Because of a special need, the main emphasis was placed on a particular off-design geometry, namely with the 20mm diameter throat. During a series of repeated shots, the repeatability of the achieved condition with respect to the set-up and tube fillings, was shown to be quite good.

The main results of this study were that the standard deviations of the burst pressure, reservoir pressure and reservoir enthalpy did not exceed 5%. The radial pitot pressure distribution in the exit plane of the nozzle exhibited a clear minimum near (but surprisingly not always on) the nozzle axis in all cases. The repeatability of this minimum was within ± 3% with air, and 7% with N_2. The repeatability of the second derivative of pitot pressure with radial distance was only ± 15%, with both test gases.

All of these repeatability values may be expected to apply similarly, as orders of magnitude, to the other conditions tested, though repeatability tests were not performed at all conditions.

The calibration study covers the whole T5 envelope of reservoir pressure and specific enthalpy, using both the 20mm and 30mm throat (area ratio around 225 and 100, respectively), with air and nitrogen as test gases, and a few cases with carbon dioxide and hydrogen.

New methods to reduce the test section data were successfully investigated. The pitot pressure distribution was characterized by the parameters of a parabolic fit in terms of the minimum, curvature, and location of the symmetry axis. This has turned out to be quite effective.

In every case, the minimum pitot pressure was correlated with the nozzle reservoir pressure. In fact, the ratio p_{min}/p_0 can be considered independent of the reservoir condition (neither p_0 nor h_0) throughout the whole envelope. However, the value of the ratio does depend on the given test gas and, of course, the given throat diameter.

The distribution always presented a parabolic shape with positive curvature, more or less curved, depending on the enthalpy and the reservoir pressure. When using air as the test gas, the curvature decreases with increasing enthalpy, in both throat cases. However, the trend is opposite when using nitrogen.

In most cases, a noticeable shift was observed between the location of the symmetry axis of the distribution and the nozzle centerline, especially at off-design conditions.

The ratio of the p_{min}/p_0 constant for the 30mm throat over the one for the 20mm throat, was compared to the theoretical value of the inverse ratio of the area ratios. Even though the order of magnitude is correct, the values for air, nitrogen, carbon dioxide, and

the theoretical one are all different.

Finally, experimental results were compared with various SURF simulations. Again, orders of magnitude are correct, but values are different. Computed minimum pitot pressures are higher, while computed curvatures are lower than the experimental ones.

8.2. Discussion

Beyond these conclusions, some remarks and suggestions can be made about the use of different test gases, the SURF program, and the behavior of the ratio p_{min}/p_0.

In terms of pitot pressure, the behavior of nitrogen is quite different from that of air. On the opposite, the behavior of carbon dioxide and air are quite alike, while the enthalpy ranges are complementary. The use of other test gases, especially the ones leading to far off-design conditions like hydrogen, should be avoided.

The SURF program is an inviscid code. Therefore, it does suffer the lack of viscous effects, especially a boundary layer computation, or at least an estimate. Currently, no corrections for the effect of the nozzle wall boundary layer are included. This may explain the problem of lower curvatures, and the higher minimum.

While the ratio p_{min}/p_0 is independent of h_0 and p_0 in the measurements, the computations show a significant increase with increasing h_0 and a slight increase with increasing p_0. Nevertheless, the computed curvature exhibits the same trend as the measured one in that they all decrease with increasing h_0 to quite low values close to the design point, i.e. h_0 around 25 MJ/kg.

Two possible explanations can be suggested for the different values found for the ratio of the ratios p_{min}/p_0 for the two throats. The first one is related to the final flow speed reached at the nozzle exit. The scaled pitot pressure p_t/p_0 goes in theory like ρu^2. The ρu part of it should go inversely with the area ratio. But it may happen that for a given enthalpy h_0, the exit velocity u is still significantly lower than the terminal speed $\sqrt{2h_0}$, and this would be even more so for the area ratio of 100 than for 225. This may be significant when chemical effects are strongly involved (dissociation/recombination), as, for example, in air and carbon dioxide, in comparison with nitrogen.

The second explanation is related to the throat. Exposed to severe conditions and gradients, the flow may detach at the throat entry. Also, the boundary layer may be thicker than expected, especially at this location. This would imply a smaller effective throat minimum area, leading to a different ratio of the area ratios. This may depend on the test gas.

8.3. Recommendations

In the light of the experience gained during this investigation, the author would like to make the following recommendations.

The flow quality in a contoured nozzle is seriously impaired when it is used at off-design conditions. This includes too low enthalpies, the use of reduced throat diameter, or the use of a different test gas. In the off-design tests of this investigation, high curvatures of the pitot pressure distribution, or some centerline focusing effects, were observed. In other words, a contoured nozzle should be only used at, or quite close to the designed condition.

However, for T5, working within such a wide envelope of conditions, this would imply several contoured nozzle, which would be quite expensive. Instead, a more reasonable choice is to use a conical nozzle, which would provide the flexibility of throat exchange without causing radial nonuniformity of the pitot pressure. However, this would be at the expense of working with an axial pitot pressure gradient and divergent flow. Actually, a 8 degree half-angle conical nozzle has already been built, and is ready to be tested.

This calibration study was limited to pitot pressure survey, at least as far as the test section is concerned. Other studies involving heat fluxes, and enthalpies were also investigated [Chihyung Wen, 1994]. These are important for the confirmation of the value of h_0. Other quantities, such as the flow composition and the static temperature are also very important. Methods for measuring these and their application to T5 are needed.

To acquire precise values of the reservoir parameters is extremely important, in order to know the exact condition in the test section. This implies being very careful with the nozzle reservoir pressure transducers, as far as the maintenance, the calibration, the data acquisition, the complete derivation, are concerned. Furthermore, they are the only current trigger signals. In view of the significant decrease of the shock speed along the shock tube, methods for the measurement of the variation of h_0 with time are also needed.

Finally, the throat design is still a main concern. On one hand, finding some new materials capable of sustaining such heat fluxes and pressures experienced in T5, is under investigation. On the other hand, it would be useful to know more about the flow through the current throats, e.g., the boundary layer thickness, or even whether the flow separates. Practically, it could be useful to know the exact throat minimum diameter before every shot, to record its history, and to evaluate the damage.

REFERENCES

References Specific to T5

ADAM Philippe & ROUSSET Bernard (1993) ; "Electre Experiments in T5", GALCIT Report FM 93-2, Graduate Aeronautical Laboratories California Institute of Technology, Pasadena, California, September 1993.

BELANGER Jacques (1993) ; "Studies of Mixing and Combustion in Hypervelocity Flows with Hot Hydrogen Injection", Ph.D. Thesis, California Institute of Technology.

BELANGER Jacques and HORNUNG Hans G. (1994) ; "Numerical Predictions and Actual Behavior of the Free Piston Shock Tube T5", AIAA Paper 94-2527, 18^{th} AIAA Aerospace Ground Testing Conference, Colorado Springs, CO, June 1994. (on the piston motion in the CT and the viscous losses in the ST)

BROUILLETTE Martin (1991) ; "Design modifications to T5 and their implementation", GALCIT Report FM 91-3, California Institute of Technology.

CUMMINGS Eric (1993) ; "The Design of T5 Diaphragm Indenter", GALCIT Report, California Institute of Technology.

GERMAIN Patrick, CUMMINGS Eric, and HORNUNG Hans G. (1993) ; "Transition on a Sharp Cone at High Enthalpy; New Measurements in the Shock Tube T5 at GALCIT", AIAA Paper 93-0343, 31^{st} Aerospace Sciences Meeting & Exhibit, Reno, Nevada, January 1993. (on flow visualization and the sodium technique)

GERMAIN Patrick (1994) ; "The Boundary Layer on a Sharp Cone in High-Enthalpy Flow", Ph.D. Thesis, California Institute of Technology.

HORNUNG Hans G. and BELANGER Jacques (1990) ; "Role and Techniques of Ground testing for Simulation of Flows Up to Orbital Speed, California Institute of Technology", AIAA Paper 90-1377, AIAA 16th Aerodynamic Ground Testing Conference, Seattle, Washington, June 18-20.

HORNUNG Hans G. (1992) ; "Performance Data of the New Free-Piston Shock Tunnel at GALCIT", AIAA Paper 92-3943, AIAA 17th Aerospace Ground Testing Conference, Nashville, Tennessee, July 6-8.

McINTOSH, M. K. (1970) ; "A Computer Program for the Numerical Calculation of Equilibrium and Perfect Gas Conditions in Shock Tunnels", Australian Defence Scientific Service, Technical Note CPD 169, Salisbury, South Australia. (on ESTC)

NOELKER Matthias (1994) ; "Design Study of a New Contoured Nozzle for a Free-Piston Shock Tunnel", GALCIT Report, California Institute of Technology.

REIN Martin (1989) ; "SURF : A Program for Calculating Inviscid Supersonic Reacting Flows in Nozzles", GALCIT Report FM 89-1, Graduate Aeronautical Laboratories California Institute of Technology, Pasadena, California, 1989.

REIN Martin (1991) ; "Partial Chemical Equilibrium : Theory and Implementation in the Program SURF", GALCIT Report FM 91-1, California Institute of Technology.

TOGAMI Kenji (1993) ; "Hypervelocity Dissociating Flow over a Spherically Blunted Cone", Ae.E. Thesis, California Institute of Technology.

References Specific to Other Shock Tubes

EITELBERG George (1993) ; "Calibration of the HEG and its Use for Verification of Real Gas Effects in High Enthalpy Flows", AIAA/DGLR Fifth International Aerospace Planes and Hypersonics Technologies Conference, 30 Nov - 3 Dec 1993, Munich, Germany, AIAA-93-5170.

FITCH C. R. (1966) ; "Flow Quality Improvement at Mach 8 in the VKF 50-inch Hypersonic Wind Tunnel B", AEDC-TR-66-82.

JACOBS P. A. and STALKER R. J. (1991) ; "Mach 4 and Mach 8 Axisymmetric Nozzles for a High-Enthalpy Shock Tunnel", Aeronautical Journal, Vol 95 (949), Nov 1991. (about T4 in Australia)

JONES Robert A. and FELLER William V. (1970) ;"Preliminary Surveys of the Wall Boundary Layer in a Mach 6 Axisymmetric Tunnel", Langley Research Center, NASA TN D-5620 (Feb 1970).

MIDDEN Raymond E. and MILLER III Charles G. (1985) ; "Description and Calibration of the Langley Hypersonic CF_4 Tunnel", NASA Technical Paper 2384, March 1985.

MUYLAERT J., WALPOT L., HAUSER J., SAGNIER P., DEVEZEAUX D., PAPIRNYK O., and LOURME D. (1992) ; "Standard Model Testing in the European High Enthalpy Facility F4 and Extrapolation to Flight", AIAA Paper 92-3905.

SIVELLS James C. (1963) ; "Aerodynamic Design and Calibration of the VKF 50-inch Hypersonic Wind Tunnels", AEDC-TDR-62-230 (March 1963).

References in Hypersonics

ANDERSON Jr. J. D. (1989) ; "Hypersonic and High Temperature Gas Dynamics", McGraw-Hill, New York.

HORNUNG Hans G. (1992) ; "Ae234 Hypersonic Aerodynamics Lecture Notes, California Institute of Technology.

JOHNSON C. B., BONEY L. R., ELLISON J. C., and ERICKSON W. D. (1963) ; "Real-Gas Effects on Hypersonic Nozzle Contours with a Method of Calculation", Langley research Center, NASA TN D-1622 (April 1963). (on BL thickness computation)

LIEPMANN Hans W. and ROSHKO Anatol (1957) ; "Elements of Gasdynamics", John Wiley and Sons, New York.

PIRUMOV U. G. and ROSLYAKOV G. S. (1985) ; "Gas Flow in Nozzles", from the original Russian version "Techeniya gaza v soplakh" (1978), Springer-Verlag.

SHEPHERD Joseph E. (1994) ; "Ae201c Hypersonic Aerodynamics Lecture Notes, California Institute of Technology.

VINCENTI W. G. and KRUGER Jr. C. H. (1986) ; "Introduction to Physical Gas Dynamics", Krieger, Florida (reprint of 1965 John Wiley and Sons).

VKI (Von Karman Institute for Fluid Dynamics) (1993) ; "Methodology of Hypersonic Testing", Lecture Series 1993-03. Specially Chp 4, 5 ,& 6.

APPENDIXES

APPENDIX 1

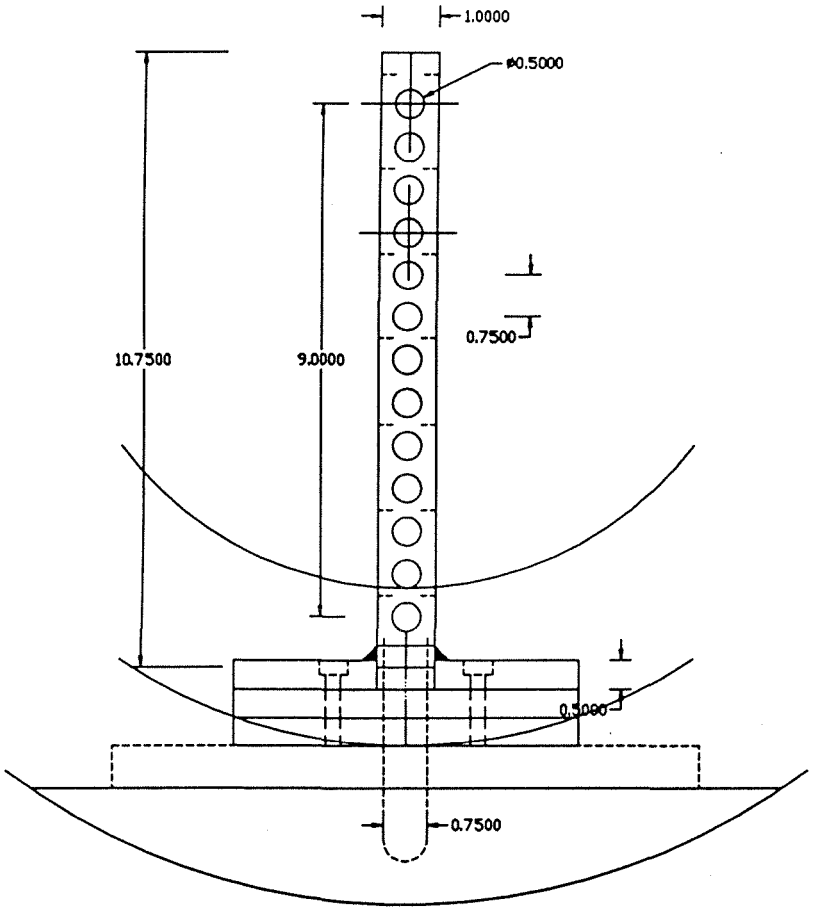

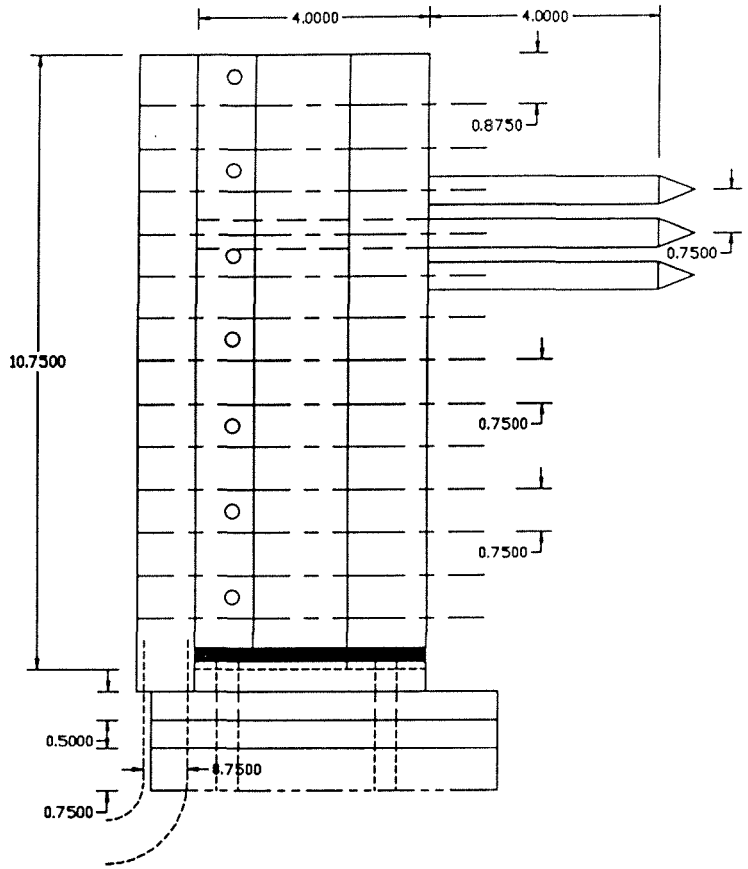

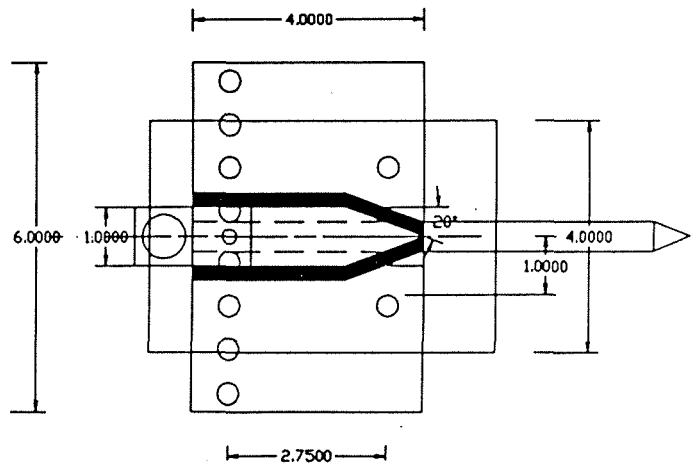

B. ROUSSET	March 93	S. Steel			INCHES
DRAWN: BY	DATE	MATERIAL	FINISH	ASS,Y REF.	SCALE

GALCIT
T5 Laboratory
Caltech, Pasadena

R13 TRANSDUCER RACK
by
Bernard ROUSSET

DRAWING REF.

B. ROUSSET	March 93	Brass			INCHES
DRAWN: BY	DATE	MATERIAL	FINISH	ASS,Y REF.	SCALE
GALCIT T5 Laboratory Caltech, Pasadena	PITOT TRANSDUCER TIP by Bernard ROUSSET (based on Simon SANDERSON 's Design) NAME				

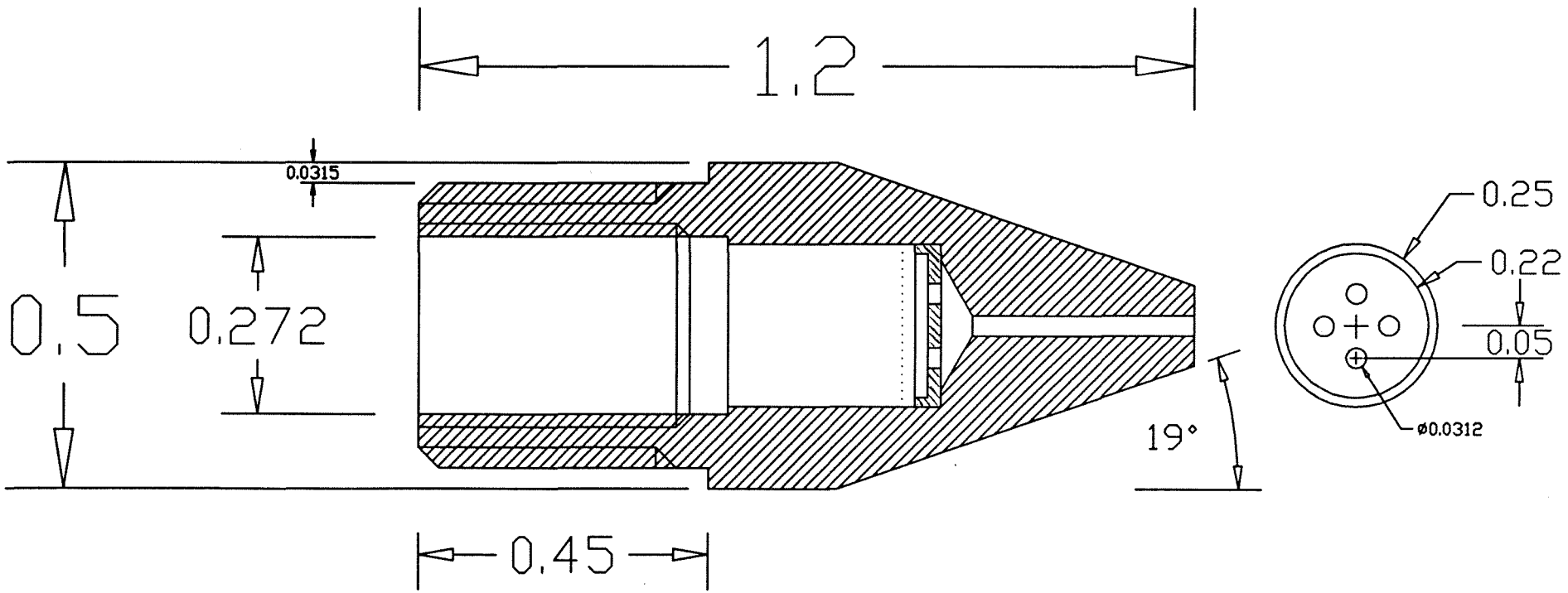

PCB®
PIEZOTRONICS

SPECIFICATIONS
PRESSURE TRANSDUCER
VOLTAGE MODE

REVISIONS -137-
-D-Rev # 3861

SHEET 1 OF 1

MODEL 113A26

DYNAMIC

Range (5V Output)	psi (Bars)	500 (34.5) ≈ 3.5 MPa
Useful Overrange	psi (Bars)	1000 (69)
Maximum Pressure	psi (Bars)	10000 (690)
Resolution	psi (Bars)	0.01 (0.00069)
Sensitivity (nominal)	mV/psi (mV/[Bars])	10 ±0.5 (145)
Resonant Frequency	kHz	≥500
Low Frequency (-5%)	Hz	0.001
Rise Time	µs	1
Overload Recovery	µs	10
Amplitude Non-Linearity [1]	% FS	≤1
Acceleration Sensitivity	psi/g ([Bars]/[m/s²])	0.002 (0.000014)
Vibration (max)	g (m/s²) peak	2000 (19620)
Shock (max)	g (m/s²)	20000 (196200)

ELECTRICAL

Excitation		
Constant Current	mA	2-20
Voltage	VDC	24-27
Discharge Time Constant (@R.T.)	s	≥50
Output Impedance	ohm	<100
Output Bias	+volt	8 to 14
Polarity		Positive

ENVIRONMENTAL

Temperature Coefficient	%/°F (%/°C)	≤0.03 (0.054)
Maximum Flash Temperature	°F (°C)	3000 (1648.8)
Temperature Range	°F (°C)	-100 to +275 (-73 to +135)

PHYSICAL

Case/Diaphragm	material	17-4/Invar
Sealing		Epoxy
Weight (with clamp nut)	oz (gram)	0.2 (6)
Connector (micro)	coaxial	10-32

Notes:
[1] Zero based best straight line.

Supplied Accessories:
Model 065A02 Seal
Model 060A03 Clamp Nut

APP'D	TC	12/82	SPEC NO.
ENGR	MTR	12/82	113-1260-80
SALES	RCM	12/82	

APPENDIX 2

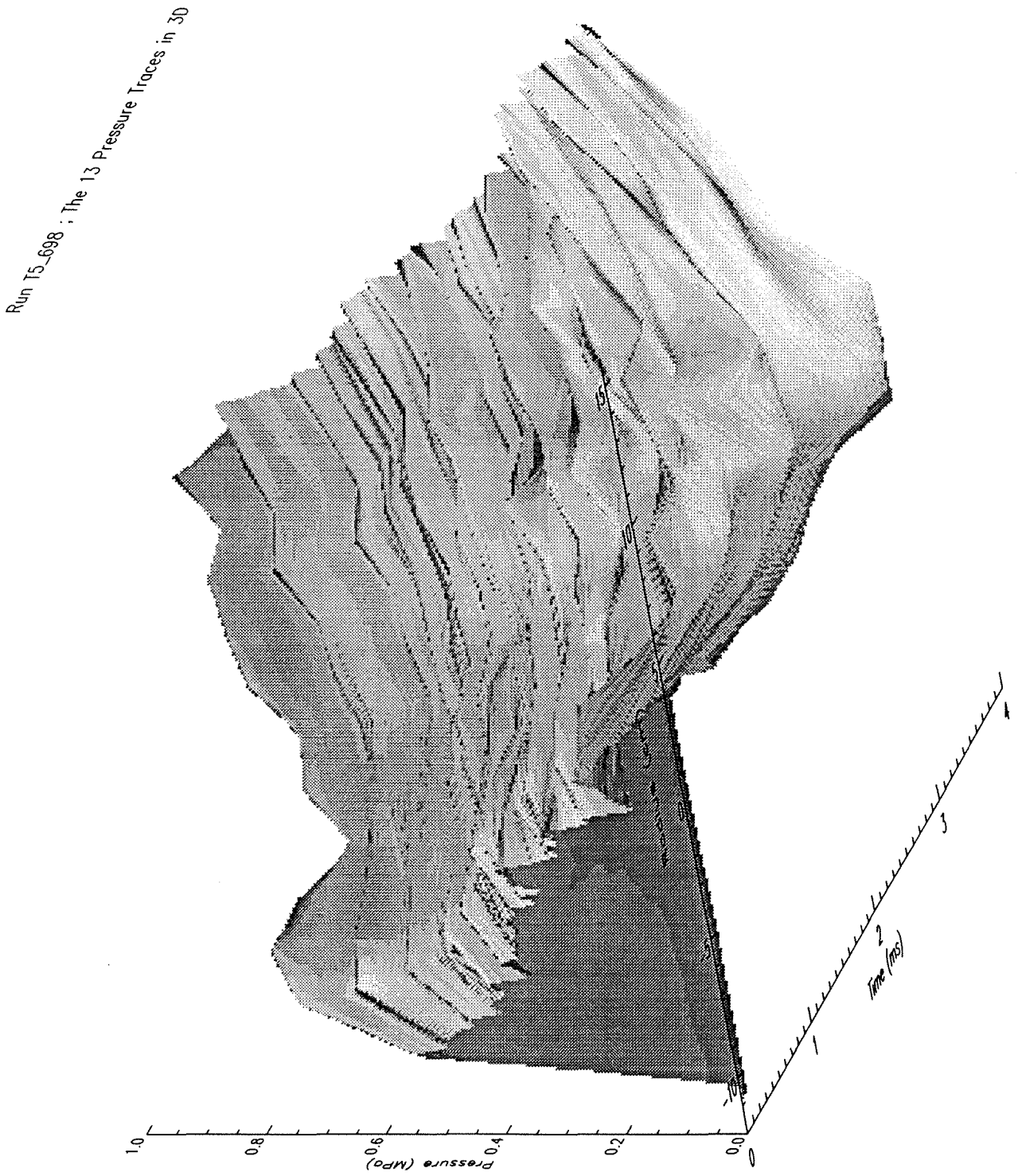
Run T5_698 ; The 13 Pressure Traces in 3D
Pressure (MPa)
0.0
0.2
0.4
0.6
0.8
1.0
Time (ms)
0
1
2
3
4
-10
10
50

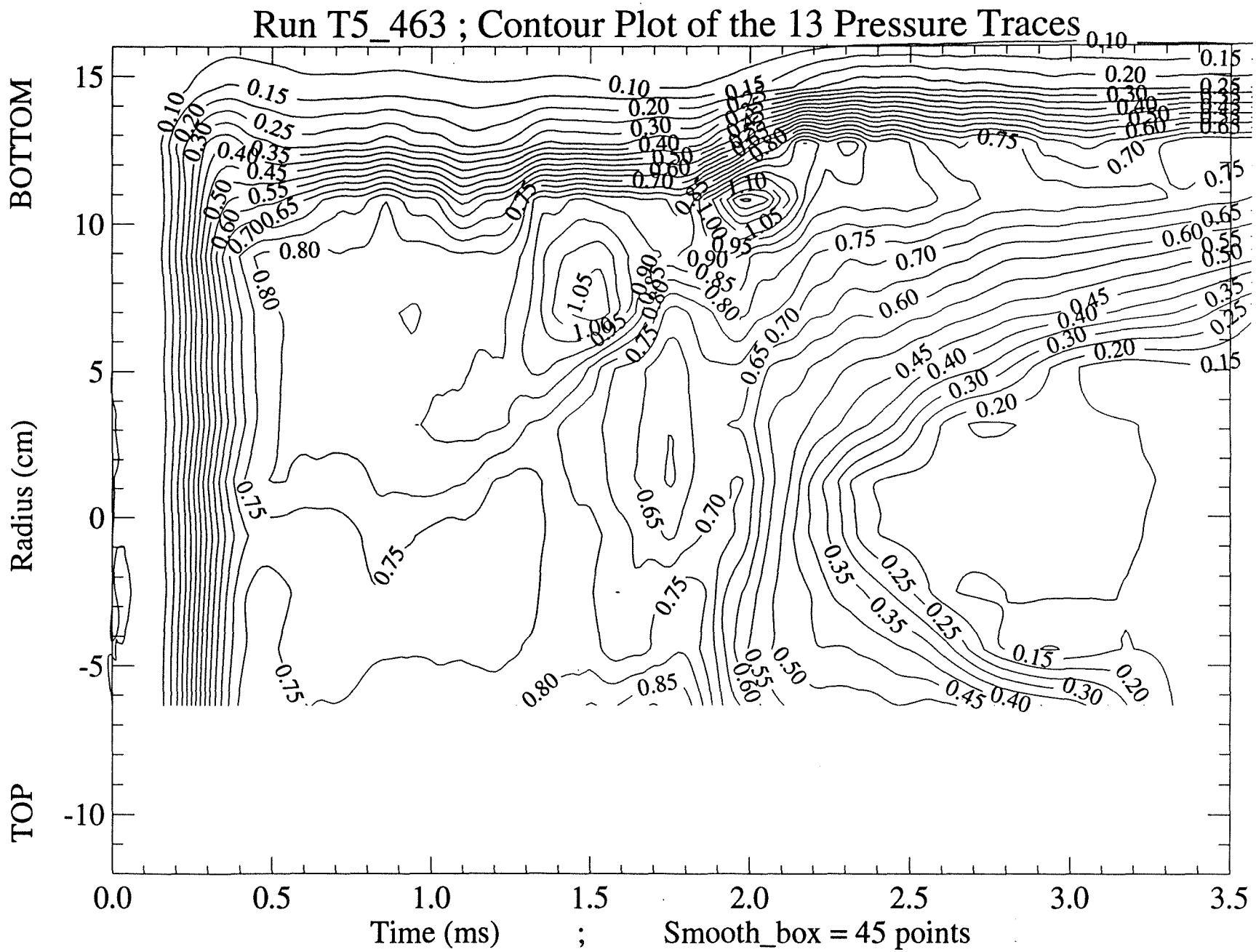
Run T5_463 ; Contour Plot of the 13 Pressure Traces
BOTTOM
TOP
Radius (cm)
15
10
5
0
-5
-10
0.0
0.5
1.0
1.5
2.0
2.5
3.0
3.5
Time (ms) ; Smooth_box = 45 points

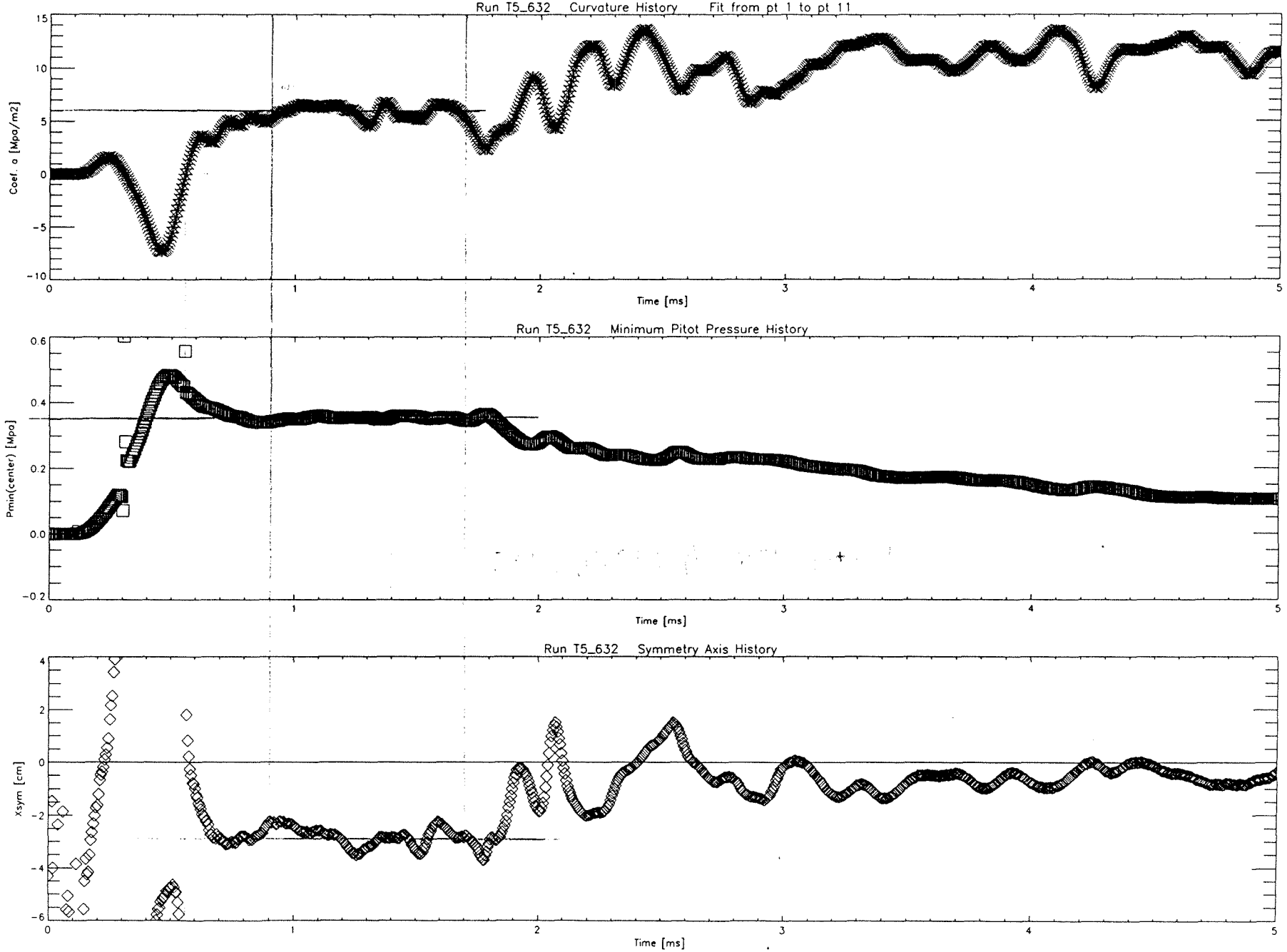
Run T5_632 Curvature History Fit from pt 1 to pt 11
Coef. a [Mpa/m2]
Time [ms]
Run T5_632 Minimum Pitot Pressure History
Pmin(center) [Mpa]
Time [ms]
Run T5_632 Symmetry Axis History
Xsym [cm]
Time [ms]

APPENDIX 3

This table is the log of the series of repeated shots, with some comments on specific events or on test section changes.

Note that the "unit" of height for the rake position is one spacer of 3/4 of an inch ; as to the axial position denominations, please see paragraph 3.1.

Shot	Position Axial	Position High	Test Gas	Conditions	Comments
627	-4.0cm	+2.5	Air	950 psig in 2R, 30 kPa in ST	High response time in some traces
628	-4.0cm	+2.5	Air	1000 psig in 2R, 30 kPa in ST	To increase P_0; Transd. 4 & 10 checked
PS 628 Copper deposit on the rake; Transd. 04 changed to 00					
629	-0.5cm	+2.5	Air	35 kPa in ST	To decrease h_0 and taylored P_0
Note on 629 : The copper sleeve melted, creating a turbulent flow; Transd. 13 checked					
PS 629 Changed ST end sleeve, holders of nozzle res. transd., piston front ring, remachined the throat					
630	-0.5cm	+2.5	Air	32.5 kPa in ST	Everything went normal
631	+3.0cm	+2.5	Air	1000 psig in 2R, 30 kPa in ST	PS: interch. the whole tip 4 & 10
632	+3.0cm	+2.5	Air	as 631, transd. interchanged	PS: interch. the whole tip 3 & 11
633	+3.0cm	+2.5	Air	as 632, transd. interchanged	No ST cleaning
634	+6.5cm	+2.5	Air	same as 633	ST cleaning
635	+6.5cm	+1.5	Air	Rake down by 3/4"	Transd. 3 traces clearly bad
636	+6.5cm	+1.5	Air	acq. syst. interchanged	CT cleaning, transd. 3 poorly connected
PS 636 New CT-ST throat in steel					
637	+6.5cm	+2.0	Air	up by 3/8"	Everything went normal
638	+3.0cm	+2.0	Air	same as 637	P4 transd. checked before the shot
639	-0.5cm	+2.0	Air	same as 638	Good data, good symmetry
640	-0.5cm	+2.0	N_2	N_2 as test gas	Pb filling ST (quick vacuum again)
641	-0.5cm	+2.5	Air	up by 3/8", high as 627	Good symmetry
642	-0.5cm	+2.5	N_2	N_2 as test gas	P4 South checked before the shot
643	+6.5cm	+2.5	N_2	N_2 as test gas	Change holder of $P_{0,South}$, piston leaked
644	-0.5cm	+2.5	Air	30 mm throat	Low P4 !
646	-0.5cm	+2.5	N_2	30 mm throat	P_0 South transd. SN 2444

Table App.3 - Conditions and Rake Positions (Shots 627-646)

APPENDIX 5

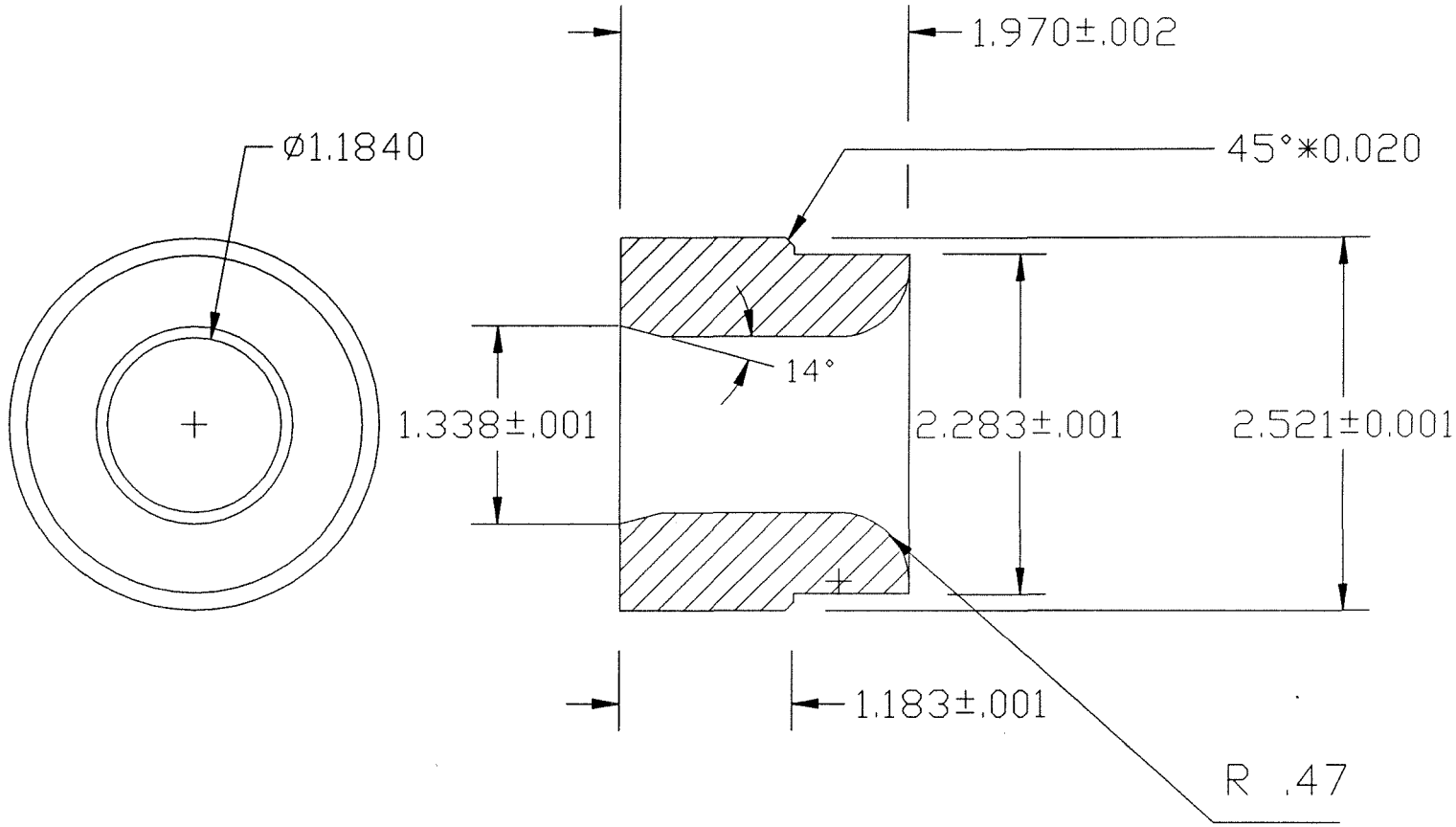

BAHRAM V.	7-29-92	MOLYBDENUM	MACHINE	3709 17 01	1:1, INCH	UNLESS OTHERWISE NOTED
DRAWN:BY	DATE	MATERIAL	FINISH	ASS,Y REF.	SCALE	TOLERANCES : +- 0.004 OR 1/64
GALCIT T5 Laboratory Caltech, Pasadena		30mm nozzle THROAT NAME				3709-17-04-B DRAWING NO.

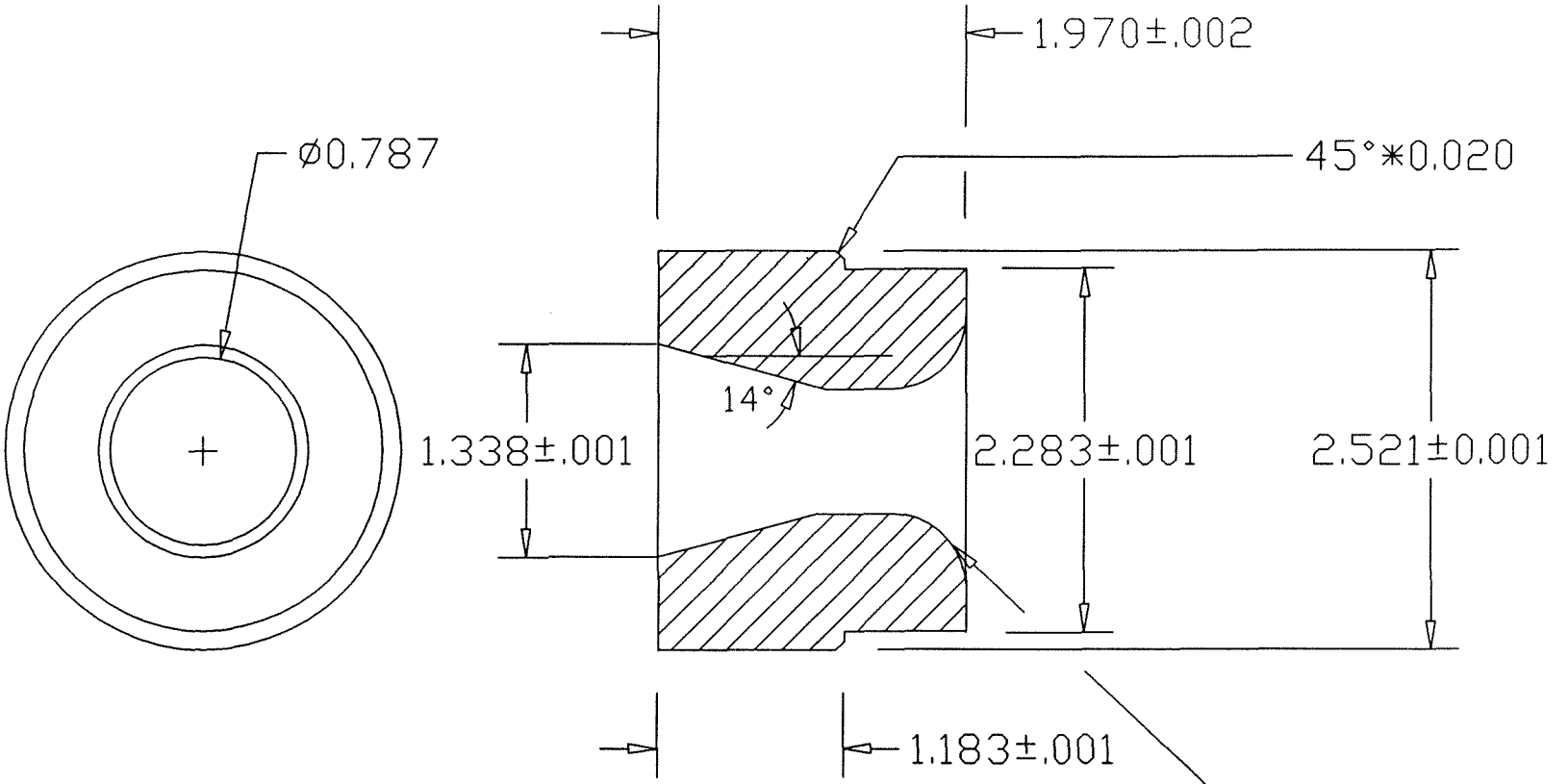

20 mm THROAT

BAHRAM V.	7-29-92	MOLYBDENUM	MACHINE	3709 17 01	1:1, INCH	UNLESS OTHERWISE NOTED
DRAWN BY	DATE	MATERIAL	FINISH	ASS'Y REF.	SCALE	TOLERANCES : +- 0.004 OR 1/64
GALCIT T5 Laboratory Caltech, Pasadena		nozzle THROAT NAME				3709-17-04-B DRAWING NO.

APPENDIX 6

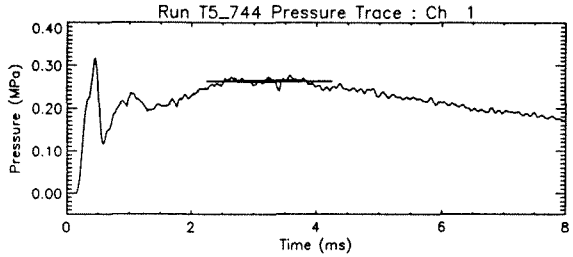
Run T5_744 Pressure Trace : Ch 1
Pressure (MPa)
Time (ms)

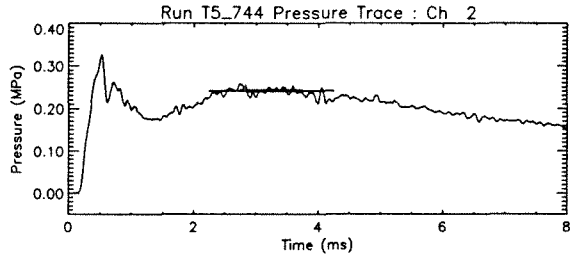
Run T5_744 Pressure Trace : Ch 2
Pressure (MPa)
Time (ms)

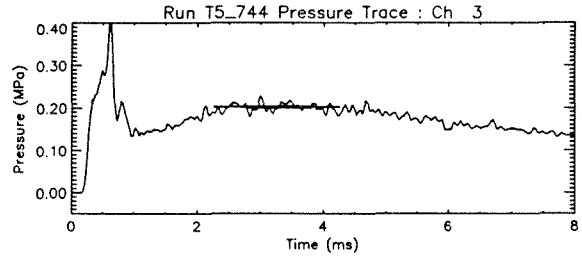
Run T5_744 Pressure Trace : Ch 3
Pressure (MPa)
Time (ms)

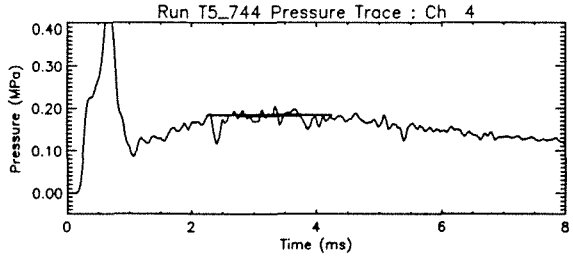
Run T5_744 Pressure Trace : Ch 4
Pressure (MPa)
Time (ms)

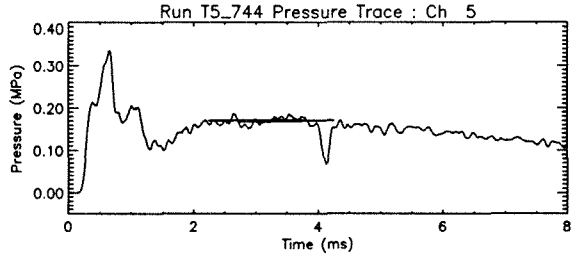
Run T5_744 Pressure Trace : Ch 5
Pressure (MPa)
Time (ms)

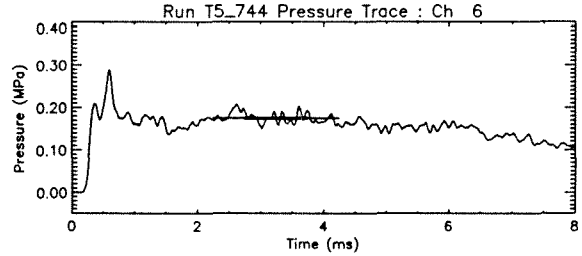
Run T5_744 Pressure Trace : Ch 6
Pressure (MPa)
Time (ms)

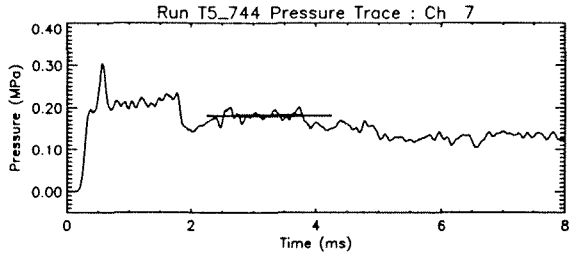
Run T5_744 Pressure Trace : Ch 7
Pressure (MPa)
Time (ms)

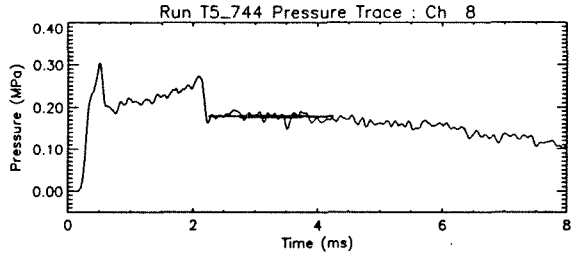
Run T5_744 Pressure Trace : Ch 8
Pressure (MPa)
Time (ms)

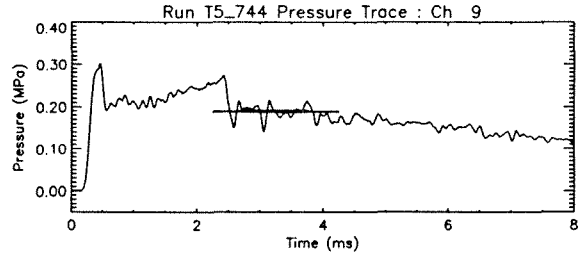
Run T5_744 Pressure Trace : Ch 9
Pressure (MPa)
Time (ms)

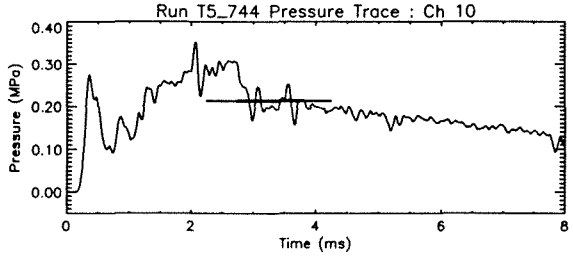
Run T5_744 Pressure Trace : Ch 10
Pressure (MPa)
Time (ms)

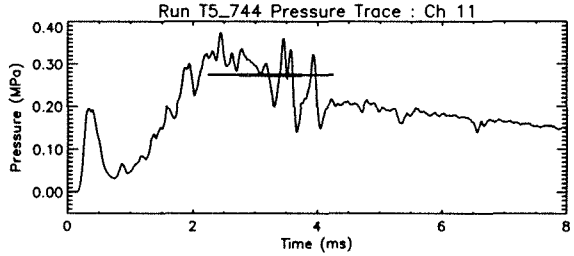
Run T5_744 Pressure Trace : Ch 11
Pressure (MPa)
Time (ms)

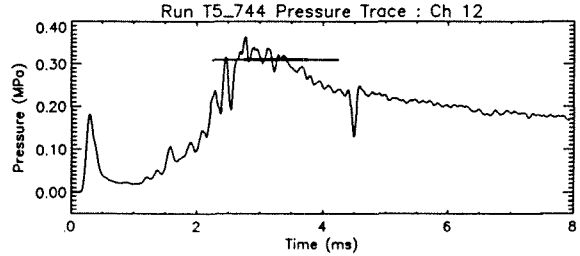
Run T5_744 Pressure Trace : Ch 12
Pressure (MPa)
Time (ms)

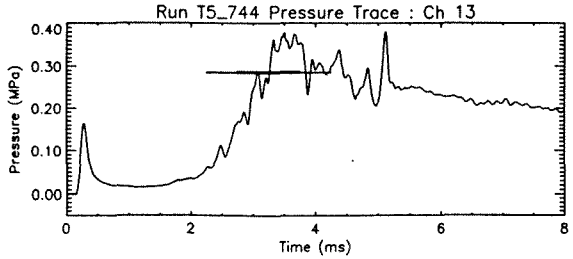
Run T5_744 Pressure Trace : Ch 13
Pressure (MPa)
Time (ms)

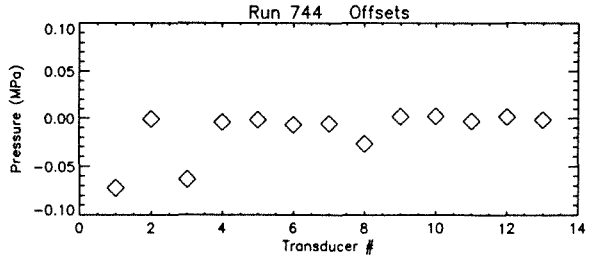
Run 744 Offsets
Pressure (MPa)
Transducer #

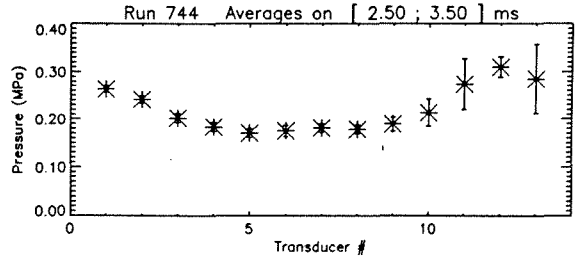
Run 744 Averages on [2.50 ; 3.50] ms
Pressure (MPa)
Transducer #

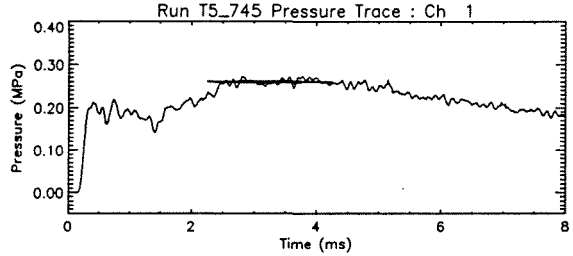
Run T5_745 Pressure Trace : Ch 1
Pressure (MPa)
Time (ms)

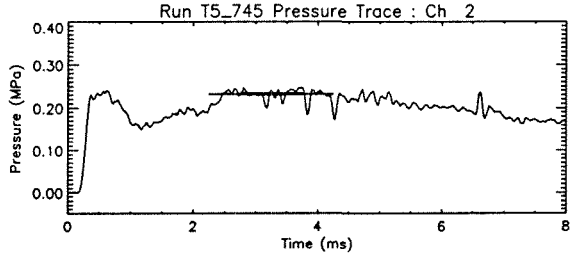
Run T5_745 Pressure Trace : Ch 2
Pressure (MPa)
Time (ms)

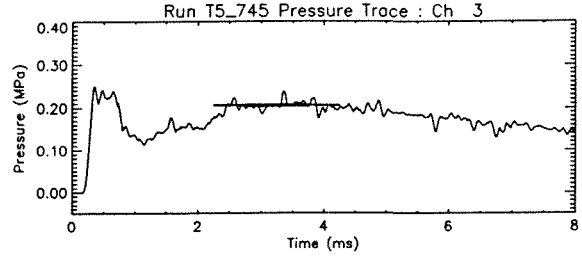
Run T5_745 Pressure Trace : Ch 3
Pressure (MPa)
Time (ms)

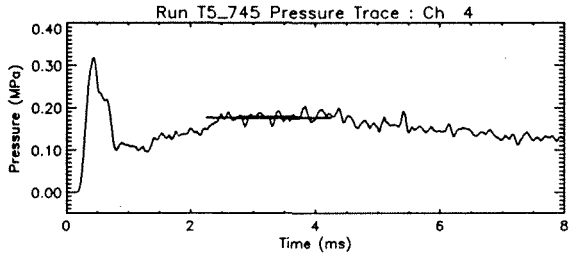
Run T5_745 Pressure Trace : Ch 4
Pressure (MPa)
Time (ms)

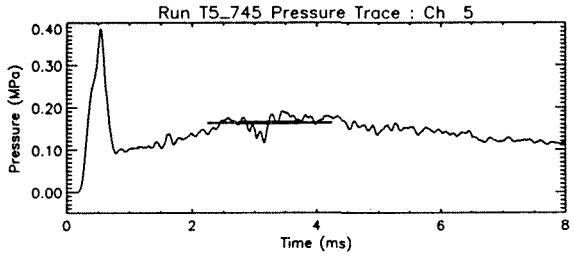
Run T5_745 Pressure Trace : Ch 5
Pressure (MPa)
Time (ms)

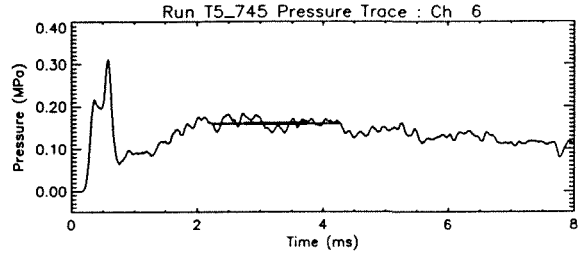
Run T5_745 Pressure Trace : Ch 6
Pressure (MPa)
Time (ms)

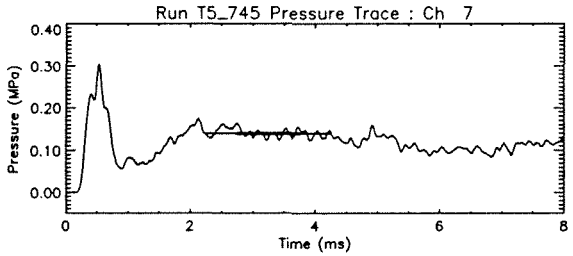
Run T5_745 Pressure Trace : Ch 7
Pressure (MPa)
Time (ms)

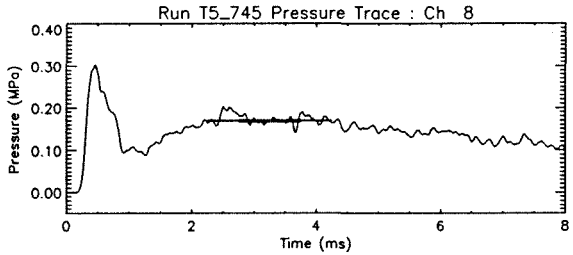
Run T5_745 Pressure Trace : Ch 8
Pressure (MPa)
Time (ms)

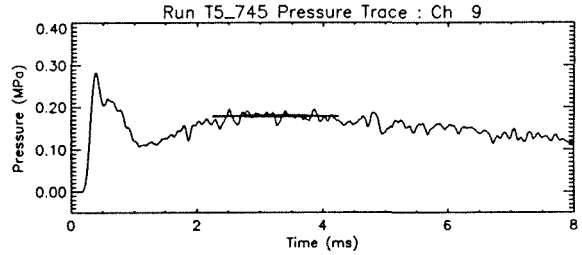
Run T5_745 Pressure Trace : Ch 9
Pressure (MPa)
Time (ms)

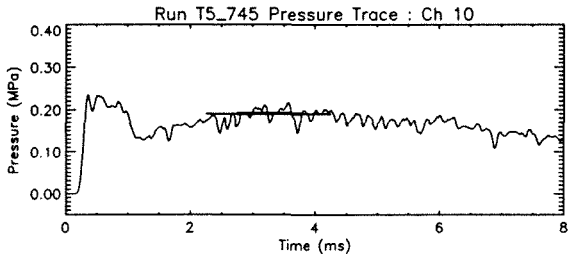
Run T5_745 Pressure Trace : Ch 10
Pressure (MPa)
Time (ms)

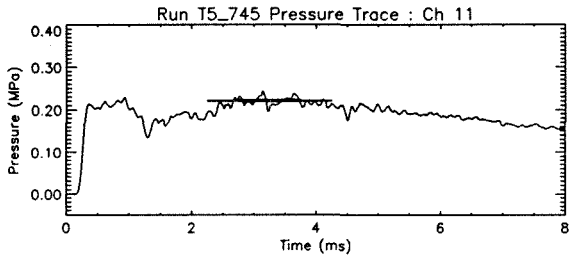
Run T5_745 Pressure Trace : Ch 11
Pressure (MPa)
Time (ms)

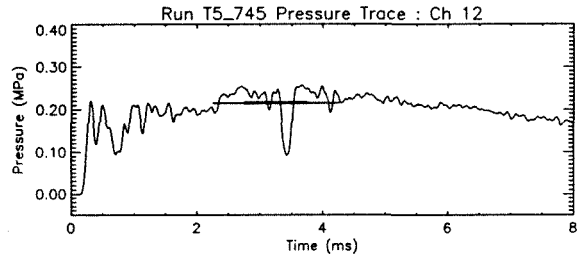
Run T5_745 Pressure Trace : Ch 12
Pressure (MPa)
Time (ms)

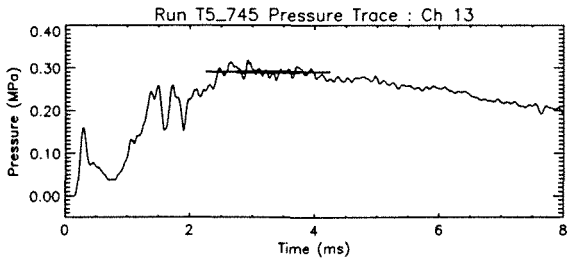
Run T5_745 Pressure Trace : Ch 13
Pressure (MPa)
Time (ms)

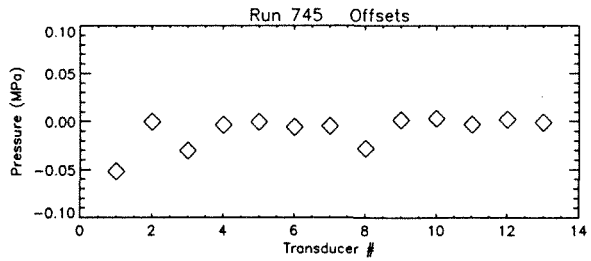
Run 745 Offsets
Pressure (MPa)
Transducer #

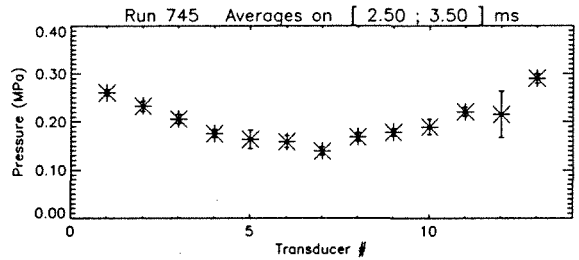
Run 745 Averages on [2.50 ; 3.50] ms
Pressure (MPa)
Transducer #

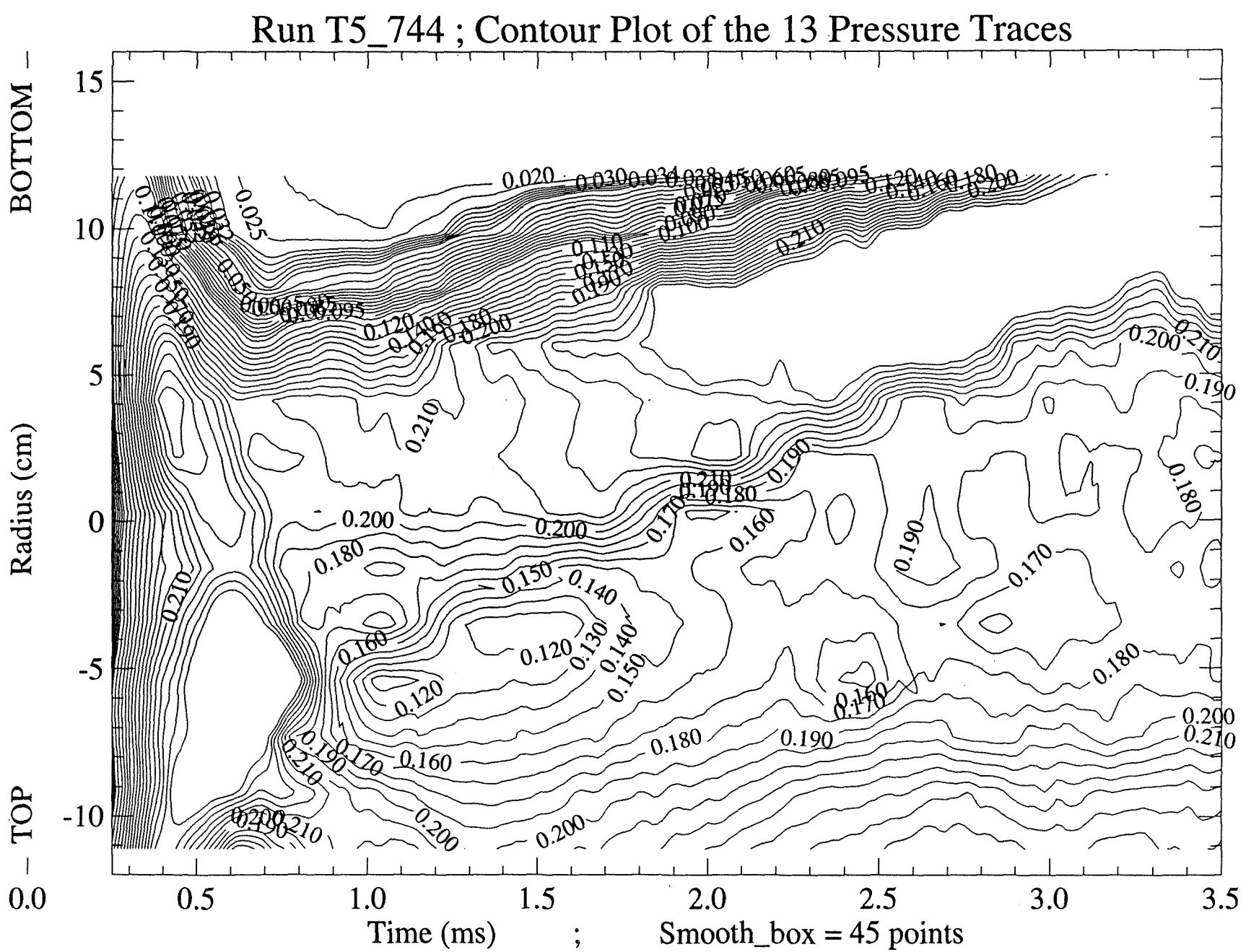
Run T5_744 ; Contour Plot of the 13 Pressure Traces
BOTTOM
TOP
Radius (cm)
15
10
5
0
-5
-10
0.0
0.5
1.0
1.5
2.0
2.5
3.0
3.5
Time (ms) ; Smooth_box = 45 points

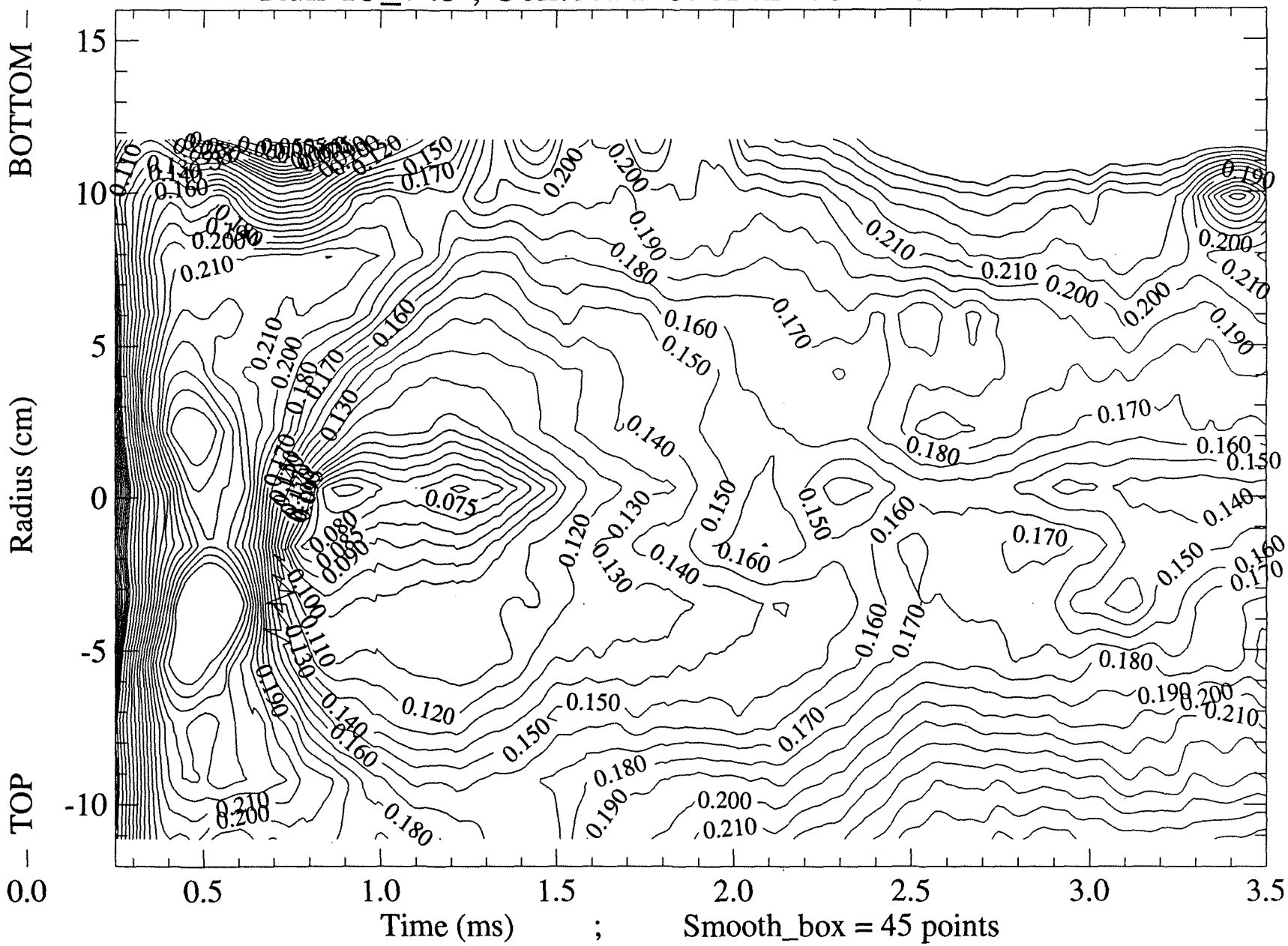
Run T5_745 ; Contour Plot of the 13 Pressure Traces
BOTTOM
TOP
Radius (cm)
15
10
5
0
-5
-10
0.0
0.5
1.0
1.5
2.0
2.5
3.0
3.5
Time (ms) ; Smooth_box = 45 points